Titre: Title:	Towards an Implantable Biosensor for Continuous Detection and Quantification of Antiseizure Medications in Blood
Auteur: Author:	Abbas Hammoud
Date:	2021
Type:	Mémoire ou thèse / Dissertation or Thesis
Référence: Citation:	Hammoud, A. (2021). Towards an Implantable Biosensor for Continuous Detection and Quantification of Antiseizure Medications in Blood [Thèse de doctorat, Polytechnique Montréal]. PolyPublie. https://publications.polymtl.ca/9909/

URL de PolyPublie: PolyPublie URL:	https://publications.polymtl.ca/9909/
Directeurs de recherche: Advisors:	Yvon Savaria, Mohamad Sawan, & Dang Khoa Nguyen
Programme: Program:	Génie électrique

POLYTECHNIQUE MONTRÉAL

affiliée à l'Université de Montréal

Towards an implantable biosensor for continuous detection and quantification of antiseizure medications in blood

ABBAS HAMMOUD

Département de génie électrique

Thèse présentée en vue de l'obtention du diplôme de *Philosophiæ Doctor*

Génie électrique

Octobre 2021

POLYTECHNIQUE MONTRÉAL

affiliée à l'Université de Montréal

Cette thèse intitulée :

Towards an implantable biosensor for continuous detection and quantification of antiseizure medications in blood

présentée par **Abbas HAMMOUD**

en vue de l'obtention du diplôme de *Philosophiæ Doctor*

a été dûment acceptée par le jury d'examen constitué de :

Yves AUDET, président
Yvon SAVARIA, membre et directeur
Mohamad SAWAN, membre et codirecteur
Dang Khoa NGUYEN, membre et codirecteur
Raphaël TROUILLON, membre
Yong Peter LIAN, membre externe

DEDICATION

To me beloved parents, Amal and Younes, and to my lovely wife, Gynan,

Who supported me throughout my journey, gave me strength, and never left my side.

ACKNOWLEDGEMENTS

First and foremost, I would like to thank God, the Almighty, for blessing me throughout my whole life, especially this journey. He is the cause and reason for every aspect of my existence.

I would like to express my sincere gratitude to my supervisors Prof Mohamad Sawan, Dr. Dang Khoa Nguyen, and Dr. Yvon Savaria for giving me the opportunity to do a Ph.D. and providing me with invaluable guidance throughout this research. Achieving my goals would not have been possible without your constant motivation and guidance. For that, I am forever grateful.

Besides my advisors, I would like to thank Dr. Steen Brian Schougaard for giving me access to his laboratories and guidance as I was a student of his own. I would also like to thank Dr. Danny Chinn, his student, for sharing his knowledge with me, permitting me to conduct valuable research.

My sincere gratitude to the jury members, namely Dr. Audet, Dr. Trouillon, Dr. Lian, and Dr Cheriet, who accepted the invitation despite their busy schedules.

I am extremely grateful to my parents for their love, prayers, caring and sacrifices for educating me and helping me carve a wonderful future. I am thankful to my beloved wife for her unconditional love and support in times where it was most necessary. Also, I would like to express my gratitude to my brothers Hussein and Mostafa, for their support and valuable prayers.

And last but not least, I would like to thank all my colleagues at Polystim Neurotech Laboratory, especially Hussein Assaf, Charles Sawma, and Elie Bou Assi. It was a pleasure being amongst great researchers, sharing meals, thoughts, and common goals.

RÉSUMÉ

L'épilepsie est l'une des maladies neurologiques les plus courantes. C'est une condition chronique caractérisée par des crises récurrentes. La première ligne de traitement de l'épilepsie passe par la prescription de médicaments antiépileptiques qui doivent être pris quotidiennement pour prévenir d'autres crises et pour une durée prolongée. Pour diverses raisons (ex. déterminer si la concentration est dans les marges thérapeutiques et ajuster la posologie en conséquence, vérifier l'adhérence au traitement etc…), il est nécessaire de procéder à des dosages sériques.

La surveillance thérapeutique précise des médicaments antiépileptiques dans le sang est actuellement limitée aux grands laboratoires et nécessite l'expertise de cliniciens qualifiés. La chromatographie liquide à haute performance est la principale technique qui permet une détection sélective et sensible du dosage de médicaments antiépileptiques. Cependant, elle est complexe, nécessite une préparation d'échantillon et ne peut pas être rendue portable. D'autre part, les méthodes miniatures existantes reposent souvent sur des techniques électrochimiques qui, malgré leur bonne sensibilité, manquent de sélectivité. D'où le besoin d'un biocapteur portable, miniature, facile à utiliser, sélectif et sensible. Un biocapteur potentiellement implantable permettrait une surveillance continue en temps réel et fournirait aux cliniciens des informations critiques qui pourraient aider à un traitement personnalisé de l'épilepsie.

Dans une première approche, nous avons émis l'hypothèse que grâce à l'analyse de l'impédance électrique de la carbamazépine (CBZ), un médicament antiépileptique, nous pourrions être en mesure d'enregistrer une réponse distincte et de quantifier sélectivement les concentrations de CBZ. Par conséquent, le premier objectif était de construire un capteur miniature de spectroscopie d'impédance électrique CMOS et de mesurer la réponse à la présence de CBZ à l'aide d'électrodes en or. Les résultats in vitro ont montré une relation linéaire entre les concentrations de CBZ et l'impédance électrique à la surface de l'électrode. Cependant, l'enregistrement d'une réponse distincte des molécules de CBZ, basée uniquement sur la spectroscopie d'impédance électrique, s'est avéré un objectif fastidieux.

Dans une deuxième approche, notre équipe a émis l'hypothèse suivante: la capture des molécules de CBZ à la surface de l'électrode isolera la réponse de la CBZ et donnera une mesure distincte de sa concentration en solution. Par conséquent, nous avons recherché des méthodes possibles pour permettre la liaison sélective entre la CBZ et la surface de l'électrode. En effet, un nouveau

polymère à empreinte moléculaire (MIP), Poly(3,4- ethylenedioxythiophene (PEDOT), a été synthétisé sur des électrodes de carbone vitreux. L'électropolymérisation du PEDOT et la quantification de la CBZ ont été réalisées par voltamétrie cyclique (CV) à l'aide d'un potentiostat commercial. Les électrodes modifiées ont montré une grande sensibilité et une grande sélectivité aux molécules de CBZ avec une limite de détection de 0,98 mM.

Comme approche finale pour atteindre la sélectivité, la sensibilité et la portabilité, notre équipe a conçu un potentiostat basé sur une puce CMOS de 1x1 mm2. Cette puce est combinée à une configuration à trois électrodes. Dans le premier mode de ce potentiostat miniature, un signal de CV suffisant pour l'électropolymérisation est appliqué. Pour le deuxième mode, un autre signal CV est généré pour mesurer les courants redox permettant d'enregistrer les concentrations de CBZ. La sélectivité du capteur a été validée en mesurant l'effet des médicaments antiépileptiques courants tels que l'acide valproïque et la phénytoïne, et aucune réponse significative n'a été enregistrée. Le polymère formé a été visualisé à l'aide d'un microscope électronique à balayage. Ainsi, l'extraction de CBZ a été confirmé par la spectroscopie ultraviolet visible. Enfin, une courbe d'étalonnage de la concentration de CBZ en fonction des pics de courant redox a été formée. La limite de détection atteinte est de 8,6 µM, ce qui améliore notablement celle publiée précédemment.

Le biocapteur proposé peut être modifié pour détecter une panoplie de médicaments. La MIP est une technique prometteuse qui ne se limite pas à la CBZ. Elle permet d'imprimer divers médicaments antiépileptiques. De plus, le biocapteur est un grand pas vers les capteurs implantables et offre de grands avantages par rapport aux systèmes de détection complexes et encombrants existants. Avec sa détection de faible puissance, sans étiquette, simple et rapide, le biocapteur permet un traitement personnalisé et pourrait être utilisé par des patients ayant des compétences cliniques minimales.

ABSTRACT

Epilepsy is one of the most common neurological diseases. It is a chronic condition characterized by recurrent seizures. The first line of treatment of epilepsy is through the prescription of antiseizure medications (ASMs). Such medications need to be taken regularly on a daily basis and for an extended period to prevent the occurrence of seizures. For various reasons (ex. determining if drug concentrations are within the therapeutic range to guide dose adjustments, assessing treatment adherence etc…), blood levels are sometimes necessary.

Monitoring the levels of ASMs in patients' blood is referred to as therapeutic drug monitoring (TDM). Accurate TDM is currently limited to large laboratories and require the expertise of trained clinicians. High-performance liquid chromatography (HPLC) aided with spectroscopy is the main technique which yields both selective and sensitive ASM level detection. However, it is complex, requires sample preparation, and cannot be rendered portable. On the other hand, existing miniaturized methods often rely on electrochemical techniques but despite their good sensitivity, simplicity, and speed, they lack selectivity. Therefore, constructing a state-of-the art miniature biosensor necessitates the combination of the selectivity and sensitivity offered by HPLC-based biosensors with the simplicity, speed and portability offered by electrochemical-based biosensors. Such a potentially implantable biosensor would enable continuous real-time monitoring and provide clinicians critical information which might aid in personalizing the treatment of epileptic patients.

As a first approach, we hypothesized that through the analysis of the electrical impedance of carbamazepine (CBZ), a common ASM, we may be able to record a distinct response and selectively quantify CBZ concentrations. Therefore, the first objective was to construct a miniaturized CMOS electrical impedance spectroscopy (EIS) sensor and measure the response of CBZ using gold electrodes. *In vitro* results showed a linear relationship between CBZ concentrations and electrical impedance at the electrode's surface. However, recording a distinct response from CBZ molecules based solely on EIS proved a tedious and maybe risky objective.

As a second approach, our team hypothesized that capturing CBZ molecules at the electrode's surface would isolate CBZ's response and yield measurement distinct to its concentration in solution. Therefore, we researched possible methods to enable the selective binding to CBZ at the electrode's surface. As a result, a novel molecular imprinted polymer (MIP) Poly(3,4-

ethylenedioxythiophene (PEDOT) was synthesized on glassy carbon electrodes (GCEs). Both PEDOT electropolymerization and CBZ quantification was performed by cyclic voltammetry (CV) using a commercial potentiostat. The modified electrodes showed great sensitivity and selectivity to CBZ molecules with a limit of detection (LOD) of 0.98 mM.

As a final approach to achieve selectivity, sensitivity, and portability, our team fabricated a 1x1 mm^2 CMOS chip combined with a three-electrode setup. In mode 1 of the miniature potentiostat, a CV signal required for electropolymerization is applied. In mode 2, another CV signal is applied to measure redox currents and record CBZ concentrations. The selectivity of the sensor was validated through measuring the sensor's response to competing ASMs such as valproic acid (VPA) and phenytoin (PHT) with no recorded significant response. Scanning electron microscopy (SEM) images further validated the polymer's formation, and ultra-violet visible (UV-vis) spectroscopy confirmed the proper extraction of CBZ from the MIP post synthesis and quantification. Finally, a calibration curve of CBZ concentration versus redox current peaks was constructed, and the achieved LOD of 8.6 µM was superior to that previously published.

Furthermore, the biosensor is a great step towards implantable sensors and offers great advantages over existing complex, and bulky detection systems. MIPs are not limited to CBZ and can be synthesized to attach to many analytes of interest. With its low-power, label-free, simple, and fast detection, the biosensor enables personalized treatment, could be utilized by patients with minimal clinical skills, and developed to detect a wide range of ASMs.

TABLE OF CONTENTS

LIST OF TABLES

LIST OF FIGURES

LIST OF SYMBOLS AND ABBREVIATIONS

AC	Alternating current
ACN	Acetonitrile
AED	Antiepileptic drug
ASM	Antiseizure medication
CBZ	Carbamazepine
CBZE	Carbamazepine 10,11 epoxide
CE	Counter electrode
CEDIA	Cloned enzyme donor immunoassay
CMOS	Complementary metal-oxide-semiconductor
CMRR	Common-mode rejection ratio
CPE	Carbon paste electrode
CV	Cyclic voltammetry
DPV	Differential pulse voltammetry
EDOT	3,4-Ethylenedioxythiophene
EIS	Electrochemical impedance spectroscopy
FPIA	Fluorescence polarization immunoassay
GCE	Glassy carbon electrode
HPLC	High-performance liquid chromatography
HPLC-MS	High-performance liquid chromatography coupled with mass spectrometry
IA	Instrumentation amplifier
LEV	Levetiracetam
LOD	Limit of detection
LOQ	Limit of quantification
LSPR	Localized surface plasmon resonance
LTG	Lamotrigine
MIP	Molecular imprinted polymer
MIPEDOT	Molecular imprinted poly(3,4-ethylenedioxythiophene)
NIP	Non-imprinted polymer
NIPEDOT	Non-imprinted poly(3,4-ethylenedioxythiophene)
NP	Nano-particle
Op-Amp	Operational amplifier
PBS	Phosphate buffered saline
PEDOT	Poly(3,4-ethylenedioxythiophene)
PHB	Phenobarbital
PHT	Phenytoin
PPy	Polypyrrole
PTP	Post-tetanic potentiation
QCM	Quartz crystal microbalance
RE	Reference electrode
SEM	Scanning electron microscopy
SERS	Surface enhanced Raman spectroscopy
SPCE	Screen-printed carbon electrode
SPM	Surface plasmon resonance
SWV	Square wave voltammetry

TDM	Therapeutic drug monitoring
UV-Vis	Ultraviolet–visible
VPA	Valproic acid
WE	Working electrode

CHAPTER 1 INTRODUCTION

1.1 Motivation

Epilepsy is the most common chronic neurological disorder after stroke that affects over 70 million people worldwide with a prevalence of 1% [1]. Common causes include brain tumors, stroke, head traumas, prescription drug use and drug withdrawal, and genetic mutations [2, 3]. Antiseizure medications (ASMs), previously referred to as antiepileptic drugs (AEDs), are the first line of treatment and most patients will need to take them daily over an extended period of time or for their whole life [3]. ASMs are generally taken by mouth once, twice or three times a day depending on their pharmacokinetic properties.

In the routine management of epileptic patients, physicians frequently order punctate blood levels of these ASMs for various reasons such as a) to ensure that the patient has reached a sufficiently protective dosage, especially in the context of liver or renal disease, pregnancy, and polypharmacy (due to the possibility of drug interactions); b) to assess treatment adherence; c) to detect or avoid therapeutic overshoot of dosing and development of over clinical toxicity. The current practice of ordering ASM levels has several limitations: a) there are numerous conditions which may affect drug levels, some of which are unpredictable and others for which the physician may be unaware of before it is too late (e.g. poor adherence, new onset co-morbid condition, new drug prescribed by another physician which may interact with ASMs such as oral contraceptive pills, grapefruit consumption which may elevate for example CBZ levels etc.); b) results from ASM testing will vary according to the time of measurement (before the ASM was taken versus several hours after the dose was taken); c) obtaining ASM levels can be time consuming and sometimes logistically difficult, especially for elderly patients and those who require frequent drug level assessments.

Unfortunately, continuous, real-time measurements are currently only possible for a handful of targets, such as glucose, lactose, and oxygen and the few existing platforms for continuous measurement are not generalizable for the monitoring of other analytes, such as small-molecule therapeutics. Present portable epileptic treatment related systems are only limited to pill reminders enhancing drug consumption whereas they provide no insight on drug levels in bloodstream. Therefore, personalized treatment would not be possible with such systems.

1.2 Epileptic seizures and antiseizure medications:

Epileptic seizures can be classified as focal or generalized. Focal seizures appear in one area of the brain, whereas, generalized seizures tend to involve all areas of the brain [1]. Furthermore, focal epileptic seizures are divided into seizures without loss of consciousness, in which the patient does not suffer from loss of consciousness but may experience an alteration in emotions, taste or smell, and into seizures with impaired awareness, where patients lose consciousness and stop responding normally to his/her environment. On the other hand, generalized epileptic seizures can be characterized into six different types such as: (a) "Grand Mal" or Generalized tonic-colonic which is the most dramatic where the patient loses consciousness and usually collapses; (b) Absence which causes a short loss of consciousness with few or no recorded symptoms; (c) Myoclonic seizures which consists of irregular brief electric shocks; (d) Clonic which causes repetitive jerks involving both sides of the body simultaneously; (e) Tonic which causes the stiffening of the muscles; (f) Atonic which consists of a sudden and general loss of muscle tone [1].

ASMs are the first line of treatment, and most patients will need to take them daily over an extended period or for their whole life. The main goals of ASMs are: to eliminate seizures or reduce their frequency to the maximum degree possible, to evade the adverse effects associated with long-term treatment, and to aid patients in maintaining or restoring their usual psychosocial and vocational activities, and in maintaining a normal lifestyle [3]. ASMs are generally taken by mouth once, twice or three times a day depending on their pharmacokinetic properties [4]. After absorption of the medication, ASMs will eventually reach a peak level (point where theoretically the patient is most protected against a seizure and when the risk of dose-related side effects is highest) and then gradually decrease to a trough level (when protection against seizures is lowest). ASM levels will again rise with the intake of the next dose.

Medication choice is influenced by individual circumstances such as age, sex, child-bearing potential, comorbidities, and tolerability issues in one hand, and seizure type and epileptic syndrome in the other hand [1]. Per diagnosis, epileptic patients are initially prescribed a single ASM since monotherapy decreases the risk of poor adherence, drug interactions, and long-term toxicity. Drug administration must be conducted with small doses while constantly monitoring any symptoms. Afterwards, the dose may be increased to the maximum tolerated if seizures persist. If the prescribed drug is ineffective it is replaced by an alternative drug. However, if monotherapy

did not enable seizure control, additional ASMs may be administered simultaneously. Amongst the most commonly prescribed ASMs for both generalized and focal seizures are levetiracetam (LEV), and lamotrigine, and valproic acid (VPA), whereas ASMs limited for focal seizures include phenytoin (PHT) and CBZ [1]. Hence, they are suggested as primary targets of therapeutic drug monitoring.

1.2.1 Phenytoin:

PHT is an ASM, also known as 5,5-diphenyl-2,4 imidazolidinedione, which operates on the motor cortex in order to minimize seizure spread. Though yet unclear, PHT seems to reduce repetitive firing through increasing the threshold of the action potential by slowing the rate of the sodium channel recovery [5]. Mani et. al [6] conducted a study by administering PHT to patients with focal or generalized tonic-clonic seizures. According to their findings, the proportion with terminal remission at each of 4 successive years of follow-up ranged from 58 % to 66 % of a sample of 60 patients. Common side effects of PHT include fatigue, involuntary eye movements and loss of coordination [7].

The recommended dose of PHT is 3-5 mg/kg/day [8]. The drug's steady-state therapeutic levels can be reached after 10 days of treatment initiation, this accumulates to 7 half-lives. Only by then, monitoring PHT levels in serum becomes relevant in order to adjust drug dosage or add other ASMs to the treatment.

1.2.2 Carbamazepine:

CBZ is another commonly used ASM, also known as 5H-dibenz[b,f]azepine-5-carboxamide. Evidence showed that 80 % of children with either focal or generalized seizures are responsive to CBZ treatment [9]. CBZ minimizes the release of glutamate, which in terms reduces seizures. Additionally, CBZ inhibits the build-up of electrical signals in the nerve cells in the brain. Common side effects of CBZ include dizziness and headaches [10]. However, these side effects are minor and dose-related and can be usually reduced by decreasing dose without necessitating a change of therapy.

The recommended dose of CBZ is 20-30 mg/kg/day [11]. The majority of CBZ in blood is affixed to plasma protein with levels of 0.5 to 25 μg/mL. Therapeutic levels of CBZ are between 4 and 12

μg/mL [12]. CBZ's half-life is about 30 hours after the administration of the first dose and reaches its peak blood level between 6 and 26 hours following a therapeutic dose [12].

1.2.3 Valproic Acid:

VPA, also known as 2-propylpentanoic acid, is an ASM used to treat both generalized and focal seizures. The process by which VPA operates is still unknown, however, it is speculated that it increases gamma-aminobutyric acid levels in brain [13]. Additionally, VPA indirectly modulates neurotransmitter release and strengthens the threshold for seizure activity [14]. Common side effects of VPZ include drowsiness, nausea, weight gain, and may cause a decrease in fertility [13].

The recommended dose of VPA is usually started at 10-15 mg/kg/day without exceeding 60 mg/kg/day [15]. VPA's therapeutic range is reported to be between 50 to 125 μg/mL [16]. Its half-life ranges from 9 to 16 hours for oral dosages of 250 to 1000 mg [13].

1.3 Therapeutic Drug Monitoring:

There are various reasons that necessitate clinicians to constantly monitor ASM levels in blood. Amongst these reasons are: ASMs are given as a prophylactic treatment and seizures happen irregularly, hence, predicting whether the given dose is sufficient to control seizures for a long-term period is challenging; signs of ASM toxicity are often faint and not distinguishable from manifestations of other disorders; toxicity cannot be easily determined through direct laboratory markers [17]; during pregnancy the pharmacokinetics of ASMs are altered due to changes in clearance capacity [18]; ensuring patients compliance is important in order to ensure successful treatment. Therapeutic drug monitoring (TDM) helps optimize patients' outcome and provides them with a safe course of treatment.

TDM is especially necessary when the therapeutic range of the drug is narrow and it is important to optimize dosage to obtain a desired therapeutic response while avoiding unwanted or harmful side-effects. Additionally, TDM provides a better understanding of (intra- or inter-individual) drug level variations whether it can be over 24h, days, weeks, or years, at various ages, during certain concomitant physiological (e.g. pregnancy, sleep) or pathological conditions (surgery, alcohol intoxication etc.). Finally, in order to establish individual therapeutic concentrations, it is important to provide clinicians with information on ASM dosage versus treatment progression.

1.4 Biosensors:

The road towards *in vivo* ASM monitoring and personalized therapy contains various challenges. Currently, TDM is conducted in large laboratories with complex equipment that can only be operated by trained clinicians. High-performance liquid chromatography coupled with mass spectrometry (HPLC-MS) is the main technique used for ASM level detection. Such technique is costly in terms of labor, price, preparation time and pre-sample treatment, affecting the integration of TDM in medical practices. Therefore, it is necessary to invent fast, reliable, and inexpensive tools capable of overcoming TDM challenges.

Fortunately, with the advances in biosensors, it may be possible to satisfy such requirements. A biosensor comprises three main components: a biological sensing element, a transducer, and a computing/signal-processing unit. The biological sensing element is responsible for recognizing and attaching to the target molecule/analyte. Examples of such elements are enzymes, aptamers, or antibodies. The second element transduces the recognition that occurs into a measurable signal, usually electrical or optical. Whereas the third element displays a user-friendly visualization of the measurable signal. The selectivity of the biological sensing element, and the sensitivity of the transducing element, offer a unique opportunity at synthesizing a rapid, portable, sensitive, and selective biosensor [19].

Biosensors can be grouped and classified according to their signal transduction readout and working principles into: optical [20], mass-based [21], and electrochemical biosensors [22].

1.4.1 Optical biosensors:

Optical sensors measure changes in light absorption caused by the interaction of the sensing element or surface with the analyte of interest. They have been widely used in various medical and environmental applications. Such applications include measuring temperature [23], pH [24], etc.

The basic instruments required for optical sensing are a light emitter (source) and a light detector. After light is propagated at a certain surface or object, the reflected light is then detected and measured to provide certain properties about the surface or object.

1.4.1.1 Surface plasmon resonance:

Surface plasmon resonance (SPR) is the main optic sensing technique. It involves the measurement of the changes in the dielectric environment of a metal film in contact with a glass prism as shown in Figure 1.1. SPR is not limited to certain types of analytes and enable selective, label-free, and real-time analysis. However, since small molecules, such as ASMs, do not significantly affect the refractive index, their detection is often difficult [17].

s

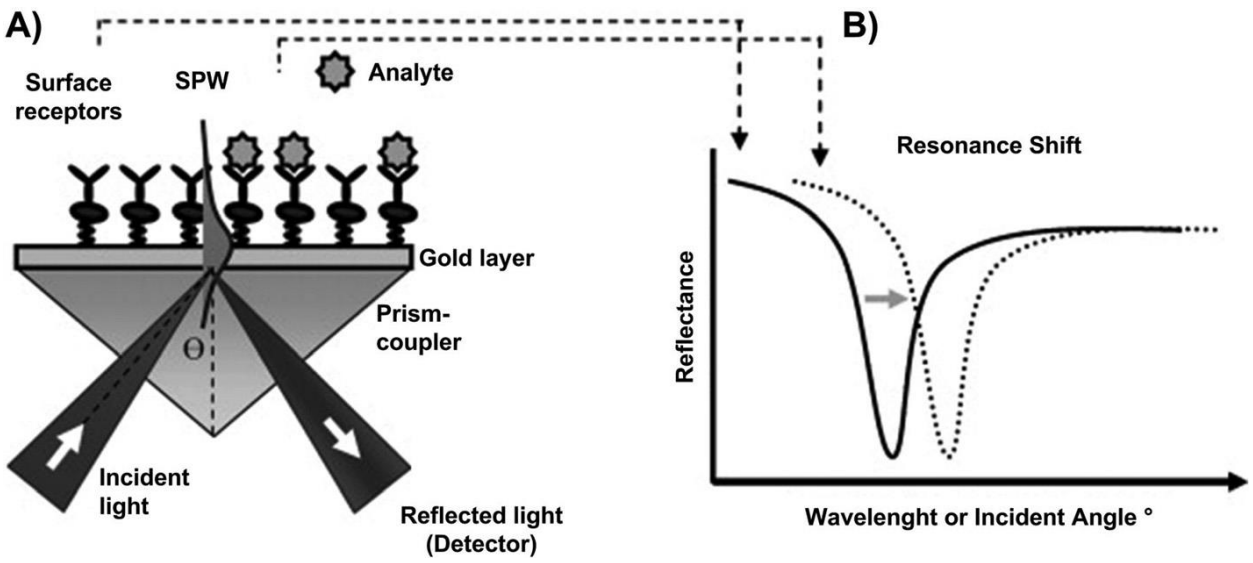

Figure 1.1 Illustration of the SPR light pathway (left) and illustration of the shift in the resonance wavelength when a binding event takes place on the sensor surface (right) [25]

1.4.1.2 Localized surface plasmon resonance spectroscopy:

Localized surface plasmon resonance (LSPR) spectroscopy is defined as the collective oscillation of conduction band electrodes produced after light interacts with noble metal nanoparticles such as silver or gold [25]. The target analyte binds to the nanoparticle's surface and causes a change in the refractive index which affects the LSPR peak frequency. A resonance condition occurs when the incident field is equal to that of the oscillating electrons on the nanoparticle's surface [26].

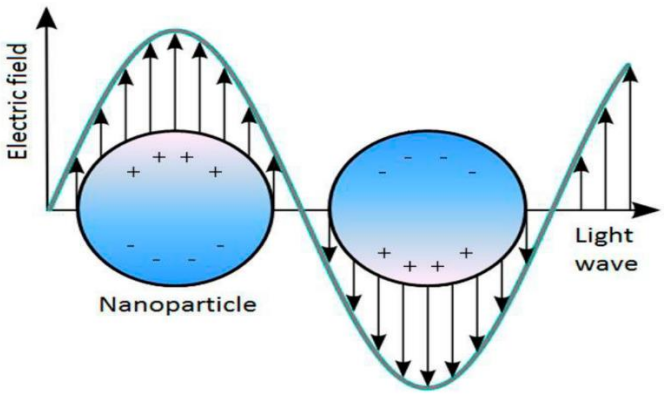

Figure 1.2 Diagram illustrating the localized surface plasmon on a nanoparticle surface [25]

This resonant oscillation generates large wave-selective increases in absorption, scattering, and electromagnetic field at the nanoparticle's surface. Many factors affect the absorption and scattering processes such as: the shape of the nanoparticle, the wavelength of the incident light, the type of the material, and the surrounding media.

1.4.1.3 Surface enhanced Raman spectroscopy:

Surface enhanced Raman spectroscopy (SERS) is an improved form of normal Raman scattering grace to two mechanisms: an electromagnetic mechanism and a chemical mechanism [27]. Due to the chemical mechanism, after the chemisorption of the molecules to the metal surface, the electrons from the molecules interact with the electrons at the surface. Such mechanism enhances the signal up to 10^2 [28]. On the other hand, the electromagnetic enhancement is a wavelength-dependent effect arising from the excitation of the LSPR. This collective oscillation of conduction electrons can occur in noble metal nanoparticles (NPs), sharp metal tips, or roughened metal surfaces, and enhances the incident electric field intensity $|E|^2$ by 10^2–10^4 times in the vicinity of the metal surface (viz. 0–50 nm of the surface) [28]. SERS enhancement factors ranging from 10^6 to 10^8 have been observed from a variety of substrates [29].

However, TDM is difficult in undiluted crude matrices when fluorescence techniques are used, because the fluorescent signal cannot easily be measured through an opaque fluid such as serum or blood [17].

1.4.2 Mechanical biosensors:

1.4.2.1 Quartz crystal microbalance:

Quartz crystal microbalance (QCM) is a piezoelectric technique that detects very low quantities of analytes [30]. An alternative current is applied to a quartz crystal that oscillates and produces acoustic waves. These waves are measured by means of two electrodes as shown in Figure 1.3.

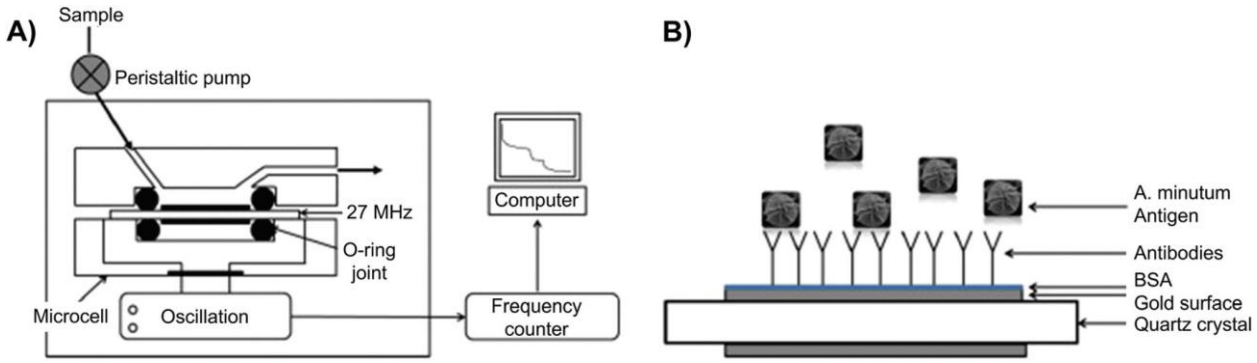

Figure 1.3 (A) A QCM setup for liquid analysis and (B) A bioassay that can be performed with QCM [31]

1.4.2.2 Microcantilevers:

Microcantilevers act as a microbalance in which the adsorption of molecules to the surface cause a variation in the cantilever's resonance frequency [32]. Microcantilevers are used in various applications such as: RNA detection [33], differentiation of DNA single-nucleotide mismatches [34], and quantifying prostate-specific antigen (PSA) [35].

1.4.3 Electrochemical biosensors:

Electrochemical methods are a class in analytical chemistry which rely on either current or voltage to detect and measure the analyte. Located in an electrochemical cell, the analyte is subjected to an excitation signal followed by measuring the response signal representing concentration of this analyte. Response signals vary according to the type of electrochemical method used. Such methods are mainly potentiometry, voltammetry, and impedance spectroscopy.

1.4.3.1 Potentiometry:

Potentiometric methods of analysis are based on measuring the potential of electrochemical cells without drawing appreciable current. The equipment for potentiometric methods is simple and inexpensive. It may simply include 2 electrodes, a reference electrode (RE) and an indicator electrode, commonly referred to as a working electrode (WE), along with a potential-measuring device (Figure 1.4).

The reference electrode is a half-cell with an accurately known electrode potential, E_{ref}, that is independent of the concentration of the analyte or any other ions in the solution under study. The indicator electrode, which is immersed in a solution of the analyte, develops a potential, E_{ind}, that depends on the activity of the analyte. Most indicator electrodes used in potentiometry are selective in their responses. The third component of a potentiometric cell is a salt bridge that prevents the components of the analyte solution from mixing with those of the reference electrode.

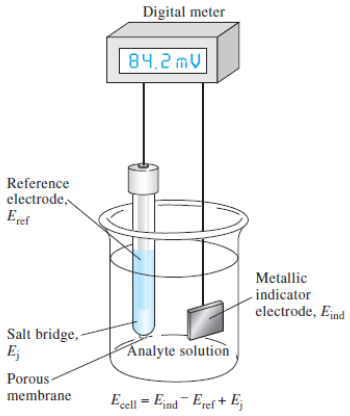

Figure 1.4 A cell for potentiometric analysis [36]

Ion concentrations are measured directly from the potential of ion-selective membrane electrodes. These electrodes are relatively free from interferences and provide a rapid, convenient, and non-destructive means for quantitatively determining numerous important anions and cations [37]. Jansod, et al. [38] report the selective detection of PHT by potentiometry using anion-selective membrane containing tetradodecylammoniun chloride as an anion exchanger. Whereas, in [39] a

potentiometric study was performed using ion selective electrodes for PHT prepared with sodium tetraphenyl borate ionophore and various plasticizers.

1.4.3.2 Voltammetry:

In voltammetry, a voltage is applied across the cell, between the WE and RE. This voltage causes a current to be produced. By measuring the resulting current various information may be extracted about the cell's characteristics. Figure 1.5 presents the potential waveforms utilized in four main voltammetry techniques.

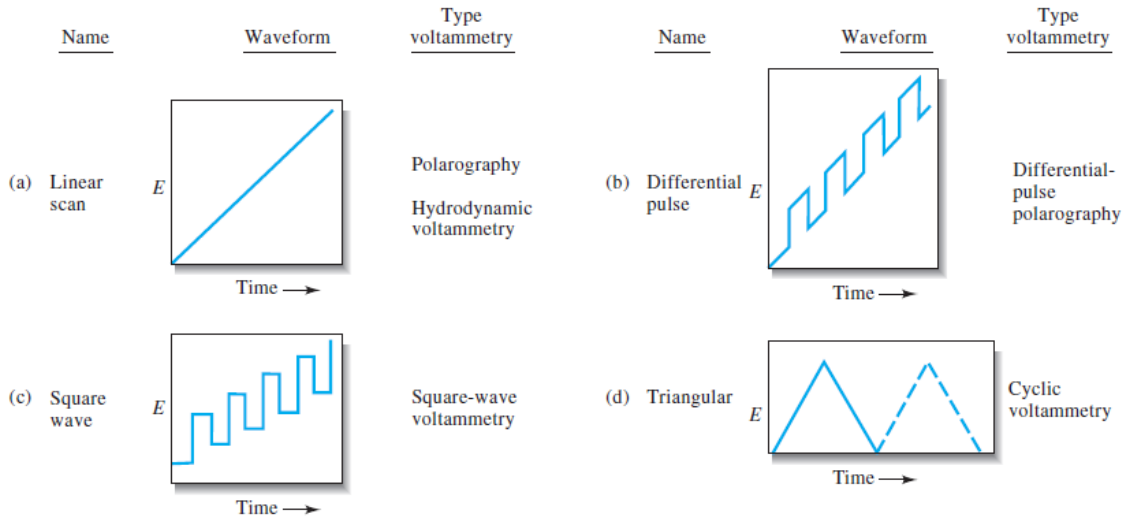

Figure 1.5 Voltage versus time excitation signals used in voltammetry [36]

Figure 1.5(a) is a linear sweep of cell voltage as a function of time. Figure 1.5(b) and 1.5(c) present two pulse excitation signals. Furthermore, Figure 1.5(d) presents a cyclic excitation signal where the potential is cycled linearly from a low voltage to a high voltage then back from the high voltage to a low voltage. In all potentiometric techniques, numerous factors may be controlled such as the cycling voltages and periods.

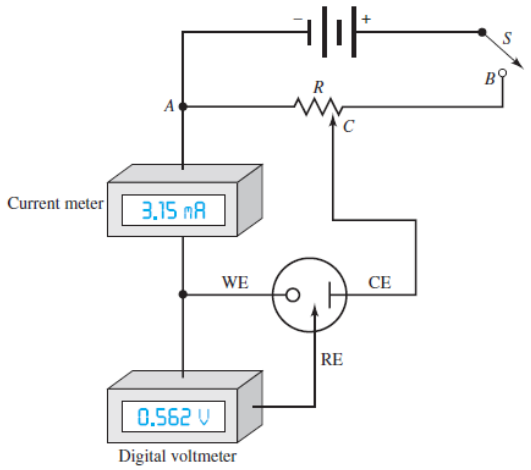

Figure 1.6 A manual potentiostat for voltammetry [36]

Figure 1.6 shows the components of a circuit used for carrying out linear sweep voltammetric measurements. The cell consists of 3 electrodes in a solution containing the analyte and supporting electrolytes. The potential of the cell is varied with respect to time across the WE and the RE. A RE must be chosen so that its potential remains unchanged throughout the experiment. Typically, Ag/AgCl is used as a RE. The third electrode is the counter electrode (CE), which is often a coil of platinum wire or a pool of mercury. The current in the cell passes between the WE and the CE. The signal source is a variable dc voltage source consisting of a battery in series with a variable resistor R. The desired excitation potential is selected by moving the contact C to the proper position on the resistor. The digital voltmeter has such a high electrical resistance that there is essentially no current in the circuit containing the meter and the reference electrode. Thus, virtually all the current from the source passes between the CE and the WE. A voltammogram is recorded by moving the contact C in Figure 1.6 and recording the resulting current as a function of the potential between the WE and the RE.

Performance of differential pulse voltammetry (DPV) compared with fluorescence polarization immunoassay (FPIA) for CBZ detection in precision, accuracy, linearity and detection limit has been established [40]. Both FPIA and DPV were comparable at most clinical used levels. Furthermore, ACAR and Onar [41] investigated the detection of VPA using square wave voltammetry (SWV) and cyclic voltammetry (CV).

1.4.3.3 Electrical impedance spectroscopy

Impedance is an important parameter used to characterize electronic circuits, components and materials and is defined as the total opposition a device offers to the flow of an alternating current (AC) at a given frequency. It consists of a real part (resistance, R) and an imaginary part (reactance, X) provided in Figure 1.7.

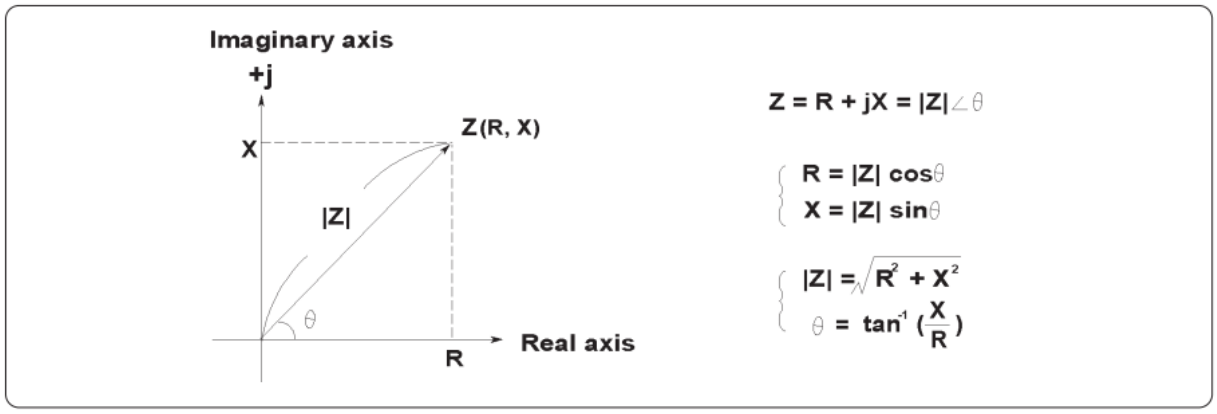

Figure 1.7 Impedance parameterization [42]

Polar coordinates of impedance are magnitude and phase. An example of a phase difference is when current passes through a capacitor or an inductor. Voltage across an ideal capacitor lags the current passing through it by a phase of 90° (Figure 1.8(a)) whereas voltage across an ideal inductor leads the current passing through it by a phase of 90° (Figure 1.8(b)).

Impedance detection has been widely utilized due to its reliability and accuracy. However, impedance detection methods are multiple and not all could be utilized for ASM detection. Below are the main impedance detection concepts.

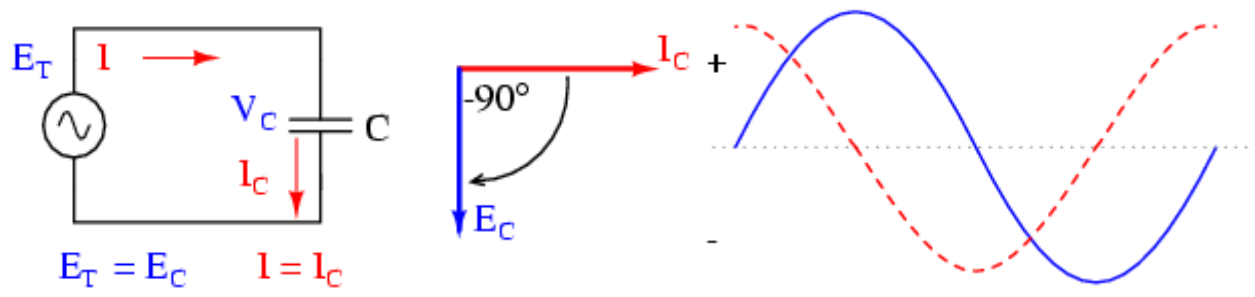

(a)

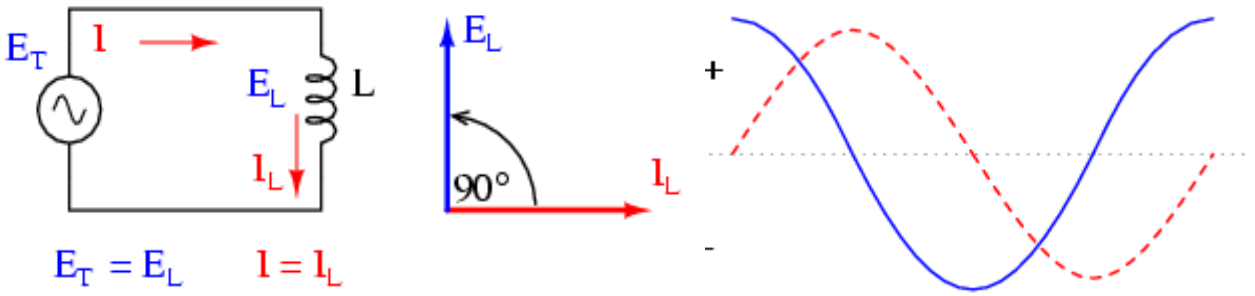

(b)

Figure 1.8 Pure capacitive (a) & inductive (b) circuits and waveforms [42]

1.4.3.3.1 Bridge method

When no current flows through the detector (D), the value of the unknown impedance (Zx) is calculated (Figure 1.9).

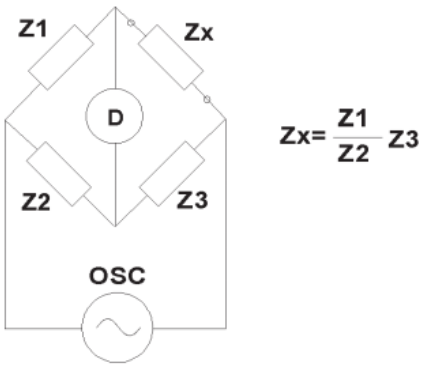

Figure 1.9 Bridge method for impedance measurement [42]

1.4.3.3.2 Resonant method

The circuit is adjusted to resonance by adjusting a tuning capacitor (C). The unknown impedance Lx and Rx are then obtained from the test frequency, C value, and Q value. The quality factor (Q) could be calculated by dividing the reactance (X) by the resistance (R) (Figure 1.10).

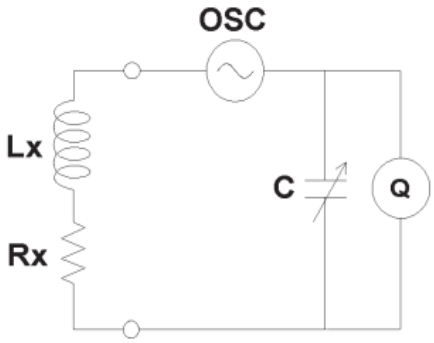

Figure 1.10 Resonant method for impedance measurement [42]

1.4.3.3.3 I-V method

The unknown impedance (Zx) is calculated from the measured current and voltage values. Current is calculated using the measured voltage across a known low value resistor (R) (Figure 1.11). Compared to other impedance measurement methods, the I-V method does not require any calibration. The unknown impedance is calculated with regards to a known value Resistor. Due to its feasibility and independency of calibration, the I-V method detection is utilized in biosensor applications.

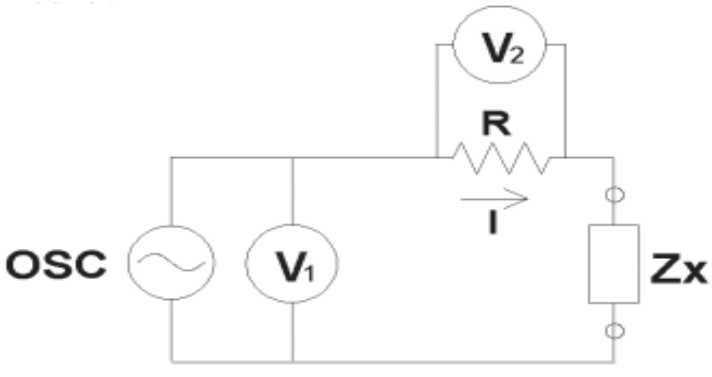

$$V_1 = V_2 + Z_x I$$

$$V_1 = RI + Z_x I$$

$$Z_x = \frac{V_1}{I} - R$$

$$\frac{V_1}{I} \gg R$$

$$Z_x = \frac{V_1}{I} = \frac{V_1}{V_2} R$$

Figure 1.11 I-V method for impedance measurement [42]

1.5 Optimal detection technique

Detection techniques are selected according to their feasibility, accuracy, precision, speed, labor intensity, power consumption, and cost. Since the proposed biosensor is intended to be implantable on the long run, the major considered aspects were feasibility, accuracy, labor intensity and power consumption. Table 1.1 presents such comparison.

Table 1.1 Comparison of detection techniques

Sensors	Non-Electroactive	Precision	Speed	Labor
Optical	✓		✓	
Mechanical	✓		✓	
Voltammetry		✓	✓	✓
EIS	✓	✓	✓	✓

Both optical and mechanical approaches although sensible and label free are not readily applied in any high throughput or practical point of care settings. Electrochemical approaches such as, voltammetric as well as electrochemical impedance spectroscopy (EIS) are alternatively used. Voltammetry may potentially detect non-electroactive analytes, however that would require electrode pre-treatment or modification. Hence, EIS is known to offer the most suitable tool when seeking for methodologies with high levels of sensitivity for the detection of biomarkers without target labeling, pre-synthesis, or the use of sandwich formats requiring two specific antibodies per target [43-45].

1.6 Research objectives and work overview

Due to their ease-of-application, sensitivity, low-cost, and minimal need for labor, voltammetry and EIS were chosen to be implemented in our proposed sensor. Thus, our main research objective is to propose and fabricate a miniature biosensor capable of selectively detecting and measuring

the concentration of ASMs within blood or a similar medium. This biosensor is designed to be potentially implantable and offer great sensitivity and ease-of-application.

Our specific aims are as follows:

AIM 1: To design a complementary metal-oxide-semiconductor (CMOS) EIS circuit capable of detecting ASM CBZ with a high degree of sensitivity.

Our team has found that the concentration of CBZ in a solution affects the impedance at the surface of gold electrodes; therefore, the design of a CMOS EIS circuit would be a big step towards a miniature biosensor capable of detecting CBZ through measuring electrical impedance at the electrode's surface. Work related to this first aim is reported in:

Article 1: **Abbas Hammoud**, Ahmad Chamseddine, Dang K. Nguyen and Mohamad Sawan, "Towards an implantable bio-sensor platform for continuous real-time monitoring of anti-epileptic drugs." 2016 38th Annual International Conference of the IEEE Engineering in Medicine and Biology Society (EMBC). IEEE, 2016.

This work was also presented in the 9th NAMIS International Summer School - Nano and Micro Systems (Montreal, July 2015).

AIM 2: To design and synthesize an electrode interface capable of measuring ASM CBZ concentration via selectively binding to CBZ molecules within a complex medium.

Despite its sensitivity, in order to selectively measure CBZ concentration, the biosensor must be capable of binding to CBZ molecules prior to quantification. Our team hypothesized that molecular imprinted polymers (MIPs) deposited on the electrodes surface would bind to CBZ molecules and enable their selective detection once paired with voltammetry. Work related to this second aim is reported in:

Article 2: **Abbas Hammoud**, Danny Chhin, Dang K. Nguyen and Mohamad Sawan, "A new molecular imprinted PEDOT glassy carbon electrode for carbamazepine detection." Biosensors and Bioelectronics 180 (2021): 113089.

AIM 3: To propose and fabricate a CMOS biosensor chip capable of polymerizing the MIP on the electrodes surface along with performing voltammetry to detect CBZ molecules.

Once proven effective at selectively binding CBZ molecules, MIPs could be utilized in the proposed biosensor. Therefore, our team hypothesized that the fabrication of a miniature biosensor chip capable of both synthesizing the polymer and conducting voltammetry would diminish the need for bulky equipment and be a big step towards personalized treatment. Work related to this third aim is reported in:

Article 3: **Abbas Hammoud**, Hussein Assaf, Yvon Savaria, Dang K. Nguyen and Mohamad Sawan, "A Molecular Imprinted PEDOT CMOS Chip-based Biosensor for Carbamazepine Detection" Submitted to Transactions on Biomedical Circuits and Systems (2021)

The work performed as part of this thesis also lead to an additional related article:

Abbas Hammoud, Dang K. Nguyen, and M. Sawan. "Detection methods and tools of administered anti-epileptic drugs-a review." Biosensors and Bioelectronics Open Access: BBOA-146. DOI 10 (2018): 2577-2260.

1.7 Thesis Organization

This thesis is organized as follows: Chapter 2 concerns a literature review of the existing sensors dedicated for ASM measurement and compares them based on various criteria. A review paper was published by the author of this thesis [46]. Chapter 2 borrows freely from that paper. Chapters 3, 4, and 5 consist of published/submitted papers addressing the main objectives of our work. We elaborate in chapters 6 and 7 a general discussion and conclusion of the entire thesis along with suggestions for future work.

CHAPTER 2 LITERATURE REVIEW

2.1 Introduction

The history of biosensors dates to as early as 1906 when Cremer demonstrated that the concentration of an acid in a liquid is proportional to the electric potential that arises between parts of the fluid located on opposite sides of a glass membrane [47]. However, a first complete biosensor was only developed in 1956 by Leland Clark Jr for oxygen detection [48, 49]. After these initial contributions, much attention has been allocated to the research and development of a large variety of biosensors. A biosensor is an analytical device which often contains immobilized biological material which specifically interact with an analyte and produce a physical, chemical or electrical signal proportional to the amount of analyte present in the solution [49]. Among commonly immobilized material are enzymes, antibodies, nucleic acid chains, and hormones. An analyte is defined as a component of interest generally measured by its chemical or physical properties [48, 50, 51].

Biosensors are nowadays ubiquitous in biomedical diagnosis as well as a wide range of other areas such as point-of-care monitoring of disease treatment or progression [50], environmental monitoring [50], food quality control [51], drug discovery [52], forensics and personalized treatment [48, 50]. One of their main applications is the detection of biomolecules that are either indicators of a disease or targets of a drug [49]. In particular, electrochemical biosensors can be used as clinical tools to detect protein cancer biomarkers [53-55]. Currently, glucose biosensors are the most widely used biosensor accounting for 85% of home-used biosensors worldwide as diabetes mellitus treatment involves precise control of blood-glucose levels [56, 57].

Figure 2.1 illustrates the general layout of a biosensor. The elements that interact, recognize, or detect an analyte are referred to in this text as biosensing elements, and components that generate or help generate a signal related to a certain physical or chemical property of an analyte are referred to as transducing elements.

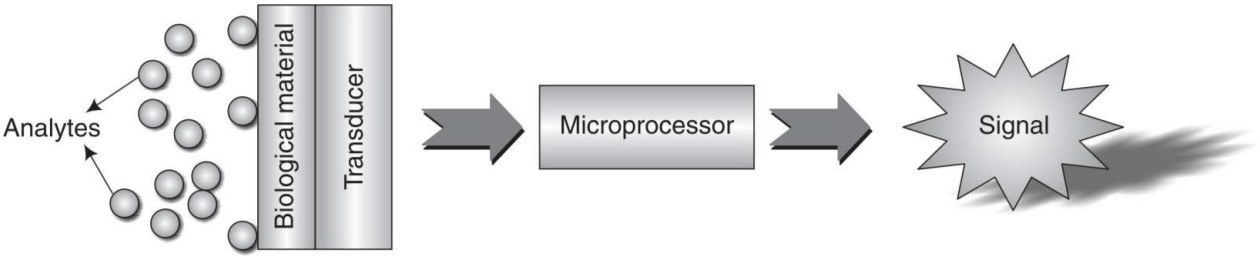

Figure 2.1 The general layout of a biosensor [58]

Biosensors essentially involve the quantitative analysis of various substances by converting their biological properties into measurable signals. Figure 2.2 illustrates the process of generating a signal from an analyte. The performance of a biosensor is mostly dependent on the specificity and sensitivity of the biological reaction, which is highly determined by the sensor's biosensing and transducing elements [51, 59]. This review presents the latest biosensing, transducing and computing units applied to the detection of ASMs. Biosensors were categorized according to two main blocks: a transducing element, coupled with a computing unit, and a biosensing element. Sections were assigned to the different categories with a focus on methods deployed, results and efficacy.

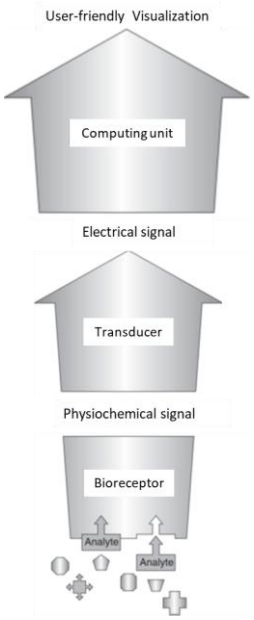

Figure 2.2 Transducer signaling process in a biosensor

2.1.1 Biosensor Characteristics

When analyzing biosensors, there are numerous characteristics that allows us to assess their performance including selectivity, reproducibility, stability, sensitivity, and linearity. Selectivity is the ability of a bioreceptor to detect a specific analyte in a sample containing contaminants. The best example of selectivity is depicted by the interaction of an antigen with the antibody. Reproducibility, on the other hand, is the ability of the biosensor to generate identical responses for a duplicated experimental set-up. Furthermore, reproducibility is characterized by the precision and accuracy of the transducer and electronics in a biosensor [51, 59]. Reproducible signals provide high reliability and robustness to the biosensor's inference. Stability, the most crucial feature of a biosensor, is the degree of susceptibility to ambient disturbances in and around the biosensing system.

These disturbances can cause a drift in the output signals of a biosensor under measurement causing an error in the measured concentration and can affect the precision and accuracy of the biosensor. Sensitivity is the biosensor's signal strength, which along with the sensor's stability, affects the limit of detection (LOD) and the limit of quantification (LOQ) of the biosensor. Both LOD and LOQ are terms utilized to describe the smallest concentration of the analyte that can be measured. LOD is defined as the lowest concentration that can be detected with a stated probability, although not quantified as an exact value. On the other hand, LOQ is defined as the lowest concentration that can be quantified with a specified acceptable precision and accuracy [60]. Linearity is the attribute that shows the accuracy of the measured response (for a set of measurements with different concentrations of analyte) to a straight line [49]. The linearity of the biosensor can be associated with the resolution of the biosensor and the range of analyte concentrations under test. Finally, the resolution of the biosensor is defined as the smallest change in the concentration of an analyte that is required to bring a change in the response of the biosensor [49].

In addition to all above characteristics, biosensor miniaturization has proved to be beneficial for various reasons. For instance, reducing the size of the biosensor to the micro- or nanoscale can result in a better signal-to-noise ratio as well as the possibility of using smaller sample volumes, which means lower assay costs. Moreover, when going towards nanoscale dimensions, the surface-to-volume ratio of the sensing active area increases, and the sizes of the detecting electrodes and that of the target biomarker become comparable. This reduces non-specific binding and increases

binding efficiency towards the target molecule. As a result, the bioreceptor becomes an active transducer for the sensing system and it becomes possible to perform single-molecule detection [49, 61]. Miniaturization also allows for easier integration of these sensors in point-of-care monitoring allowing them to be implantable.

2.1.2 Antiseizure Medications and Therapeutic Drug Monitoring

ASMs are the first line of treatment offered to epileptic patients. These drugs are generally taken by mouth once, twice or three times a day depending on their pharmacokinetic properties. Post absorption, ASM levels reach a point where the patient is most protected against seizures, and where risks of dose-related side effects are highest. Levels will then gradually decrease until reaching a level where the patient has the least seizure protection. Anew, levels will rise with the intake of the next dose. While low serum concentrations may have no therapeutic effect, high serum concentration may cause side effects [62].

Common dose-related side effects of ASMs include dizziness, blurred vision, dysarthria, ataxia, somnolence, and psychomotor slowing. Currently, more than fifteen ASMs are available on the market. The most used ones include CBZ, VPA, PHT, LEV and Lamotrigine (LTG) [63]. TDM of concentrations of drugs in body fluids, usually plasma, can be used during treatment. This information is used to individualize dosage so that drug concentrations can be maintained within a target range. In the routine management of epileptic patients, physicians will frequently order punctate blood levels of ASMs for various reasons such as a) to ensure that the patient has reached a sufficiently protective dosage, especially in the context of elderly patients, liver or renal disease, pregnancy, and polypharmacy (due to the possibility of drug interactions); b) assessing adherence or compliance; c) detect or avoid therapeutic overshoot of dosing and development of over clinical toxicity.

The current practice of ordering punctate ASMs levels has several limitations: a) there are numerous conditions which may affect drug levels, some of which are unpredictable and others for which the neurologist may be unaware of before it is too late (e.g. poor compliance, new onset co-morbid condition, pregnancy, prescription by another physician of a drug which can interact with ASMs such as oral contraceptives pills, grapefruit consummation which may elevate for example carbamazepine levels etc.); b) results from ASM testing will vary according to the time of measurement (before the ASM was taken versus several hours after the dose was taken); c) because

patients need to go to a health care facility and wait in line for blood collection, obtaining these ASM levels can be time consuming and sometimes logistically difficult, especially for elderly patients and those who require frequent drug levels.

A sensor capable of continuously measuring ASM levels in the bloodstream or tissue *in vivo* would give clinicians a valuable window into patients' health and their response to therapeutics. This device could allow for example: a) a better understanding of (intra- or inter-individual) drug level variations whether it can be over 24h, days, weeks or years, at various ages, during certain concomitant physiological (e.g. pregnancy, sleep) or pathological conditions (surgery, alcohol intoxication etc.); b) a comprehensive assessment of compliance by patients; c) a thorough causality assessment between drug levels and side effects or seizure protection; d) a better assessment of the impact of switching from brand-name to generic ASMs. Unfortunately, continuous real-time measurements are currently only possible for a handful of targets, such as glucose, lactose, and oxygen and the few existing platforms for continuous measurement are not generalizable for the monitoring of other analytes, such as small-molecule therapeutics.

2.2 The Transducing Element

A biosensor is a sensing device that compromises a biological component, referred to as a sensing element in this text, a transducer that transforms biochemical activity into a measurable signal proportional to the quantity of analyte present, and a computing unit that transforms the signal into a user-friendly visualization. In this section, the transducing element of the biosensor will be discussed and categorized into chromatography-based, optical-based, and electrochemical-based sensors. Additionally, the computing unit coupled with the transducer element will be mentioned when necessary.

2.2.1 Chromatography Based Methods

Chromatography-based methods are one of the most adopted methods for TDM of ASMs because of their high accuracy, sensitivity and selectivity [64-69]. Drawbacks include that they require expensive bulky instruments and a long time for sample pre-treatment. The four main types of chromatography techniques are liquid chromatography, gas chromatography, thin-layer chromatography and paper chromatography. In liquid chromatography, the liquid solvent containing the sample mixture travels by gravity through a column containing solid adsorbent

material. Contingent upon the mixture's interaction with the adsorbent material, different flow rates separate the components as they flow out of the column. An improved version of liquid chromatography is high-performance liquid chromatography (HPLC) [70-72] where the solvent is pressurized by a pump through the column reducing the time of separation. In gas chromatography, helium is used to move a gaseous mixture through a column of absorbent material. Gas chromatography is applied in analytical chemistry for separating and analyzing compounds that can be vaporized without decomposition for testing the purity of a substance or separating the different components of a mixture [73].

Both thin-layer chromatography and paper chromatography use an absorbent material on flat glass or plastic plates as stationary phases; however, in contrast to paper in paper chromatography, silica or alumina is used in thin-layer chromatography. All mentioned chromatography techniques are often coupled with mass spectroscopy to enhance detection after separation [74, 75]. The latter is an optical-based detection technique which relies on quantifying particles through measuring their mass-to-charge ratio after ionization. Due to their precision, accuracy and high selectivity, HPLC and gas chromatography are the most widely used techniques for therapeutic drug monitoring. Shah et al. [76], implemented a HPLC technique by taking a sample of dried blood spots from patients for the simultaneous determination of ASMs LEV, LTG, Phenobarbital (PHB), CBZ and carbamazepine 10,11 epoxide (CBZE). Dried blood spots sampling provides multiple advantages over conventional venous sampling such as: a) only a small volume of blood is required, beneficial for amassing samples from newborns, youth and seniors; b) it can be performed by non-professionals; c) the dried blood spots samples do not need to be processed and prepared; e) most importantly, once dried, many analytes including antibodies are stabilized on filter paper [77]. However due to the use of minimal sample volumes, there is a high risk of false negatives with dried blood spots sampling [78]. Prior to analysis, whole blood aliquots were prepared from the dried blood spots samples by adding 75% buffer (25 mM phosphate buffer pH 6.2), 15% acetonitrile (ACN) and 10% methanol.

Afterwards, 10 mL of analyte diluted in methanol at concentrations corresponding to recorded therapeutic ranges were added to 0.95 mL of the prepared blood aliquots. HPLC analysis using an XBridgeT M C_{18} column (150 mm x 4.6 mm, 3.5 μm; Waters, UK) combined with ultraviolet detection was then carried out for a total run time of 28 min. The method was then validated by evaluating selectivity, linearity, LOD, accuracy, and recovery. It was found that the mobile phase

consisting of the above-mentioned mixture enabled the best chromatographic conditions to achieve good resolution of all analytes, including LEV which is highly polar and requires a mobile phase with little organic strength. Ultraviolet detection using a wavelength of 205 nm was then carried out to monitor the absorbance of the analyzed ASMs. Ultraviolet detection was used adjacent to liquid chromatography mass spectrometry since all the ASMs of interest are active at relatively high concentrations (μg/mL, rather than ng/mL). Apart from good selectivity, linearity, and accuracy within 15% at all quality control concentrations, acceptable LOQ and LOD values were achieved as provided in Table 2.1. Finally, it was found that extraction of ASMs from the tested samples using methanol:ACN (3:1, v/v) gave the best recovery enabling the extended use of blood samples.

Table 2.1 Calculated LOD and LOQ for ASMs in dried blood spots samples [76]

ASM	**LOD (μg/mL)**	**LOQ (μg/mL)**
LEV	0.38	1.15
LTG	0.223	0.676
PHB	0.318	0.963
CBZE	0.3	0.908
CBZ	0.258	0.78

De Almeida, et al. [79] on the other hand, used liquid chromatography coupled with mass spectrometry for the determination of ASMs bromazepam, lorazepam, CBZ, and diazepam. Specifically, samples were pre-concentrated with the aid of C18 Premium 300 mg/3 mL cartridges pre-conditioned with 10 mL methanol and 10 mL water (pH 2.0), and the analytical determinations were carried out using a liquid chromatograph equipped with a binary pump, a degasser, a column oven and an automatic injector. Furthermore, the operational conditions were the following: analytical column = Zorbax SB C18 5 μm, 4.6 x 150 mm; mobile phases = water and methanol, both containing 1.0% v/v formic acid. The gradient program adopted began with 10% mobile phase methanol, then the mobile phase was increased linearly up to 80% for 5.5 min. Afterwards, it was

kept at 80 % until 8 min was reached, then increased again to 90% until 11 min, finally increased to 100% from 13 min to 15 min before dropping it back to initial conditions (Table 2.2).

Table 2.2 HPLC gradient program [79]

Time (min)	Flow rate (mL/min)	Injection volume (µL)	Methanol %
Initially	0.7	25	10
0 - 5.5	0.7	25	10 - 80
5.5 - 8	0.7	25	80
8 - 11	0.7	25	80 - 90
11 - 13	0.7	25	90
13 - 15	0.7	25	90 - 100
Final	0.7	25	10

After separation, the compounds were quantified using a mass spectrometer equipped with an electrospray ionization source. The spectrometer was optimized by infusing the working solution of each analyte and determining both the ionization mode and precursor ion. Furthermore, the ionization conditions were found by injecting a standard solution of each analyte at a rate of 100 µg/L. The mass spectrometer parameters used are presented in Table 2.3. De Almeida et al. were able to achieve satisfactory precision and exactitude with intra-day precision values between 3.6 % and 5.8 % and inter-day precision values between 5.1 % and 9.5 %. Finally, the LOD values were found to be between 4.9 and 6.1 ng/L, and the LOQ between 30 and 50 ng/L.

Hashem, et al. [80] implemented an HPLC method that is simple, rapid, accurate, and stable for the quantification of PHB and PHT in various forms: powder forms, dosage form and in urine samples. Prior to analysis, stock solutions of PHB (1 mg/mL) and PHT (1 mg/mL) were dissolved in methanol and ACN respectively. Furthermore, apart from control samples, others were loaded with either HCl, NaOH or H_2O_2 or exposed to ultraviolet radiation in order to perform forced degradation studies. The different samples containing PHB were separated using an isocratic binary mobile phase of MeOH/H_2O (38.0/62.0, v/v) at a flow rate of 3 mL/min at a temperature of 40°C and detection was achieved at 214 nm. Whereas the PHT

containing samples were separated using an analytical column with an isocratic binary mobile phase of ACN/H_2O (25.0/75.0, v/v) at a flow rate of 1 mL/min at 40°C and detected at 220 nm. PHB showed a strong degradation with NaOH, and a weak degradation with HCl, H_2O_2, and upon exposure to ultraviolet radiation. PHT, on the other hand, showed weak a degradation with all NaOH, HCl, H_2O_2, and upon exposure to ultraviolet radiation. To study the detection limit of the HPLC method developed, 13 concentrations of PHB and PHT solutions ranging from 0.061-100 μg/mL were prepared. The graph of the peak area versus concentration provided linearity in the range of 1 - 20 μg/mL for PHB and 1 - 50 μg/mL for PHT. The LOQ values were found to be 0.250 μg/mL for PHB and 0.500 μg/mL for PHT. Both drugs were further analyzed, PHB in suppository, and PHT in capsules and spiked urine. Results are provided in Table 2.4.

Table 2.3 Mass spectrometer parameters used [79]

Drug	**Precursor Ion (m/z)**	**Product Ion (m/z)**	**DP.**	**CE. (%)**	**CCEP.**
Bromazepam	316	214	106	39	12
		156	106	45	10
CBZ	237	194	130	53	10
		179	130	53	10
Clonazepam	316	270	101	35	14
		181	101	67	8
Diazepam	285	193	56	53	10
		154	130	53	10
Lorazepam	321	275	101	53	10
		302	106	47	10
DP: Declustering Potential; CE: Collision energy; CCEP: Collision Cell Exit Potential					

Table 2.4 Determination of PHB and PHT in Dosage forms or in Urine [80]

	PHB		**PHT**		
	Recovery	St. Addition (suppository)	Recovery	St. Addition (suppository)	Spiked urine
Average	100.78	99.3	96.91	96.05	96.69
RSD	2.62	2.94	1.06	1.67	0.68
SD	2.6	2.96	1.09	1.74	0.7

Shah, et al. [81] developed an accurate, simple, rapid, precise, and linear technique using reverse phase HPLC for simultaneous estimation of PHT and PHB. The term reverse phase describes the chromatography mode that is opposite of a normal phase, namely the use of a polar mobile phase and a non-polar hydrophobic stationary phase. Shah et al. tested different chromatographic conditions for better separation and resolution. A mobile phase of methanol: phosphate buffer (pH 5) adjusted with 0.1 M NaOH (50:50), a flow rate of 1.0 mL/min and a run time of 9 min were found to be fit for the analysis. Furthermore, ultraviolet detection was at 215 nm for both drugs. The mobile phase was also used as the solvent to prepare the drug solutions. The linearity of the test solutions for the assay using 5 different concentrations of each drug was found to be within the concentration range of 10 – 30 μg/mL and 3 - 9 μg/ml for PHT sodium and PHB respectively. The retention time for PHT was 3.97 min and 6.90 min for PHB. The LOD for PHT was 1.44 μg/mL and 4.36 μg/mL; the LOD for PHB was 0.4 and 1.35 μg/mL. The proposed reverse phase HPLC method used methanol and phosphate buffer which are both easily available and achieved a recovery rate of 98 % to 100 % for each drug which made it simple, easy to perform and economical.

2.2.2 Optical Based Methods

Optical biosensors employed in ASM detection offer great advantages because they enable direct, real-time, and label-free detection of many biological and chemical substances [82, 83]. Their advantages also include high specificity, sensitivity, smallness, and cost-effectiveness. Optical-based detection is performed by exploiting the interaction of an optical field with a biorecognition element [84]. Spectrophotometry is a simple optical technique that relies on measuring the

absorbance of a medium to light. It requires a photometer to measure the intensity of light through an analyte containing medium by studying the wavelength. This simple technique has been employed in ASM detection systems [85-91] to detect and characterize analytes according to their absorbance spectra. Revanasiddappa, et al. [92] used an ultraviolet visible (UV-Vis) spectrophotometer to study the determination and degradation of oxycarbamazepine, a keto analog of CBZ, in HCl, NaOH, H_2O_2, thermal and UV radiation. They concluded that the absorbance spectra of oxycarbamazepine solution prepared in methanol:ACN (50:50, v/v) showed a direct correlation with the amount of analyte present at a wavelength of 255 nm. The LOD and LOQ measured by Revanasiddappa were 0.0550 μg/mL and 0.1667 μg/mL respectively. However, despite good sensitivity, Revanasiddappa's method does not claim to be selective.

On the other hand, Rezaei, et al. [93] used partial least-squares regression combined with UV-spectrophotometry to achieve selective detection of both CBZ and PHT. Partial least-squares regression is a linear statistical method that measures the correlation of two variables and has been utilized in spectrophotometric-multicomponent analysis of various drugs in biological and pharmaceutical samples [94-100]. Authors found a correlation with the drugs and their respective absorbance spectra and reported recovery percentages of CBZ and PHT to be 98.4 and 98.2 respectively. However, the authors do not yet propose this method as an alternative to HPLC for in plasma detection which is a complex medium. In addition to spectrophotometry, surface plasmon resonance, the most common optical technique, relies on a phenomenon that occurs on the surface of metals (or other conducting materials) at the interface of two media (usually glass and liquid) when it is illuminated by polarized light at a specific angle.

This generates surface plasmons and consequently a reduction of the intensity of reflected light at a specific angle known as the resonance angle. This effect is proportionate to the mass on the surface. As a result, a sensogram can be obtained by measuring the shift of reflectivity, angle or wavelengths against time. Figure 1.1 demonstrates the basic schematics of a surface plasmon resonance setup as well as the sensogram measurements. Multiple and various interacting molecules or biosensing elements could be immobilized depending on the analyte of interest, which makes surface plasmon resonance a universal technique suitable for various biosensing applications. For example, to measure a ligand-analyte interaction, one interacting molecule must be immobilized on the sensor surface. However, small molecules, such as most therapeutic drugs, once captured on the surface, may not affect the refractive index significantly, which makes their

direct detection and quantification difficult. Furthermore, nonspecific binding is an issue that occurs in most universal detectors and is defined as the adsorption or binding on the sensor's surface of molecules that are not related to the analysis [17].

Fu, et al. [101], developed a prototype biosensor that takes advantage of surface plasmon resonance for the detection of PHT in saliva. Saliva is not often used as a sample for TDM; however, it is an ideal sample for patients since its collection is non-invasive and painless, and samples can be obtained more frequently than would be practical with blood [102]. Nevertheless, analytes, especially PHT, are often present in saliva at concentrations that correlate well with their free levels in the blood. PHT was tested in both phosphate buffered saline (PBS) and human saliva. Saliva was preconditioned by a 0.2-μm-pore conventional polymeric filter and a microfluidic diffusion-based separations device, the flat H-filter [103, 104]. This combination of filters removes 98 % of the glycoprotein/mucin content and 92 % of the protein content, while retaining 27 % of the small-molecule analytes [105].

To act as a source, a near infrared light-emitting diode was used along with stationary wide-field image imaging optics. A compact liquid crystal polarizer enabled electronic switching of the source between a transverse magnetic mode, where the magnetic field is perpendicular to the wave-guide axis, and a transverse electric mode, where the electric field is perpendicular to the wave-guide axis. Additionally, the concept of folded optics, to miniaturize the optical module whilst still achieving a long optical path producing a strong and focused beam.

Apart from that, Fu, et al. [101] utilized a 1/3" charge coupled device with 640 x 480 pixels' image detector with a fast readout to enable improvement of image statistics through averaging and a low background noise to operate at high light levels. The charge coupled device, integrated into a camera with a powerful digital signal processor was able to acquire and sum images at 30 frames per second. Fu, et al. [101] then used a custom-coded software to control both data acquisition functions such as light-emitting diode translation, polarization switching and image acquisition, and fluid motion such as valve and pump actuation. Finally, the data analysis function was created using MATLAB and implemented on a tablet-style paper chromatography enabling large processing power and a high-resolution display.

In order to produce a change in the refractive index, the unknown amount of PHT was mixed with a known amount of anti-PHT which was then introduced to the PHT-surface immobilized detection

zone. Only the free unbound anti-PHT binds to the immobilized PHT causing a change in the refractive index quantifiable by the SPR imaging system. The SPR signals provided in Figure 2.4 indicate that both the rate of binding and the total coverage of anti-PHT are inversely correlated with the concentration of PHT. Furthermore, in order to detect different ASMs, antibodies for the ASM of interest could replace that of PHT and by a small-range translation of the source the instrument response can be optimized.

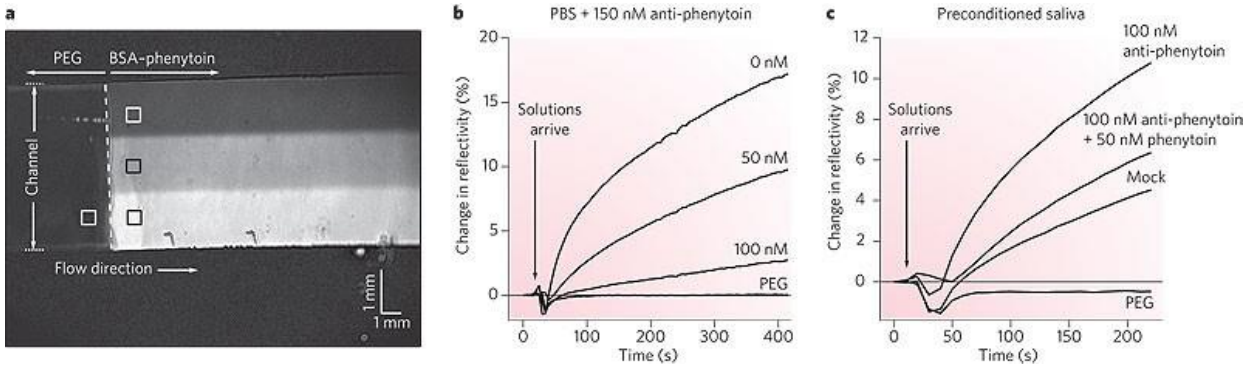

Figure 2.3 Parallel indirect immunoassays for PHT conducted using multiple flows. (A) The SPR difference image shows the outcome of anti-PHT binding to the surface from samples containing 0, 50, or 100 nM PHT in phosphate buffer premixed with 150 nM anti-PHT after 5 min (B) Assay results for PHT spiked into PBS (C) Assay results for PHT spiked into preconditioned saliva [105]

2.2.3 Electrochemical Methods

Electrochemical methods are a class in analytical chemistry which rely on either current or voltage to detect and measure the analyte. Located in an electrochemical cell, the analyte is subjected to an excitation signal followed by measuring the response signal representing the concentration of the analyte. Such methods are mainly potentiometry, voltammetry, and impedance spectroscopy. Due to ease-of-application, sensitivity, low-cost, minimal need for labor and least damage to analyte, electrochemical methods are highly reliable. Biosensing elements could be immobilized on the surface of the WE to improve upon its selectivity. However, the WE could also be modified with different materials to amplify the strength of the signal which will improve the signal-to- noise ratio [106, 107]. Several factors may affect electrochemical evaluation, such as the electric

conductivity of the electrode, solvent type, scan rate, and distance between electrodes. Therefore, it is important to control such factors in order to achieve reproducible results.

Raoof et al. [108] developed a highly sensitive voltammetric sensor for the determination of PHB in the presence of acetaminophen. CV and DPV were conducted using a multiwalled carbon nanotube paste electrode as the working electrode, a platinum wire as the counter electrode and an Ag|AgCl|KCl (3 M) electrode as the reference electrode. Multiwalled carbon nanotubes are allotropes of carbon with cylindrical nanostructures possessing large-surface area, high stability at nanoscale, and high thermal, electrical and mechanical conductivity. They were able to attain a detection limit of PHB of 0.1 M.

On the other hand, chemical doping at the electrode's surface has proved to be effective for chemo-biosensing applications [109-111]. Lavanya et al. [112], developed an electrochemical sensor for the determination of CBZ levels. They modified the WE by Fe-SnO_2 doped with Fe^{3+}. The added active elements stabilize the SnO_2 surface and promote a decrease in grain size which enhances higher catalytic activity and sensor response than that of pure SnO_2. The behaviour of CBZ at the WE was investigated using CV and SWV. Despite achieving oxidation peaks at 0.78 V for a bare screen-printed carbon electrode (SPCE) which is much lower than literature values ~1.15 V [61, 108, 112, 113], modifying the electrode resulted in a significant increase in anodic peak currents of CBZ (Ipa = 14.8 μA) (Figure 2.5). This increase in anodic current is due to the large effective electrode surface area and higher electron conductivity of the Fe doped SnO_2 NPs. To conclude, their fabricated sensor displayed a good electro-oxidation response towards the detection of CBZ at a lower oxidation potential of 0.8 V in phosphate buffer solution at pH 7.0 with a wide linear range of 0.5-100 μM and a low detection limit of 0.5-100 μM.

On the other hand, Balasubramanian, et al. [114] developed a CBZ detection biosensor based on both graphene oxide and Graphitic Carbon Nitride Composite (GO/g-C_3N_4). Despite its specific electronic structure, low toxicity and stability, g-C_3N_4 was found to be limited due to its low electrical conductivity [115, 116]. Therefore, graphene oxide was added along with g-C_3N_4 to the electrodes surface. This improves electrocatalytic activity along with the detection limit, sensitivity, and linear range. Cyclic Voltammetry was used to prove the superior electro-catalytic activity of (GO/g-C_3N_4). Performance of the GO/g-C_3N_4 modified glassy carbon electrode (GCE) was compared g-C_3N_4 /GCE, in a N_2 -purged 0.05 M phosphate buffer solution.

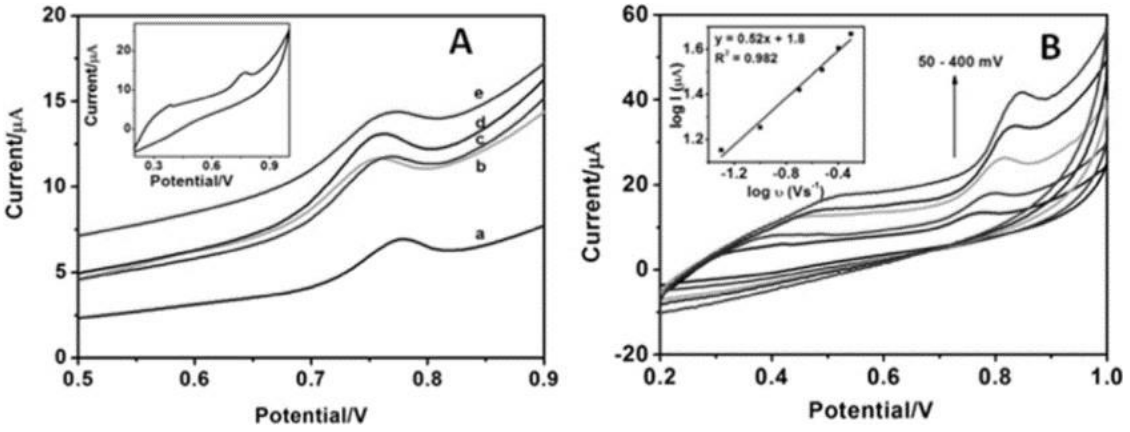

Figure 2.4 A) Anodic scan of CVs of 50μM CBZ at a) bare SPCE, b) Sno2; B) CVs obtained at different scan rates [112]

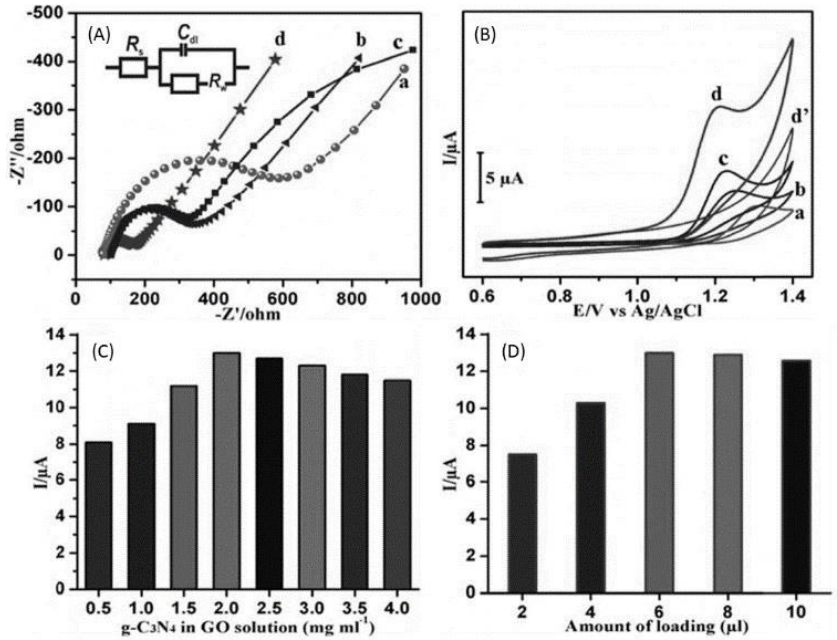

Figure 2.5 A) EIS spectrum of bare GCE (a), g-C3N4/GCE (b), GO/GCE (c), and GO/g-C3N4/GCE (d). (B) CVs of bare GCE (a), g-C3N4/GCE (b), GO/GCE (c), and GO/g-C3N4/GCE (d) in 0.05 M PBS (pH 7) containing 20 μM CBZ and GO/g-C3N4/GCE (d') absence of 20 μM CBZ at scan rate of 50 mVs-1. (C) Anodic current response of 20 μM CBZ on various amount of g-C3N4 loaded GO. (D) The effect of loading amount of GO/g-C3N4 composite on GCE [114]

The working electrode had excellent electro-catalytic activity with an overpotential of only 0.1 V. and attained the best rate of the electron transfer as can be seen in Figure 2.6. Furthermore, an Amperometric assay calculated the LOD of CBZ on the modified electrode along with the sensitivity to be 10.5 nM and 1.727 μA $\mu M^{-1} cm^{-2}$ respectively.

Lin et al. [113], developed a biosensor to find serum levels of CBZ in rabbits. This was accomplished using DPV with GCE as the WE. Initially, dropping mercury electrodes were to be used; however, mercury is not only toxic to the environment but can also enter the human body by inhalation or ingestion, potentially resulting in acute mercury intoxication, which can manifest as chills, chest pain, dyspnea, and pulmonary infiltration, or chronic mercury intoxication, which can cause tremors, social withdrawal, irritability, perspiration, rash, and paresthesia [117]. Furthermore, pre-treatment of the test samples with acetonitrile was crucial to maintain a good performance of the DPV method which would be affected by the presence of N, S, or O the common elements in serum. Blood samples from rabbits that were fed CBZ were obtained and added to a 3-electrode setup containing a GCE as the WE, a platinum wire as CE, and an Ag/AgCl, KCl as RE. Different concentrations of CBZ were tested: 4, 8, 12 μg/mL. The detection limit was 0.14 μg/mL for the DPV technique. For comparison reasons Lin also performed the FPIA method which resulted in a detection limit of 0.2 μg/mL. The correlation between the CBZ concentrations from DPV compared with those by FPIA was good (R-squared value = 0.998). Lin concluded that the electrochemical sensor had a superior detection limit, precision and accuracy compared to FPIA.

In a work similar to Lin, Wang, et al. [40], also developed a biosensor for the determination CBZ levels in serum using DPV and a bare GCE as the WE. Furthermore, the performance of the sensor was also compared with FPIA. The tested samples were prepared in 7 different concentrations (0, 2, 4, 8, 12, 20 and 23.6 μg/mL) by dissolving CBZ in 0.1 M tetrabutylammonium perchlorate/ACN (Figure 2.7). The DPV parameters were the following: pulse amplitude: 50 mV; pulse width: 0.05 sec; sample width: 0.0167 sec; pulse period: 0.2 sec; scan rate: 20 mV/sec. The LOD was 1 μg/mL for the DPV technique however was 0.5 μg/mL for the FPIA. Despite the fact that fluorescence polarization immunoassay performance exceeded DPV in Wang's work, the performance of the DPV technique was within the Food and Drug Administration guidelines for bioanalytical methods, which ensures the clinical applicability of the DPV technique.

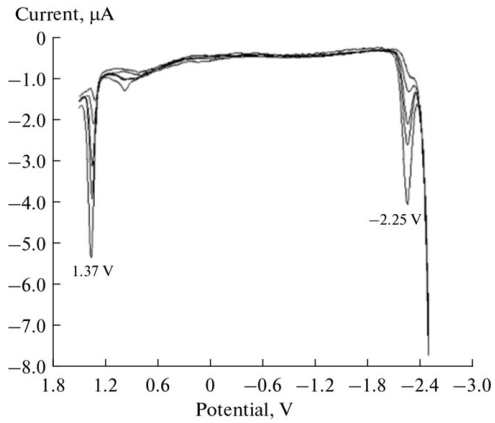

Figure 2.6 Typical DPV potential of CBZ in serum developed at +1.37 V and -2.25 V [40]

Finally Pan et al. [118] confirmed the reliability of DPV for measuring CBZ levels in human serum. The latter used a GCE with the following setup parameters: DPV pulse amplitude, 50 mV; pulse width: 0.05 sec; sample width: 0.0167 sec; pulse period: 0.1 sec; and scan rate: 20 mV/sec. Again, the correlation between the results obtained by the DPV technique and the FPIA technique were very good with a R-squared value of 0.998 (Figure 2.8).

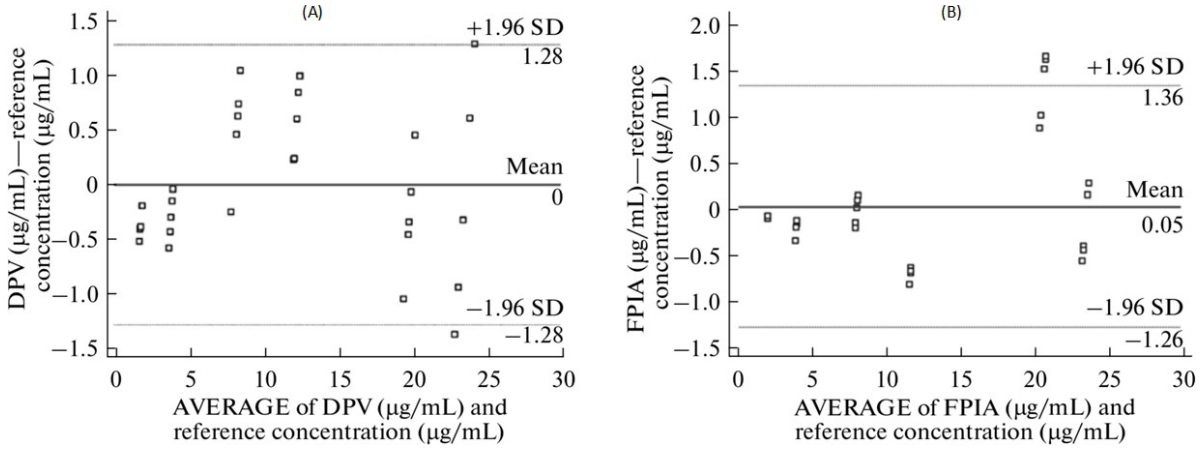

Figure 2.7 (A) Bland-Altman plots of the DPV results and reference value concentrations. The solid line represents the mean difference, and the dashed line represents 1.96 SD; (B) Bland-Altman plots of the FPIA results and reference value concentrations. The solid line represents the mean difference, and the dashed line represents 1.96 SD [40]

2.3 The Biosensing Element

In the context of biosensors, a receptor is used to aid in analyte detection; it is often immobilized on the transducer's surface to specifically bind to the target analyte, or a molecule related that target. Generally, bioreceptors include a vast category of molecules including enzymes, polymers, nucleic acids, proteins, and aptamers; however, given the paper is limited to ASM bioreceptors, the sections below will only cover bioreceptors utilized for ASM detection. According to the reviewed papers, ASM bioreceptors utilized in recent research centralize around antibodies [119-125] or MIPs [126-133].

2.3.1 Antibody-Based Bioreceptors

The concept of antibodies generated from the field of immunoassays which relies on the selective binding and high affinity of the antigen to the antibody. Not only have antibodies been incorporated on large-scale ASM sensing systems, but their use has migrated towards nanoscale systems such as microelectrodes, microcantilevers and miniature microfluidic systems. In his research, Huang [21] added PHT-antibodies to his piezoresistive microcantilever beam for PHT detection. The antibodies were incorporated into a microfluidic channel where analytes can enter and bind to the receptors. The use of a microfluid channel enhanced detection by filtering out unwanted particles, thus enabling the PHT particles to solely enter and bind to the antibodies. The binding yielded a deflection and thus an associated resistance change due to the molecular recognition. This change in resistance was then measured to interpret variations in PHT levels. The sensor had a linear detection response ranging from 10 to 80 μg/mL with a signal resolution of 0.005 Ω and a sensitivity of 2.94 x 10-6 μg/mL.

In a similar research, Huang [134] utilized VPA selective antibodies which allowed the detection of a different drug, VPA. The VPA sensor had a calculated LOD of 45 μg/mL, and a measured drug-antibody binding affinity of around 90 ± 21 μg/mL. Both biosensors were label-free and were compared to FPIA measurements of PHT/VPA in bovine and were shown to yield comparable results in the relevant clinical concentrations. Huang's research demonstrates the versatility of piezoresistive microcantilevers where all that is required is a change of the bioreceptor used. Figure 2.9 demonstrates the side-view of the biosensor and the various layers that were used in its construction.

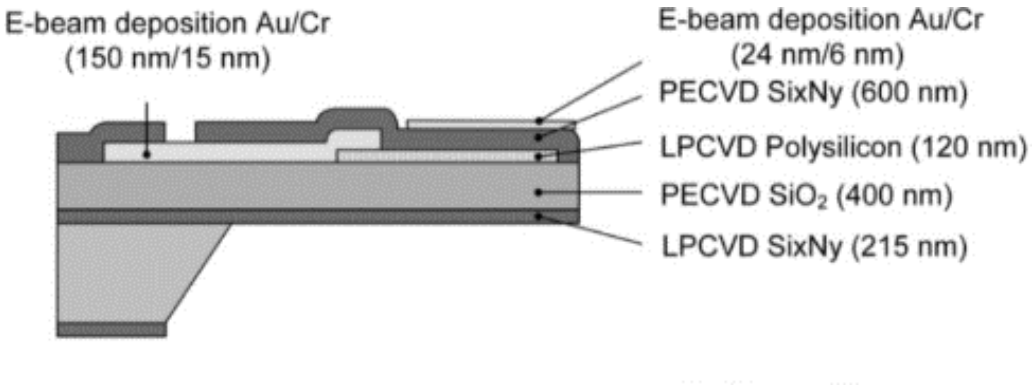

Figure 2.8 Fabrication process of a piezoresistive microcantilever sensor [134]

In an antibody-based detection sensor, Yang, et al. [125] reported the detection of CBZ, PHT, and VPA in serum utilizing a Cloned Enzyme Donor Immunoassay (CEDIA). To perform concurrent detection, they fabricated a multi-well ImmunoChip by xurography. The ImmunoChip surpasses conventional analytical devices by requiring small volume of samples, and being smaller in size due to automated manufacturing. CEDIA is an immunoassay technique where the reaction requires the addition of two separately inactive antibody-fragments. Once added together, these inactive fragments form an active antibody ready to bind to the target analyte. This procedure does not need any separation steps since fragments are initially inactive. To proceed with detection, Yang mixed ASM spiked serum samples with the first CEDIA reagent. The second CEDIA reagent was then immediately added to the solution. Once mixed, the mixture was transferred to the multi-well ImmunoChip containing freshly Beta-Glo reagent solution. Once exposed to a bright luminescent signal, graphs of relative light intensity versus ASM concentrations were generated. Although the LOD and LOQ was not specified, Yang provided evident graphs that relative light intensity varied over the range of ASM concentration. Furthermore, the highest calculated coefficients of variation intra-assay and inter-assay, were reported to be 6.9 % and 9.3 % for CBZ, 5.3 % and 9.6 % for PHT, and 5.6 % and 9.2 % for VPA.

2.3.2 MIP-Based Bioreceptors

As a cheap alternative to natural antibodies, MIPs have been widely researched [135-137]. MIPs are chemically synthesized molecules designed to mimic the behavior of antibodies. They typically

involve a monomer, a porogen, a cross-linker, an initiator, and the template of interest. Once the MIP is polymerized across the template, the template is removed to leave a gap which resembles its structure. This gap is similar to the target template and has an affinity to bind to a molecule with similar structure. MIPs have proven to be robust, slightly affected by pH variations, reproducible, simple to fabricate, and most importantly cheap. It is however important to determine the initiating reagents proportions and conditions to synthesize functional MIPs.

Since MIPs are robust, it is relevant to explore their usage in electrochemical based systems which highly rely on the immobilization of biosensing molecules on the electrode's surface. Commercially available electrodes are often expensive and lack selectivity, hence, it is necessary to fabricate application specific electrodes. These application specific electrodes differentiate from the aforementioned by the ease of fabrication, reproducibility, and strong affinity towards the analyte. To achieve these characteristics, MIP are added to the electrode's setup.

Gholivand et al. developed an electrochemical MIP-based biosensor for the selective detection of LTG [135]. MIPs were fabricated using a non-covalent molecular imprinting approach. After polymerizing, LTG was extracted from the polymers by soxhlet extraction; tetrahydrofuran was used and the removal of the template. The LTG-free MIP was then immobilized on the carbon paste electrode (CPE) and CV was performed. In order to confirm the ability of MIPs to bind to LTG it was compared to an electrode immobilized with non-imprinted polymers (NIPs) along with a bare CPE. NIPs have been prepared similarly to MIP without the addition of a template. CV graphs in Figure 2.10 show that MIP-CP had the highest current response, validating the selective detection of LTG.

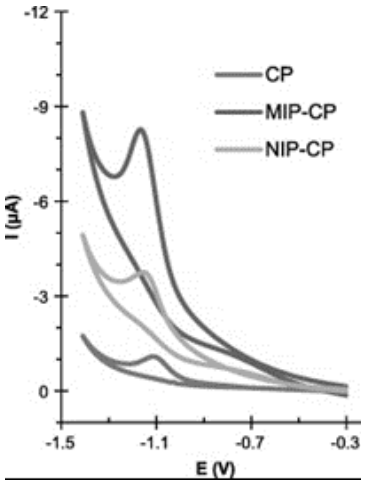

Figure 2.9 Cyclic voltammograms of different electrodes immersed in the 1.0 x 10^{-6} M LTG solutions after 7 min preconcentration. Determination conditions: acetate buffer pH = 5.5 and scan rate 100 mV/sec [135]

The selectivity of the designed MIP-based CP electrode through DPV was further evaluated by inserting the electrodes into aqueous solutions of LTG and LTG similar compounds. Figure 2.11(B) shows a distinct response to LTG when compared to LTG-similar compounds, unlike Figure 2.11(A) and Figure 2.11(C) were no significant LTG-related response could be concluded. Furthermore, the sensor's response was linear throughout LTG concentrations of 0.8-25 nM and 25-400 nM with a calculated LOD of 0.21 nM.

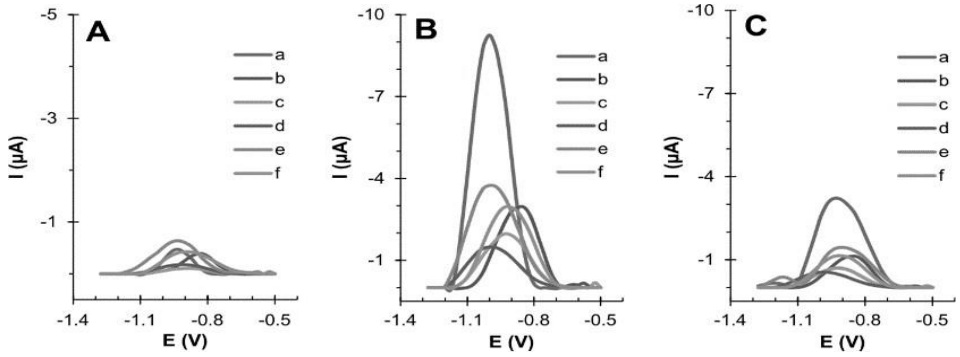

Figure 2.10 The DPV response of sensors based on a (A) CPE, (B) MIP-CPE and (C) NIP-CPE immersed in solutions containing LTG and LTG similar compounds [135]

Furthermore, MIPs have replaced antibodies and other expensive biosensing elements in chromatography-based methods. Hoshina, et al. [136] developed a MIP-based biosensor for the successive determination of four different ASMs. Rather than utilizing an electrochemical approach, they combined MIPs as biosensing elements with a chromatography-based detection method. In order to study the effect of different monomers on functionality of the imprinted polymers, polymerization was tested with MAA, 2-VP and 4-VP as monomers. It was found that the 4-VP based polymer exhibited the best selectivity when compared to other monomers. Drug induced samples were pre-treated prior to chromatographic analysis by passing through a MIP packed column, then into the analytical column. 2 mM ammonium acetate-ACN (60:40, v/v) was then administered at a flow rate of 0.2 mL/min. The proposed method was both accurate and reproducible and graphs of peak area ratio versus ASM concentrations were linear with a correlation of > 0.999. Furthermore, LOD and LOQ were as follows: PHB 15 and 5.0 ng/L, amobarbital 8.0 and 2.0 ng/L, and PHT 2.0 and 0.50 ng/L.

2.4 Discussion and Conclusion

ASMs are given as a treatment to control seizures; therefore, detecting optimal dosage on purely clinical grounds can be difficult. Furthermore, continuous ASM monitoring rises as a necessary technique to optimize patients' outcome and providing them with a safe course of treatment. TDM is currently performed in centralized laboratories equipped with bulky instruments, such as immunoassay analyzers and mass spectrometry, which can be used by trained personnel only. Particularly HPLC-MS, is routinely used in core facilities.

The financial costs related to instrumental operation and maintenance, and the time required for the preparation and analysis of samples, for processing the results, affects the application of TDM in medical practices. Therefore, a new generation of analytical tools, capable of providing rapid, sensitive, and reliable diagnosis, is necessary to respond to the timely need of drug control aiming at effectively treating epileptic patients.

Table 2.5 Various drug transducing and sensing systems along with their LOD, selectivity, linear range, and complexity

Ref.	Tran.	Sens.	Drug	LOD	Sel.	L.R.	Com.
[17]	RP-HPLC	-	PHT	1.44 μg/mL	High	PHT:10-30 mg/L; phenobarbitone 3-9 μg/mL	High
[101]	SPR	Antibodies	PHT	50 nM	High	-	High
[109]	CV and SWV	NPs	CBZ	0.34 μM	Low	0.5-100 μM	moderate
[113]	DPV	MWCNT/ Pt-NPs	PHB	0.1 μM	Low	0.4-60 μM	Low
[40]	DPV	-	CBZ	1 μg/mL	Low	-	Low
[40]	FPIA	-	CBZ	0.5 μg/mL	High	-	High
[21]	PM	Antibodies	PHT	9.5 μg/mL	High	10-80 μg/mL	High
[134]	PM	Antibodies	VPA	45 μg/mL	High	50-500 μg/mL	High
[135]	DPV	MIP	LTG	0.21 nM	High	0.8-25 and 25-400 nM	moderate
[114]	CV	GO-g-C3N4	CBZ	10.5 nM	Low	0.092-266 μM	Low
[138]	HPLC-ES-MS/MS	Protein	LTG, LEV, Primidone	50 μg/mL	High	-	High
[139]	UA-DES-LPME/HPLC–UV	-	CBZ	1.7 μg/L	High	5-200 μg/L	High
[140]	Amperometry	$NiSe_2$	CBZ	18.2 nM	Low	50nM -10 μM	Low
[141]	ICA	Antibody	CBZ	2.5 ng/mL	High	-	High

PM: Piezoresistive Microcantilever; IRTD: Iron doped tin dioxide ; UA-DES-LPME/HPLC-UV: Ultrasound-Assisted Deep Eutectic Solvent-Based Liquid-Phase Microextraction Method for HPLC–UV; ICA: Immunochromatographic assay.

With all the various assets brought forward by detection techniques, it is often hard to specify an optimal solution. Vastly developing transducing techniques along with biosensing elements are spiraling towards sensitive, accurate, label-free, cheap, and easy to operate biosensors. Because ASMs have a narrow therapeutic range, are often administered as a form of poly-treatment, and are susceptible to high toxicity reactions, ASM detection biosensors must be sensitive but also highly selective to eliminate or decrease the effect of unwanted particles. Hence, it is necessary to combine the advantages offered by both transducing and biosensing elements to produce the desired outcome. Table 2.5 sums up the common biosensors employed for ASMs detection or monitoring.

The main detection techniques regarding PHT and PHB determination have focused on techniques such as: a piezoresistive cantilever combined with the immobilization of biomolecular receptors operating as biosensing elements; electrochemical DPV using a multi-walled carbon nanotube modified Pt electrode; and HPLC combined with UV spectroscopy. For LEV, the main detection technique is HPLC-ES-MS/MS coupled with immobilized protein for selective detection. Furthermore, VPA main detection techniques are mostly piezoresistive microcantilever combined with antibody immobilization. Finally, most CBZ detection sensors are electrochemical based combined with chemically modified working electrodes. It is justifiable to say that no specific biosensor has yet been employed to detect multiple ASMs without the need for bulky equipment, sample pre-conditioning, or specialized clinicians. By examining the existing techniques provided in Table 2.5, it is possible to choose one detection technique that may be integrated into a miniature, label-free, economical, easy to operate, and accurate biosensor. Although not the most sensitive or selective, electrochemical transducing techniques such as CV, DPV, SWV, and EIS are the simplest to operate, enable label-free detection and fast response times. Combined with MIPs surface immobilized electrodes, electrochemical biosensors could become highly selective and suitable for multi ASM detection. Furthermore, using appropriate dopants or by adding graphene or carbon nanotubes, electrodes could also become highly conductive, thereby increasing the sensitivity of the sensor.

CHAPTER 3 CBZ DETECTION BY ELECTRICAL IMPEDANCE SPECTROSCOPY

3.1 Overview

In chapter 2, we described the most recent ASM detection systems by highlighting their respective biosensing and transducing elements. When designing an ASM detection biosensor, it is important to opt for the optimal combination of biosensing and transducing elements. The latter mainly affect signal quality and accuracy of the biosensor whereas biosensing elements achieve selectivity towards the analyte of interest. All aforementioned transducing elements present good signal quality and high accuracy. Particularly, electrochemical methods turn out to be least destructive, easiest to operate and suitable to be integrated on a miniature implantable chip.

Following this observation, the present chapter presents a CMOS circuit capable of performing EIS along with *in vitro* measurements conducted using a commercial potentiostat and gold electrodes. This work was published at the 38th annual international conference of the IEEE Engineering in Medicine and Biology Society (EMBC), 2016.

Citation: **Abbas Hammoud**, Ahmad Chamseddine, Dang K. Nguyen and Mohamad Sawan, "Towards an implantable bio-sensor platform for continuous real-time monitoring of anti-epileptic drugs." 2016 38th Annual International Conference of the IEEE Engineering in Medicine and Biology Society (EMBC). IEEE, 2016.

3.2 Article 1: Towards an Implantable Bio-Sensor Platform for Continuous Real-Time Monitoring of Anti-Epileptic Drugs

Abbas Hammoud[1], Ahmad Chamseddine[1], Dang K. Nguyen[2], and Mohamad Sawan[1]

[1]Polystim Neurotech Laboratory, Electrical Engineering Department, Polytechnique Montreal

[2]Notre Dame Hospital, CHUM, Université de Montréal

IEEE Engineering in Medicine and Biology Society (EMBC), August 2016

3.2.1 Abstract

The need of continuous real-time monitoring device for *in vivo* drug level detection has been widely articulated lately. Such monitoring could guide drug posology and timing of intake, detect low or high drug levels, in order to take adequate measures, and give clinicians a valuable window into patients' health and their response to therapeutics. This paper presents a novel implantable biosensor based on impedance measurement capable of continuously monitoring various antiepileptic drug levels. This portable point-of-care microsystem replaces large and stationary conventional macro-systems, and is a one-of-a-kind system designed with an array of electrodes to monitor various anti-epileptic drugs rather than one drug. The micro-system consists of (i) the front-end circuit including an inductive coil to receive energy from an external base station, and to exchange data with the latter; (ii) the power management block; (iii) the readout and control block; and (iv) the biosensor array. The electrical circuitry was designed using the 0.18-um CMOS process technology intended to be miniature and consume ultra-low power.

Keywords: Micro-system, real-time monitoring, implantable biosensor, *in vivo* detection, antiepileptic drug (AED).

3.2.2 Introduction

Epilepsy is the most common chronic neurological disorder after stroke with a prevalence nearing 1%. Common causes include brain tumors, stroke, head traumas and genetic mutations. Antiepileptic drugs (AEDs) are the first line of treatment and most patients will need to take them daily over an extended period of time or for their whole life. After absorption, these AEDs will eventually reach a peak level (point where theoretically the patient is most protected against a seizure and when the risk of dose-related side effects is highest) and then gradually decrease to a trough level (when protection against seizures is lowest). Measuring AED levels in the bloodstream or tissue in vivo would give clinicians a valuable window into patients' health and their response to therapeutics. This device could allow for example: a) a better understanding of (intra- or inter-individual) drug level variations whether it be over 24h, days, weeks or years, at various ages, during certain concomitant physiological or pathological conditions; b) a comprehensive assessment of non-adherence by patients (which could be as high as 30-60% according to some studies); c) a thorough causality assessment between drug levels and side effects

or seizure protection; d) a better assessment of the impact of switching from brand-name to generic AEDs.

There are various monitoring techniques utilized for AED detection including high performance liquid chromatography [1], gas chromatography [2], capillary chromatography [3], chemiluminescence [4], spectrometry [5], and amperometry [6], most of these techniques cannot be reproduced in portable devices, are time-consuming and rely on heavy apparatus. Thus, arises the need for a miniature, portable, and point-of-care biosensor enabling the continuous monitoring of those AEDs.

Electrical Impedance Spectroscopy (EIS) is one method performed in impedance measurement systems and has been widely used for applications such as bio-molecular, DNA, metabolites and cancer cell detection. EIS provides precise and fast impedance measurements with variations in electrode's surface. Once extrapolated, measurements are then utilized in order to detect, or specify changes in fluid concentration. However, none of existent EIS based impedance systems offer continuous detection of AEDs. Therefore, we propose the utilization of EIS as a method for the detection of AEDs.

Indeed, our group has found that carbamazepine, a drug widely used in the treatment of seizure disorders [8], has a significant effect on impedance. Impedance measurements conducted using a VMP-300 potentiostat at Polystim Labs have signified that impedance decreases with the increase of carbamazepine concentration. EIS also revealed different impedance spectra with different concentrations of AEDs.

Compared to other techniques such as voltammetry and amperometry, EIS is a more promising technique due to its precision, the ability to detect a much wider variety of particles not necessarily electroactive ones and little to no variation or damage to analyte measured. Two challenges with EIS are the need to adjust the potential of operation outside the oxidation/reduction window of unwanted particles, and the need of finding functionalized electrodes for the specific detection of the drug to be measured. This ensures that unwanted particles have minimal to zero effect on our measurements.

The proposed implantable micro-system consists of four components: (i) the front-end circuit including an inductive coil to receive energy from an external base station, and to exchange data with the latter; (ii) the power management block; (iii) the readout and control block; and (iv) the

biosensor array consisting of the fabricated ion-selective functionalized electrodes. The implantable bio-system will consume ultra-low power, display high sensitivity to AED level variations and wirelessly transmit these AED concentrations to a user's smart device (base station).

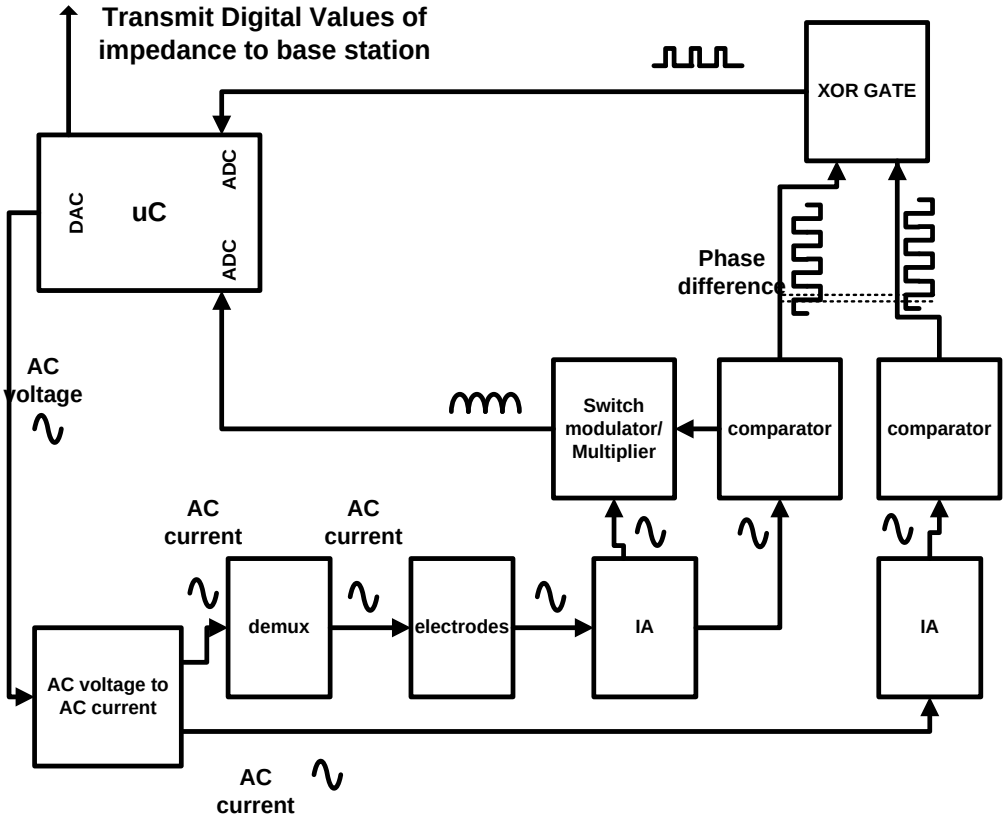

Figure 3.1 Proposed Impedance Measurement Biosensor Block Diagram

3.2.3 Biosensor Block Diagram

The complete block diagram of the proposed biosensor is presented in Figure 3.1. The microcontroller will be used to generate an AC voltage which will then be changed into an AC current to be sent to its respective electrode. Once excited, the voltage across the electrode with reference to the reference electrode will then be amplified and multiplied by its corresponding square form generated through a fast comparator. This results in the magnitude of impedance measured across the electrode's surface. The microcontroller offers a variety of amplitudes and frequencies to be adjusted according to the drug to be measured. As for the phase, the comparator

generated square wave of the voltage across the electrode will be compared with that of the original signal. This difference generated by a XOR gate will resemble the phase of our impedance.

3.2.4 Impedance Measurement Circuit

The EIS system chosen to be integrated on the implantable biosensor was proposed by P. Kassanos, I. F. Triantis, and A. Demosthenous in [7]. Figure 3.2 presents a CMOS magnitude/phase measurement chip. This technique extracts both the phase and the magnitude of the voltage across the particles tested. After applying a differential alternating current through a pair of surface electrodes to the body tissue, the resulting voltages across the unknown impedance and the known current-sense resistor (RIsense) are measured by two instrumentation amplifiers and then converted into square waves using two comparators. A XOR gate then produces a pulse signal, with the pulse width representing the phase delay introduced by the unknown impedance at that particular frequency. The square wave generated by the comparator is then used as the clock required by a switch modulator for synchronously rectifying the measured signal which is then low-pass filtered to obtain a full-wave rectified signal dc average voltage.

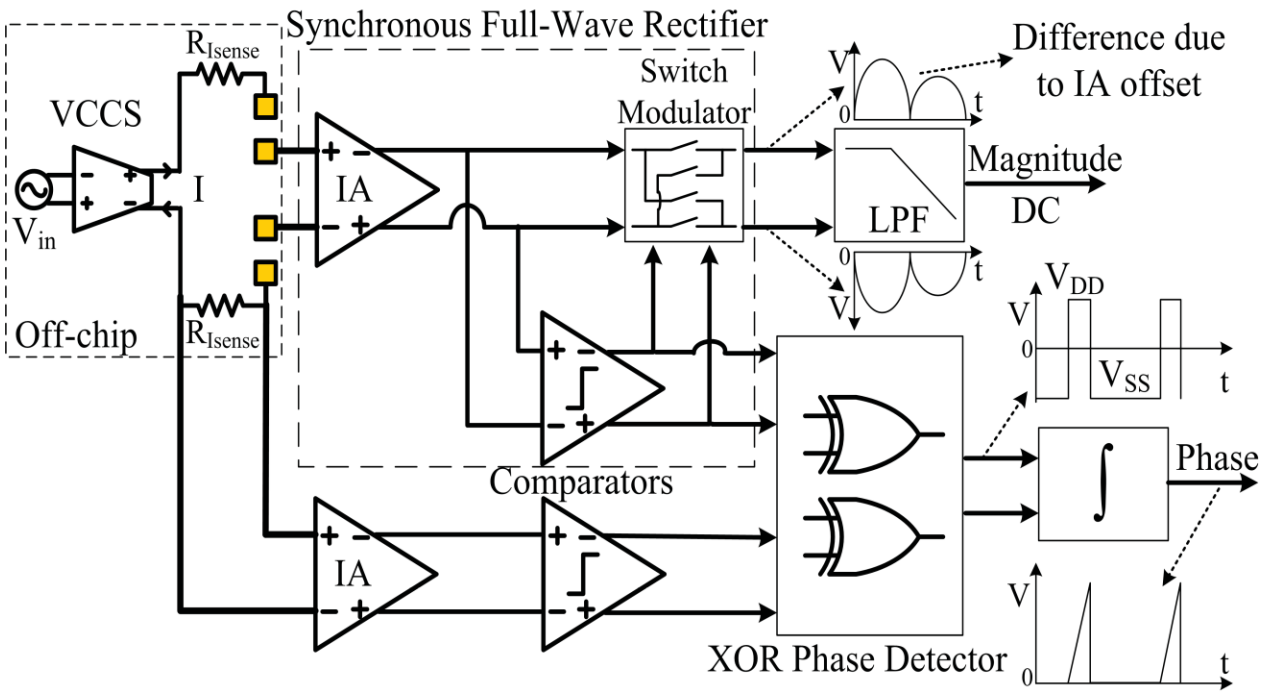

Figure 3.2 Adopted Impedance Measurement Circuit [7]

The phase (ϕ) of the unknown impedance from the output of the phase detector is then calculated by:

$$\phi = 360° \, \Delta t \, f \quad (1)$$

Δt is the pulse width and f is the frequency of the applied signal.

As for the magnitude (M) of the unknown impedance, it could be calculated by:

$$M = \pi * \frac{Vdc}{2 * Av * I} \quad (2)$$

Vdc is the full-wave rectified signal dc average voltage, A_v is the gain of the instrumentation amplifier and I is the amplitude of the injected current.

3.2.4.1 Instrumentation Amplifier (IA)

The main common-mode interference in bio-impedance measurements occurs at the working frequency and is produced by the current injected into the body to make the measurements [8]. The differential signal measured between the pair of electrodes can be as small as a few tenth of a microvolt (μV) whereas the common-mode interference can be in the hundreds of millivolt (mV) range. Therefore, a high gain amplifier with a high common mode rejection is needed in order to amplify such a small measured signal while rejecting as much noise as possible.

There are two basic approaches to the design of an IA: resistive feedback and current feed-back. Both approaches offer good performance, whereas the current-feedback offers higher CMRR because of both isolation and balancing techniques. The IA presented in Figure 3.3, uses a current feed-back topology and is comprised of an input transconductance stage and two output transimpedance stages to render it fully-differential. This design has a variable gain which can be achieved by modifying the ratio of the integrated resistors, which offers us an advantage while varying the range of impedances measured. Additionally, to having a high CMRR, this IA uses a

capacitive neutralization transistor (M0) in order to diminish the mismatch in the drain capacitances of the input pair transistors. As for the output DC voltage of the amplifier, it can be set using a DC voltage source (usually generated using a band-gap voltage reference circuit).

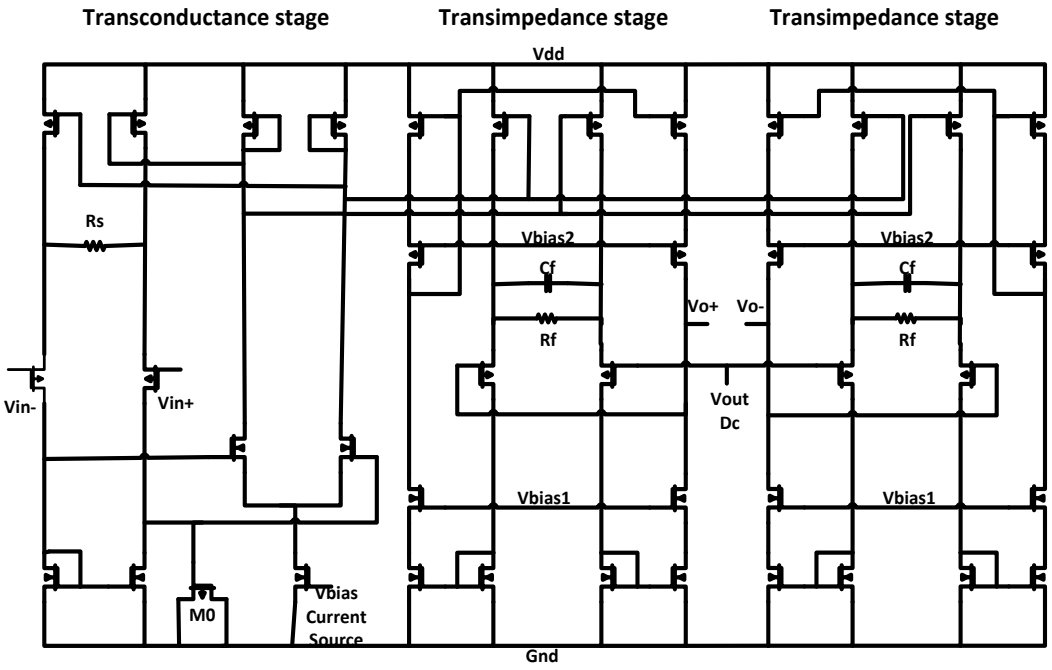

Figure 3.3 CMOS 3-stage Instrumentation Amplifier

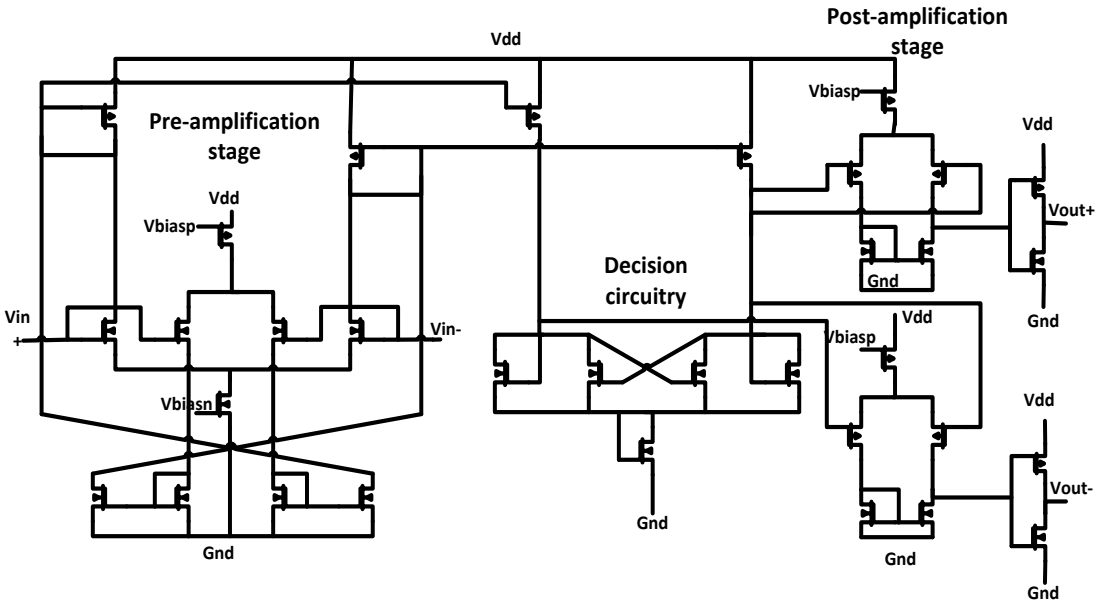

Figure 3.4 CMOS comparator with rail-to-rail input common-mode

The instrumentation amplifier was biased at a current of 37.5uA and an output DC voltage was set to 1.42V in order to be used in the comparator stage.

3.2.4.2 Multi-stage Comparator Circuit

The comparator design is a clock-less continuous time multistage comparator as provided in Figure 3.4. It includes both a PMOS and an NMOS differential amplifier feeding a decision circuit, and the output buffer is a PMOS differential amplifier driving an inverter. In order to be used as a clock for our switch modulator, the comparator must be in-phase with the signal generated from the instrumentation amplifier. The delay of the comparator will introduce an error in the calculation of the magnitude. The equation of multiplying the sine-wave output of the IA with the square wave generated from the comparator is provided below.

$$Vout = \frac{2Vo[\cos(\emptyset) - 2\cos(2\omega t + \emptyset)]}{\pi} \quad (3)$$

By providing a square wave directly in phase with IA sine wave output we remove the additional gain factor of cos(Ø). Therefore, the delay of our comparator needs to be minimized.

3.2.5 Biosensor Array

The biosensor consists of an array of electrodes upon which selectivity could be provided. Various electrodes can be modified in order to offer a certain selectivity towards the drugs, which will enable us to distinctly measure the concentration of the drugs. Such electrodes exist, and are labeled as functionalized electrodes, which exhibit a high sensitivity towards our various drugs. As an example, Graphene-Gold nanoparticle modified electrodes are highly selective to carbamazepine [9] and phenytoin selective electrodes are proposed by M. El-Tohamy [10].

In order to detect the different concentrations, there will be a switching technique which operates the electrodes separately and records the corresponding measurements. This will result in separate measurement of each drug. When necessary, these electrodes can be easily modified to render our

biosensor universal able to detect not only AED levels but lactate and glucose concentrations, dissolved O_2 and pH levels.

3.2.6 Simulation Results

In order to test the operation of the designed circuit, the IA was combined with the comparator as provided in Figure 3.5. A transient analysis was performed while varying the capacitance C and keeping R constant. Both voltage signals were recorded. The first was an amplified sinusoidal voltage signal (Va) generated by the IA, while the other was the square wave signal (Vc) generated by the comparator.

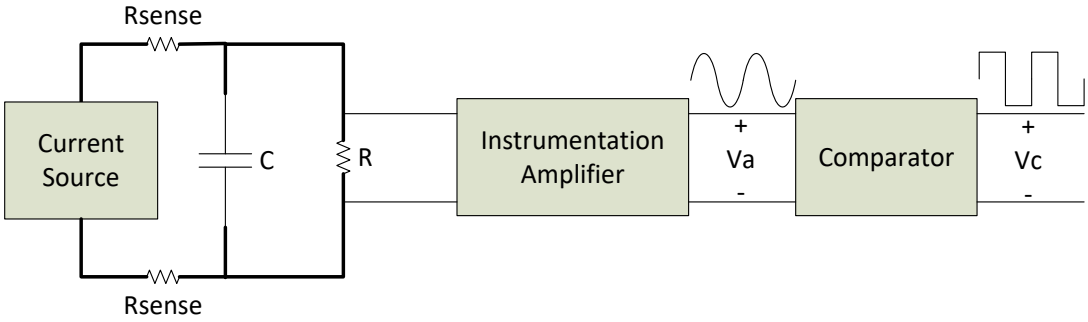

Figure 3.5 Combined IA and Comparator

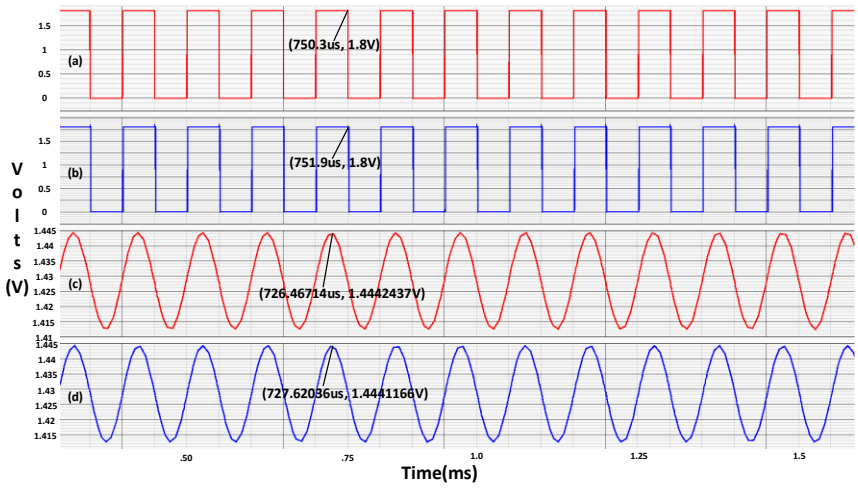

Figure 3.6 Varying C from 1 pF to 100 pF displaying variable amplitude and phase. (a) Square wave at C = 1 pF, (b) Square wave at C = 100 pF, (c) Sine wave at C = 1 pF, (d) Sine wave at C = 100 pF

The capacitance C was changed from 1pF to 100pF in order to test if the circuit can detect any changes in impedance. Effectively, as provided in Figure 3.6, a phase shift was recorded between both square waves (a) and (b), and the amplitude of the sinusoidal waves (c) and (d) varied. The phase shift is due to the increase in voltage lag caused by the capacitor, whereas the change in amplitude refers to the change in the magnitude of impedance measured.

3.2.7 *In vitro* Experimentation

Attempting to monitor the concentration of the AEDs through EIS, requires the drug to alter the impedance of the electrodes surface. This means that a change in concentration of the drugs must result in change in opposition to current flow between the working and counter electrode. In order to test the validity of this assumption we performed *in vitro* tests of impedance versus concentration of drugs.

White carbamazepine powder with a molecular weight of 236.27 was ordered from Sigma-Aldrich and dissolved in Isopropyl alcohol to form concentrations over the range of 5-40 (mg/mL). Impedance measurements were taken by a VMP-300 potentiostat at Biostim laboratories. Such is a multichannel workstation able to perform EIS measurements. A 3-electrode terminal setup was used to validate the concept with a gold working electrode, a platinum counter electrode and an Ag/AgCl reference electrode. These electrodes are used in most basic electrochemical measurement and were provided by EDAQ (ET014 EChem Electrode Kit). A 3-electrode terminal setup was chosen since it offers better measurements when compared to a normal 2-electrode setup; measurement is less affected by residual impedance and contact impedance at low frequencies.

Figure 3.7 represents the system operated on the potentiostat. In electrical impedance spectroscopy a sinusoidal voltage is varied according to both amplitude and current whilst measuring the current and varying drug concentration. The voltage is then divided by the current to generate a graph of impedance versus concentration.

Figure 3.8 provides the *in vitro* graphs generated of impedance versus concentration of carbamazepine, using impedance spectroscopy. A total of 32 measurements were conducted, four measurements for each concentration, with a total of 8 drug concentrations, and the average impedance for each concentration was calculated and plotted. The impedance decreases as

carbamazepine in isopropanol concentration increases. This implies that the drug increases the current flow in the solution; as concentration increases the current opposition decreases yielding a decreased impedance value.

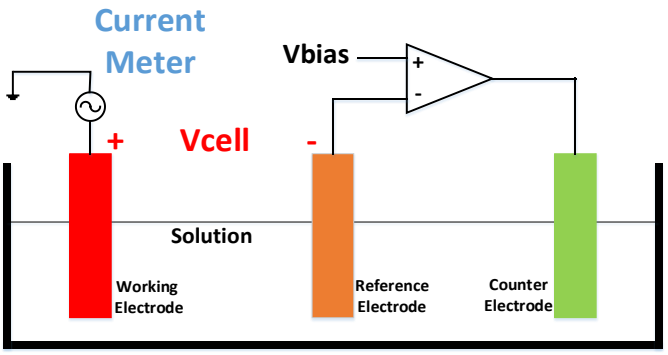

Figure 3.7 Three-Terminal Electrode Setup

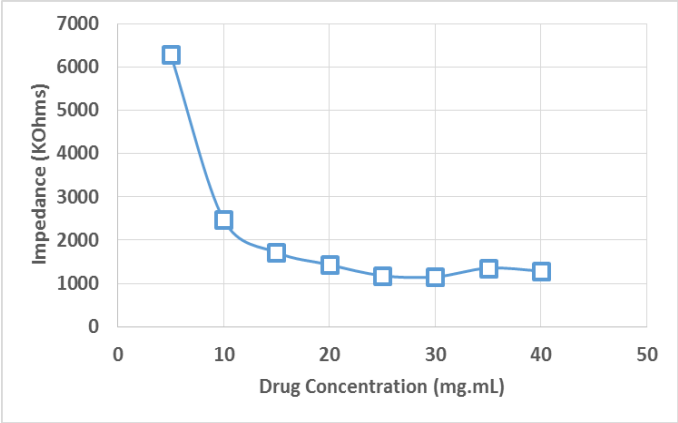

Figure 3.8 Impedance vs. Carbamazepine Concentration

3.2.8 Conclusion

Detection of AEDs using electrical impedance spectroscopy is a promising technique which offers a wide range of detection and precision. Three-electrode setup measurements performed using the potentiostat showed success when detecting the increase of concentration of drugs *in vitro*, and the circuitry designed detected change in impedance through changing the value of capacitance, resistance or inductance. Analog circuit components were designed in cadence 180nm technology

requiring a voltage supply of 1.8V. EIS enables various recording while varying electrodes, and operating ranges enabling the detection of multiple drugs.

3.2.9 Acknowledgments

Authors would like to acknowledge the support of CMC Microsystems and NSERC of Canada.

3.2.10 References

[1] R. Kelmann, G. Kuminek, H. Teixeira, and L. Koester, "Determination of carbamazepine in parenteral nanoemulsions: development and validation of an HPLC method," Chromatographia, vol. 66, pp. 427-430, 2007.

[2] J. C. Durán-Alvarez, E. Becerril-Bravo, V. S. Castro, B. Jiménez, and R. Gibson, "The analysis of a group of acidic pharmaceuticals, carbamazepine, and potential endocrine disrupting compounds in wastewater irrigated soils by gas chromatography–mass spectrometry," Talanta, vol. 78, pp. 1159-1166, 2009.

[3] E. Marziali, M. A. Raggi, N. Komarova, and E. Kenndler, "Octakis-6-sulfato-γ-cyclodextrin as additive for capillary electrokinetic chromatography of dibenzoazepines: Carbamazepine, oxcarbamazepine and their metabolites," Electrophoresis, vol. 23, pp. 3020-3026, 2002.

[4] S. H. Lee, M. Li, and J. K. Suh, "Determination of carbamazepine by chemiluminescence detection using chemically prepared tris (2, 2'-bipyridine)-ruthenium (III) as oxidant," Analytical sciences, vol. 19, pp. 903-906, 2003.

[5] Z. Rezaei, B. Hemmateenejad, S. Khabnadideh, and M. Gorgin, "Simultaneous spectrophotometric determination of carbamazepine and phenytoin in serum by PLS regression and comparison with HPLC," Talanta, vol. 65, pp. 21-28, 2005.

[6] B. Unnikrishnan, V. Mani, and S.-M. Chen, "Highly sensitive amperometric sensor for carbamazepine determination based on electrochemically reduced graphene oxide–single-

walled carbon nanotube composite film," Sensors and Actuators B: Chemical, vol. 173, pp. 274-280, 2012.

[7] P. Kassanos, I. F. Triantis, and A. Demosthenous, "A CMOS magnitude/phase measurement chip for impedance spectroscopy," Sensors Journal, IEEE, vol. 13, pp. 2229-2236, 2013.

[8] A. Worapishet, A. Demosthenous, and X. Liu, "A CMOS instrumentation amplifier with 90-dB CMRR at 2-MHz using capacitive neutralization: Analysis, design considerations, and implementation," Circuits and Systems I: Regular Papers, IEEE Transactions on, vol. 58, pp. 699-710, 2011.

[9] S. Pruneanu, F. Pogacean, A. R. Biris, S. Ardelean, V. Canpean, G. Blanita, et al., "Novel graphene-gold nanoparticle modified electrodes for the high sensitivity electrochemical spectroscopy detection and analysis of carbamazepine," The Journal of Physical Chemistry C, vol. 115, pp. 23387-23394, 2011.

[10] M. El-Tohamy, S. Razeq, M. El-Maamly, and A. Shalaby, "Construction of different types of ion-selective electrodes and validation of direct potentiometric determination of phenytoin sodium," Open Chemistry, vol. 8, pp. 937-945, 2010.

CHAPTER 4 CBZ SELECTIVE ELECTRODE DESIGN

4.1 Overview

In chapter 3 we reported an electrical impedance CMOS design with the potential of being integrated within a biosensor for the electrochemical detection of CBZ. Furthermore, *in vitro* tests were conducted to analyze the effect of CBZ concentrations on the electrical impedance of gold electrodes. Despite its promising calibration curve, EIS alone does not permit the selective detection of CBZ with a complex medium. We hypothesize that interfering drugs or substances would greatly affect the electrode's surface impedance and deteriorate the noise-to-signal ratio of our sensor. Hence, it was necessary to design special electrodes capable of selectively binding to CBZ molecules prior to quantification. To address the limitations of the device proposed in chapter 3, this chapter reports the design and fabrication of electrodes engulfed by a molecular imprinted polymer capable of selectively binding to CBZ molecules. This work was published at Biosensors and Bioelectronics, 2021.

Citation: **Abbas Hammoud**, Danny Chhin, Dang K. Nguyen and Mohamad Sawan, "A new molecular imprinted PEDOT glassy carbon electrode for carbamazepine detection." Biosensors and Bioelectronics 180 (2021): 113089.

4.2 Article 2: A New Molecular Imprinted PEDOT Glassy Carbon Electrode for Carbamazepine Detection

A Hammoud[a,*], D Chhin[b], D K Nguyen[c] and M Sawan[a,d]

[a]Department of Electrical Engineering, Polytechnique Montréal, Montréal, QC, Canada

[b]Département de chimie, UQAM, Montréal, QC, Canada

[c]Centre Hospitalier de l'Université de Montréal, Université de Montréal, Montréal, QC, Canada

[d]School of Engineering, Westlake University, and Westlake Institute for Advanced Study, Zhejiang, China

Biosensors and Bioelectronics, February 2021

4.2.1 Abstract

An electrochemical sensor for the detection of carbamazepine was fabricated by the electropolymerization of PEDOT on glassy carbon electrodes. Molecular imprinted polymer sites were synthesized by cyclic voltammetry on the electrodes' surfaces providing high selectivity and sensitivity towards carbamazepine molecules. Scanning electron microscopy validated the formation of the polymer. Extraction of carbamazepine from the polymer was performed by immersion in acetonitrile and validated by ultraviolet-visible spectroscopy along with cyclic voltammetry experiments comparing pre- and post-template extraction data. Further cyclic voltammetry and square-wave voltammetry tests aided in characterizing the electrodes' response to carbamazepine concentration in PBS solution with $[Fe(CN)_6]^{3-/4-}$ as a redox pair/mediator. The limits of detection and quantification were found to be 0.98 x 10^{-3} M and 2.97 x 10^{-3} M respectively. The biosensor was highly sensitive to carbamazepine molecules in comparison to non-imprinted electrodes, simple to construct and easy to operate.

Keywords: Sensor, Antiepileptic drug, PEDOT, Electropolymerization, Molecular imprinted polymer.

4.2.2 Introduction

Carbamazepine (CBZ) 5H-Dibenzo[b,f]azepine-5-carboxamide is amongst the most used antiepileptic drugs (AEDs) for the treatment of epilepsy. In the routine management of epileptic patients, physicians frequently sample CBZ blood concentration for various reasons such as to a) ensure sufficient dosage in the patient; b) assess treatment adherence or compliance; c) avoid overshoot of dosing and development of overt clinical toxicity. Blood levels are particularly important in the context of patients that are elderly, pregnant, have co-morbid conditions such as liver disease, or take several medications that interact with each other.

As such, the development of a potentially implantable miniature biosensor for continuous monitoring of CBZ would give clinicians a valuable window into patients' health and their response to therapeutics by correlating serum CBZ concentrations with their clinical condition.

Biosensors are nowadays ubiquitous in biomedical diagnosis as well as a wide range of other areas such as point-of-care monitoring of disease treatment or progression [1], environmental monitoring [2], food quality control [3], drug discovery [4], forensics and personalized treatment [1, 5]. They

essentially involve the quantitative analysis of various substances by converting their biological properties into measurable signals. The performance of a biosensor is mostly dependent on the specificity and sensitivity of the biological reaction, which is highly determined by the sensor's biosensing and transducing elements.

To date, only a handful of biosensors have been reported for AED detection. Furthermore, CBZ biosensors often lack selectivity, require bulky equipment and special treatment rendering *in vivo* detection illusory.

Reported studies of CBZ detection include techniques such as high-performance liquid chromatography (HPLC) [6, 7, 8], spectrophotometry [9, 10], cyclic voltammetry (CV) [11, 12], differential pulse voltammetry (DPV) [13, 14, 15], and amperometry [16, 17]. Amongst the aforementioned techniques, those based on electrochemical detection (such as CV, DPV or amperometry) are utilized in a wide range of applications in medical, biological and environmental analyses due to their excellent speed, simplicity, low-cost and the potential of being integrated within implantable devices.

Despite their excellent characteristics, electrochemical based detection systems often lack sensitivity and selectivity. Consequently, sensitivity has been improved by altering the electrode's surface prior to template detection using different material such as graphene-gold nanoparticles [11, 12], iron doped tin dioxide nanoparticles, and graphene oxide-g-C3N4 composite films to increase surface conductivity and thus enhancing sensitivity [17]. On the other hand, to permit the selective detection of CBZ, molecular imprinted polymers (MIPs) have been utilized [18, 19, 20]. MIPs have proven to be robust, slightly affected by pH variations, reproducible, simple to fabricate, and most importantly, cheap. They are molecules designed to mimic the behaviour of antibodies.

Once the MIP is polymerized across the template, the template is then removed to leave a gap which resembles its structure. This gap is similar to the target template and has an affinity to bind to a molecule with a similar structure.

Chemically synthesized MIPs have outstanding characteristics: they have high sensitivity, are robust, are easy to prepare, and can be produced in bulk. However, they are difficult to immobilize on the electrode's surface never mind control their thickness. An alternative method involves preparing MIPs through electropolymerization which permits the formation of a MIP layer directly on the electrode's surface while controlling its thickness through the regulation of the

electrochemical conditions (e.g. applied voltage, monomer concentration, etc). Electrochemical polymerization requires less time, less expertise, and costs less than additional polymerization. The most reported electropolymerized polymer for drug or bio-particle detection has been pyrrole [21, 22, 23, 24]. On the other hand, poly(3,4-ethylenedioxythiophene) (PEDOT) has been reported to have superior conductivity, increased stability, lower density and operating voltages [25]. In its doped state, PEDOT's conductivity is one order of magnitude higher than that of polypyrrole (PPy). Furthermore, its highly stable oxidized state maintains its conductivity for several months even at high temperatures [26, 27].

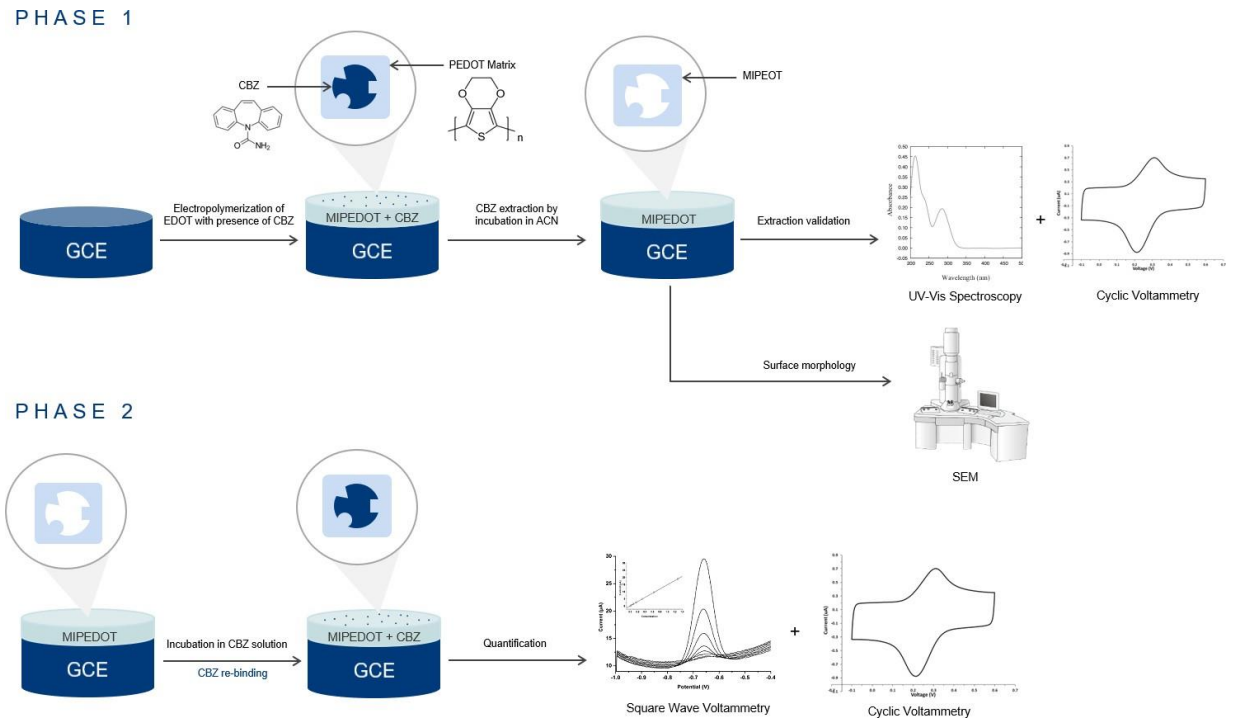

Figure 4.1 Schematic illustration of experimental protocol

In the present study, a selective electrochemical sensor for the detection of CBZ was developed based on molecular imprinting of PEDOT and PPy. PEDOT was found to have superior electrical qualities than that of PPy. As provided in Figure 4.1, in phase one of our experiment, molecular imprinted PEDOT (MIPEDOT) was prepared on GCE. Furthermore, scanning electron microscopy (SEM) images were taken to observe the sensor's morphology. Additionally, CBZ extraction validation was conducted through ultraviolet–visible (UV-vis) spectroscopy along with CV. In

phase 2, CV measurements along with SWV were conducted to study the effect of CBZ concentration on the electrochemical response of the molecular imprinted PEDOT modified glassy carbon electrode (MIPEDOT-GCE). All characterization measurements were conducted in a phosphate buffered saline (PBS) solution. To assess the effect of CBZ on the current response of the sensors, a redox couple of $[Fe(CN)_6]^{3-/4-}$ was needed since CBZ is not electroactive within the potential window of PBS.

To our knowledge this is the first report of CBZ detection by molecular imprinted PEDOT GCEs.

4.2.3 Materials and Methods

4.2.3.1 Reagents

CBZ powder was purchased from Sigma-Aldrich (Steinheim, Germany). All other commercially available reagents were purchased of analytical grade. Pyrrole along with 3,4-Ethylenedioxythiophene (EDOT) were purchased from Sigma-Aldrich, purified by distillation, purged by nitrogen, and kept in darkness at 4°C. PBS was used as the electrolyte. Stock solutions of CBZ were prepared in methanol/water mixture and stored at 4°C when not in use.

4.2.3.2 Apparatus

A three-electrode setup was used for all measurements: a MIP-modified GCE (2 mm diameter) as the working electrode; a Pt wire electrode as the counter electrode; and a potassium chloride (KCl)-saturated Ag/AgCl electrode as the reference electrode. CV and SWV electrochemical studies were conducted using a Bio-Logic VMP-300 Multi Potentiostat equipped with EC-LAB software. SEM images were conducted at an electron acceleration voltage of 10 kV.

4.2.3.3 Preparation of PPy and PEDOT films

Bare GCEs were polished using 0.3 um and 0.05 um alumina slurry on micro-cloth pads followed by sonication in distilled water for 5 minutes. The electrodes were then sonicated in pure ethanol and again in distilled water for 5 minutes each. Followed by activation in sulfuric acid 0.5 M by CV at 100 mV/s between -0.2 V and +1.6 V for 20 cycles. The response of the bare GCEs was then recorded by CV scans in PBS solution containing $[Fe(CN)_6]^{3-/4-}$. The voltage was cycled from -

0.2 V to +0.6 V at 100 mV/s until stable voltammograms were acquired. Finally, the electrodes were rinsed with distilled water followed by acetonitrile and left to dry at room temperature.

PPy was electropolymerized by immersing the GCEs in a solution of ACN containing 0.05 M $LiClO_4$ and 0.05 M pyrrole, followed by applying CV in the potential range of -0.0 V to +1.0 V for 10 cycles at a scan rate of 100 mV/s. PEDOT was prepared by dissolving 0.2 M Bu_4NBF_4 and 0.2 M EDOT in ACN and performing CV in the potential range of -0.0 V to +1.4 V for 10 cycles at a scan rate of 100 mV/s. Both PEDOT and PPy modified electrodes were slightly rinsed with ACN and left to dry at room temperature before characterization in PBS solution.

4.2.3.4 Preparation of molecular imprinted PEDOT-modified GCE

Similar to the preparation of PEDOT films, the modified MIPEDOT-GCE was prepared by washing the GCEs then immersing them in a solution of ACN containing 0.2 M Bu_4NBF_4 and 0.2 M EDOT with the addition of 0.015 M of CBZ. CV was then conducted in the potential range of -0.0 V to +1.4 V for 10 cycles at a scan rate of 100 mV/s. The imprinted template molecule was then extracted by immersing the electrode in ACN solution and constantly stirring for 30 minutes. The control (non-imprinted polymer electrode, NIP) was prepared similarly but without the addition of CBZ as a template molecule during the electropolymerization.

4.2.3.5 Electrochemical characterizations

CV measurements were conducted to study the oxidation and reduction potential of CBZ by immersing a bare GCE in a solution of CBZ dissolved in ACN and cycling its potential from -0.1 V to 1.0 V versus Ag/AgCl for 10 cycles at a scan rate of 100 mV/s.

CV measurements to compare the conductivity of PEDOT-GCE and PPy-GCE were conducted. Furthermore, the characterization of both the MIPEDOT-GCE and the NIPEDOT-GCE was carried out by CV and SWV measurements in a solution of PBS (PH=7.4) containing 0.01 M $[Fe(CN)_6]^{3-/4-}$ and 0.1 M KCl.

All SWV measurements were conducted by scanning the electrodes from -0.0 V to +0.7 V versus Ag/AgCl with a pulse height of 10.0 mV, pulse width of 50.0 ms and step height of 10.0 mV.

All other CV measurements conducted in PBS (PH=7.4) with 0.01 M $[Fe(CN)_6]^{3-/4-}$ and 0.1 M KCl were cycled from the potentials of -0.1 V to +0.6 V versus Ag/AgCl at 100 mV/s for 20 cycles.

Detection of CBZ was performed as follows: incubating the MIPEDOT-GCE and NIPEDOT-GCE in CBZ solutions for 15 minutes; measuring the electrode's response by SWV and CV; extracting entrapped CBZ molecules by immersing electrodes in ACN and stirring for 30 minutes; the electrodes were then utilized for successive detections. All measurements were undertaken at room temperatures.

4.2.4 Results and discussion

4.2.4.1 CBZ redox potentials

In order to determine the concentration of a template, its respective oxidation peak is measured. The template's concentration would have a direct effect on the electrode's response in solution. For such a relation to exist, the template must exhibit redox currents within the potential window of the solvent utilized. Initially, CV was conducted on a bare GCE in a solution of ACN with 0.1 M CBZ and 0.05 M $LiCLO_4$ and the potential of the GCE was cycled from -0.4 V to +1.0 V versus Ag/AgCl. No apparent peaks were found. This implies that no oxidation nor reduction current of CBZ are present in the redox potential window of PBS congruent with reported oxidation and reduction peaks between -2.3 V and -2.2 V versus Ag/AgCl [28]. Hence, a redox mediator such as $[Fe(CN)_6]^{3-/4-}$ is needed to electrochemically probe the presence of CBZ at the electrode's surface.

We hypothesized that CBZ molecules present inside the polymer matrix on the electrode's surface could have an effect on the conductivity and the electroactive surface of the electrode. These changes in the conducting polymer properties would translate in a current variation due to the redox activity of $[Fe(CN)_6]^{3-/4-}$.

4.2.4.2 Conductivity of PEDOT versus PPy

Conductivity of the modified electrode relies on several factors including its surface area, its composition, and its morphology. Typically, an electrode with higher conductivity is preferred in biosensors to increase sensitivity via an enhanced signal to noise ratio. Both PPy and PEDOT were electropolymerized on the GCE's surface and characterized by CV in a solution of PBS (PH=7.4) with 0.01 M $[Fe(CN)_6]^{3-/4-}$ and 0.1 M KCl. Figure 4.2 shows the polymerization graphs: PEDOT offered larger redox currents, therefore PEDOT was chosen to be the imprinted polymer rather than PPy.

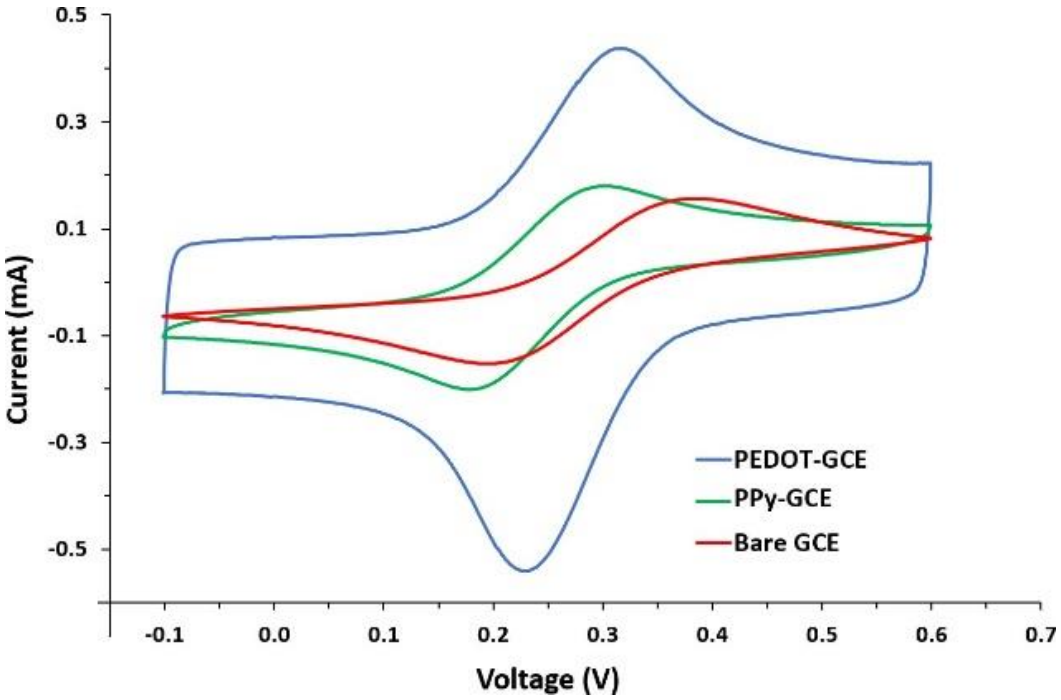

Figure 4.2 Cyclic Voltammograms of PBS solution of 0.01 M $[Fe(CN)_6]^{3-/4-}$ and 0.1 M KCl onto: Bare GCE, PPy-GCE, and PEDOT-GCE

4.2.4.3 Characterization of modified GCEs

SEM micrographs are presented in Figure 4.3. Porous structures are observed with the NIPEDOT Figure 4.3(a) yielding a different morphology than that of MIPEDOT polymer Figure 4.3(b). On the other hand, CBZ extraction Figure 4.3(c) resulted in a further change in polymer morphology which could be related to CBZ molecules being separated from the polymer matrix. A more elaborate study of the effect of CBZ imprinting and extraction was conducted through performing CV in a solution of PBS (PH=7.4) with 0.01 M $[Fe(CN)_6]^{3-/4-}$ and 0.1 M KCl.

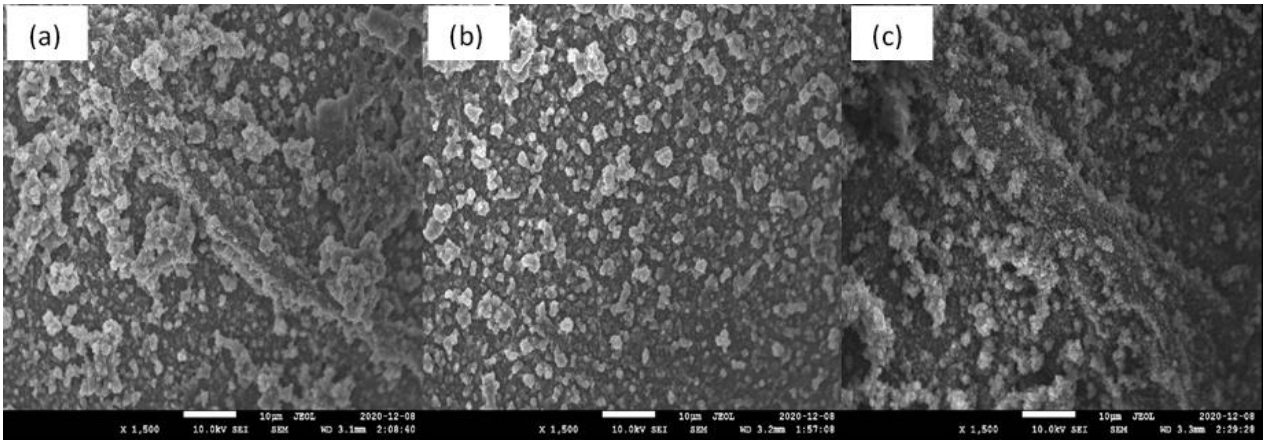

Figure 4.3 Surface morphology using SEM; (a) NIPEDOT, (b) MIPEDOT pre-extraction of CBZ, (c) MIPEDOT post-extraction of CBZ

Figure 4.4 illustrates the response of the modified electrodes post-polymerization, and post-template extraction by incubation in ACN solution for 30 minutes with stirring. For NIPEDOT-GCE which was polymerized in the absence of CBZ molecules, there is no noticeable change in current after extraction of CBZ.

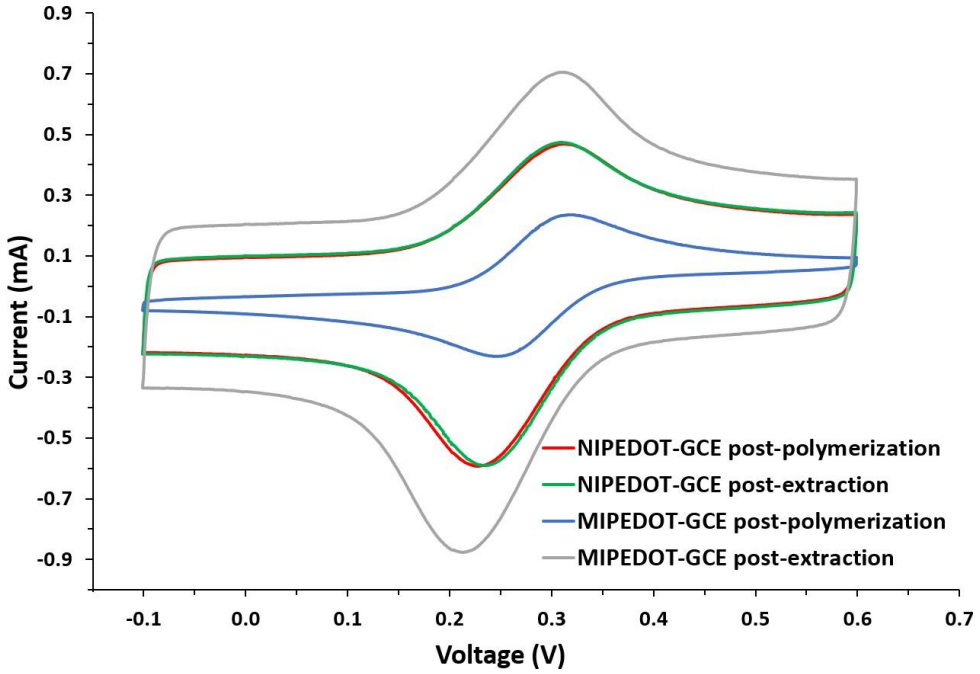

Figure 4.4 Cyclic Voltammograms of NIPEDOT-GCE post-polymerization, NIPEDOT-GCE post-extraction, MIPEDOT-GCE post-polymerization, and MIPEDOT-GCE post- extraction

On the other hand, there is a significant increase in redox currents post extraction of template from the MIPEDOT-GCE. This change in current magnitude for the MIPEDOT-GCE electrodes post extraction could be attributed to an increase of conductivity and electroactive area due to the absence of CBZ from the polymer matrix. However, more in-depth characterizations are needed to confirm this hypothesis.

4.2.4.4 Template extraction

One of the main challenges in electropolymerized-MIP-based sensors is the extraction of the template molecules from the polymer matrix. Exposing the electrode's surface to harsh extraction methods may risk delamination of the polymer. A few papers have reported extraction of the template through over-oxidation of the polymer [23, 29, 30]; however, over-oxidization of conducting polymers leads to loss of polymer activity. Alternatively, since CBZ is readily soluble in ACN, the extraction from the imprinted polymer was carried out by incubating the electrode in ACN for 30 minutes with constant stirring.

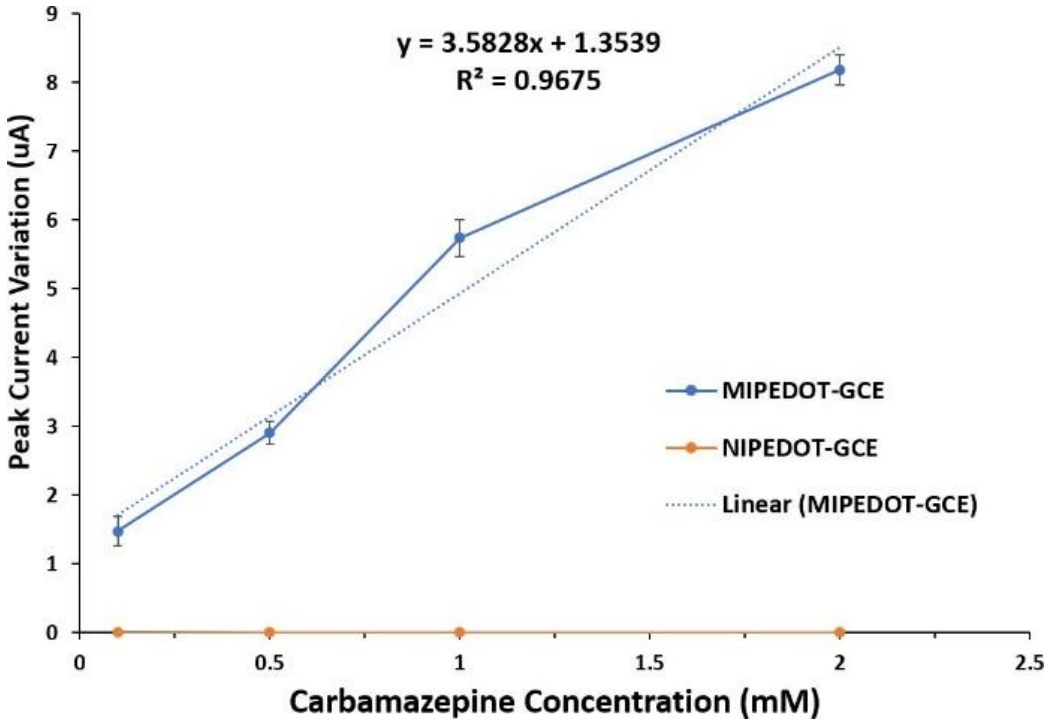

Figure 4.5 Square wave voltammogram data of MIPEDOT- GCE's and NIPEDOT-GCE's peak current variation with respect to prepared CBZ stock solutions with different concentrations

Extraction validation was implemented by conducting UV-vis spectroscopy on the ACN solution after incubation. A peak appeared at a wavelength of 230 nm reflecting successful extraction of CBZ from MIPEDOT-GCE. On the other hand, the ACN solution incubating NIPEDOT-GCE did not show any presence of CBZ.

4.2.4.5 MIPEDOT-GCE calibration curve

In order to establish the calibration curve of MIPEDOT-GCE to CBZ, both NIPEDOT-GCE and MIPEDOT-GCE were incubated in stock solutions of CBZ in methanol/water mixture (20:80). Electrodes were then removed, left to dry and then transferred into a solution of PBS (PH=7.4) with 0.01 M $[Fe(CN)_6]^{3-/4-}$ and 0.1 M KCl for SWV experiments. All measurements were performed in triplicates in order to achieve a standard deviation ensuring results are valid. SWV was conducted on a blank MIPEDOT-GCE to measure the response current. Following that, the electrode was incubated for 15 minutes in the prepared CBZ stock solutions from a range of 1.0 x 10-4 M to 2.0 x 10-3 M. SWV was conducted again to measure the variation in peak current due to the presence of CBZ molecules within the polymer matrix. The same electrode was then washed and incubated in another stock solution with different concentrations in order to finalize the experiments.

According to the SWV results there was no variation in oxidation current before and after NIPEDOT-GCE incubation; however the MIPEDOT-GCE showed a linear current response from $[Fe(CN)_6]^{3-/4-}$ redox activity with CBZ concentrations as presented in Figure 4.5. Consequently, MIPEDOT- GCE can be used for quantitative analysis of CBZ.

The limit of detection (LOD) and limit of quantification (LOQ) were calculated to be 0.98 x 10-3 M and 2.97 x 10-3 M respectively according to the linear regression method [31]. The sensitivity of the polymer is dependent on the template extraction procedure, the conductivity of the polymer and the electrode's surface area. Through further optimization of the extraction protocol, a wider number of molecular imprinted gaps would be freed hence, enhancing detection. Furthermore, increasing both surface area and conductivity may be realized through introducing conductive graphene along with the polymer.

4.2.4.6 Future work and limitations

Table 4.1 summarizes the main advantages of the proposed sensor over existing sensors; molecular imprinted PEDOT sensors are selective, rapid, robust, easy to fabricate, and cost-effective. Future work involves implementing the modified electrodes on a complete system on chip enabling continuous detection and quantification of CBZ levels. Furthermore, the sensor is not limited to CBZ detection. Applications of molecular imprinted polymers can extend to encompass a wider range of AEDs. As such, electrodes could be designed containing multiple imprinted sites selective to a combination of AEDs.

Sensitivity of the proposed sensor is inferior to that of time-consuming, and complex chromatography-based methods. However, as previously mentioned, this limitation could potentially be overcome by adding graphene to the polymer. Graphene has excellent conductive properties and could vastly increase the sensitivity of the sensor. Another limitation to the proposed sensor is the template's extraction. Since CBZ molecules are well fused within the polymer matrix, removing them with rigorous methods deteriorates the sensor's performance through the delamination of the polymer. The utilized method through ACN incubation might not fully liberate the imprinted sites. Therefore, advanced extraction methods must be researched in order to provide complete template removal.

Table 4.1 Table of comparison between proposed senor and existing ASM detection sensors

Technique	Electrode	Selectivity	Complexity	Speed	Ref.
SWV, CV	MIPEDOT-GCE	Yes	Simple	Fast	This work
CV	Au-Gr-AuNPs[1]	No	Simple	Fast	[11]
FPIA[2]	N/A	No	Moderate	Slow	[14]
DLLME[3], RP-LC[4]	N/A	Yes	Complex	Slow	[32]
LC-MS/MS[5]	N/A	Yes	Simple	Slow	[33]

[1]Graphene-gold nanoparticle composite deposited on gold electrode, [2]Fluorescence polarization, [3]Liquid chromatography-tandem mass spectroscopy, [4]Reverse-phase liquid chromatography, [5]Dispersive liquid-liquid microextraction method

4.2.5 Conclusion

Both PPy and PEDOT were polymerized and their conductive properties have been investigated through CV measurements. The latter provided superior conductivity and robustness. As such, a novel electrochemical sensor for CBZ detection was reported using the molecular imprinting of PEDOT on GCE. A mediator $[Fe(CN)_6]^{3-/4-}$ was used to study the effect of CBZ levels on the sensor's response since CBZ provided no redox peaks within the redox potential of PBS. Polymerization of PEDOT was conducted via CV and the modified electrodes were characterized using both CV and SWV. Molecular imprinted PEDOT films were immobilized on the electrodes' surface through electropolymerization. SWV experiments were conducted to validate CBZ detection followed by SEM imaging and UV-vis spectroscopy to characterize surface morphology and the extraction protocol. Afterwards, subsequent to incubation in stock carbamazepine solutions, the sensor's LOD and LOQ were found to be 0.98 x 10-3 M and 2.97 x 10-3 M respectively. The proposed biosensor achieved great sensitivity and selectivity towards CBZ molecules. Although not as sensitive as chromatography or other complex techniques, this biosensor is fast, cheap, easy to fabricate and could be implemented on a system on chip. Furthermore, the biosensor's sensitivity could potentially be improved by introducing graphene to within the polymer matrix and enhancing the extraction protocol. This would increase conductivity at the electrode's surface and free up more polymer sites for successive detection increasing the signal to noise ratio.

4.2.6 Acknowledgments

The authors would like to acknowledge Dr. Steen B. Schougaard for providing access to his laboratories, along with NSERC Canada for funding the research.

4.2.7 References

[1] Parikha Mehrotra. Journal of oral biology and craniofacial research, 6(2):153–159, 2016.

[2] J. D. Adams, S. Emam, N. Sun, Y. Ma, Q. Wang, R. Shashidhar, and N. Sun. IEEE Sensors Journal, 19(16):6571–6577, 2019.

[3] Anthony Turner, Isao Karube, and George S Wilson. Oxford university press, 1987.

[4] David G Myszka and Rebecca L Rich. Pharmaceutical science & technology today, 3(9):310–317, 2000.

[5] B Nikhil, J Pawan, F Nello, and E Pedro. Essays in Biochemistry, 60(1):1–8, 2016.

[6] N Mohamed Shah, AF Hawwa, JS Millership, PS Collier, and JC McElnay. Journal of Chromatography B, 923:65–73, 2013.

[7] Carlos Alberto A de Almeida, Carla GB Brenner, Luciane Minetto, Carlos A Mallmann, and Ayrton F Martins. Chemosphere, 93(10):2349–2355, 2013.

[8] Regina Helena Costa Queiroz, Carlo Bertucci, Wilson Roberto Malfará, Sônia Aparecida Carvalho Dreossi, Andréa Rodrigues Chaves, Daniel Augusto Rodrigues Valério, and Maria Eugênia Costa Queiroz. Journal of pharmaceutical and biomedical analysis, 48(2):428–434, 2008.

[9] Zahra Rezaei, Bahram Hemmateenejad, Soghra Khabnadideh, and Mina Gorgin. Talanta, 65(1):21–28, 2005.

[10] HN Deepakumari and HD Revanasiddappa. Chemical Sciences Journal, 5(1):1, 2014.

[11] Stela Pruneanu, Florina Pogacean, Alexandru R Biris, Stefania Ardelean, Valentin Canpean, Gabriela Blanita, Enkeleda Dervishi, and Alexandru S Biris. The Journal of Physical Chemistry C, 115(47):23387–23394, 2011.

[12] N Lavanya, C Sekar, S Ficarra, E Tellone, A Bonavita, SG Leonardi, and G Neri. Materials Science and Engineering: C, 62:53–60, 2016.

[13] ML Pan, WY Lin, HY Wang, SC Tsai, PF Hsieh, YLO Su, and PW Huang. Journal of analytical chemistry, 69(1):57–61, 2014.

[14] WY Lin, ML Pan, HY Wang, YO Su, and PW Huang. Medicinal Chemistry Research, 21(12):4389–4394, 2012.

[15] HY Wang, ML Pan, YL Oliver Su, SC Tsai, CH Kao, SS Sun, and WY Lin. Journal of Analytical Chemistry, 66(4):415–420, 2011.

[16] Binesh Unnikrishnan, Veerappan Mani, and Shen-Ming Chen. Sen- sors and Actuators B: Chemical, 173:274–280, 2012.

[17] Paramasivam Balasubramanian, TST Balamurugan, Shen-Ming Chen, Tse-Wei Chen, M Ajmal Ali, Fahad MA Al-Hemaid, and MS Elshikh. Journal of The Electrochemical Society, 165(3): B160– B166, 2018.

[18] Faezeh Khalilian and Setareh Ahmadian. Journal of separation sci- ence, 39(8):1500–1508, 2016.

[19] A Beltran, RM Marcé, PAG Cormack, and F Borrull. Journal of Chromatography A, 1216(12):2248–2253, 2009.

[20] Irshad Mohiuddin, Asnake Lealem Berhanu, Ashok Kumar Malik, Jatinder Singh Aulakh, Jechan Lee, and Ki-Hyun Kim. Environmental research, 176:108580, 2019.

[21] Bianca Schweiger, Jungtae Kim, Young Kim, and Mathias Ulbricht. Sensors, 15(3):4870–4889, 2015.

[22] Azizollah Nezhadali and Raham Shadmehri. Sensors and Actuators B: Chemical, 177:871–878, 2013.

[23] Hélder da Silva, João G Pacheco, Júlia MCS Magalhães, Subramanian Viswanathan, and Cristina Delerue-Matos. Biosensors and Bioelectronics, 52:56–61, 2014.

[24] Min Zhong, Ying Teng, Shufen Pang, Liqin Yan, and Xianwen Kan. Biosensors and Bioelectronics, 64:212–218, 2015.

[25] Y Wang. In Journal of Physics: Conference Series, volume 152, page 012023. IOP Publishing, 2009.

[26] Magatte N Gueye, Alexandre Carella, Nicolas Massonnet, Etienne Yvenou, Sophie Brenet, Jérôme Faure-Vincent, Stéphanie Pouget, François Rieutord, Hanako Okuno, Anass Benayad, et al. Chemistry of Materials, 28(10):3462–3468, 2016.

[27] Rauno Temmer, Ali Maziz, Cédric Plesse, Alvo Aabloo, Frédéric Vidal, and Tarmo Tamm. Smart Materials and Structures, 22(10):104006, 2013.

[28] S Atkins, JM Sevilla, M Blazquez, T Pineda, and Jose Gonzalez- Rodriguez. Electroanalysis, 22(24):2961–2966, 2010.

[29] Si Sun, Mengqi Zhang, Yijun Li, and Xiwen He. Sensors, 13(5):5493–5506, 2013.

[30] Hajer Hrichi, Lotfi Monser, and Nafaâ Adhoum. International Jour- nal of Electrochemistry, 2019, 2019.

[31] Alankar Shrivastava, Vipin B Gupta, et al. Chronicles of young scientists, 2(1):21, 2011.

[32] Hossein Ali Mashayekhi, Parviz Abroomand-Azar, Mohammad Saber-Tehrani, and Syed Waqif Husain. Chromatographia, 71(5- 6):517–521, 2010.

[33] Engy Shokry, Fabio Villanelli, Sabrina Malvagia, Anna Rosati, Giulia Forni, Silvia Funghini, Daniela Ombrone, Maria Della Bona, Renzo Guerrini, and Giancarlo La Marca. Journal of pharmaceutical and biomedical analysis, 109:164–170, 2015.

CHAPTER 5 MINIATURIZED BIOSENSOR

5.1 Overview

As previously discussed, selective detection of ASMs via electrochemical methods requires modification of the electrode's surface. Chapter 4 presented a new molecular imprinted PEDOT electrode which enabled successful binding to CBZ molecules and was tested via CV utilizing a large-scale commercial potentiostat. To overcome the need for large equipment and move towards an implantable biosensor, chapter 5 introduces a miniaturized CMOS chip capable of replacing the commercial potentiostat to successfully perform all necessary electrochemical measurements. This work was submitted to Transactions on Biomedical Circuits and Systems (TBioCAS), 2021.

5.2 Article 3: A Molecular Imprinted PEDOT CMOS Chip-based Biosensor for Carbamazepine Detection

Abbas Hammoud[*,1], Student Member, IEEE, Hussein Assaf[1], Yvon Savaria[1], Fellow, IEEE, Dang Khoa Nguyen[2], and Mohamad Sawan[1,3], Fellow, IEEE

[1]Department of Electrical Engineering, Polytechnique Montreal, Montreal, QC H3T 1J4, Canada

[2]Centre Hospitalier de l'Université de Montréal, Université de Montréal, Montréal, QC, Canada.

[3]School of Engineering, Westlake University, and Westlake Institute for Advanced Study, Hangzhou, Zhejiang, China, 310024

Transactions on Biomedical Circuits and Systems (TBioCAS), July 2021

5.2.1 Abstract

A miniaturized biosensor for carbamazepine (CBZ) detection and quantification was designed, implemented and fabricated. The 1×1 mm^2 CMOS chip was packaged and coupled with a 3-electrode electrochemical cell. A complete characterization of the sensor was conducted via two steps: 1) Molecular imprinting of PEDOT polymer sites by cyclic voltammetry (CV) on glassy carbon electrode (GCE) surfaces; and 2) Quantification of CBZ solutions through both CV, and a

current peak detection circuitry. The proposed biosensor offered high-selectivity and high-sensitivity to CBZ molecules. Scanning electron microscopy (SEM) was utilized to validate the synthesis of the PEDOT chains. CBZ removal from the imprinted polymer was conducted through soaking the modified GCEs in acetonitrile (ACN). Extraction was then confirmed by ultraviolet-visible (UV-vis) spectroscopy and CV analyzing data from pre- and post-template extraction. Furthermore, in order to characterize the electrodes' response to CBZ levels in phosphate buffered solution (PBS) with $[Fe(CN)_6]^{3-/4-}$ as a redox pair/mediator, CV and peak detection was conducted to obtain redox peak currents vs. CBZ concentration graphs. The limits of detection (LOD) and quantification (LOQ) were calculated to be 2.04 and 6.2 μg/mL respectively. Finally, selectivity towards CBZ was validated by studying the effect of valproic acid (VPA) and phenytoin (PHT) on the biosensor's performance. The proposed biosensor is highly sensitive and selective to CBZ molecules, simple to construct and easy to operate.

Keywords: Biosensor, CMOS, Electropolymerization, Antiseizure medication, Carbamazepine, Molecular imprinted polymer, PEDOT.

5.2.2 Introduction

Epilepsy is characterized by recurrent seizures and influences over 70 million patients across the world [1]. Primarily, clinicians prescribe antiseizure medications (ASMs) as a prophylactic treatment. Such ASMs may be taken daily or for protracted periods. Currently, more than twelve ASMs are being utilized. The most common ASM is CBZ, an anticonvulsant which works by blocking presynaptic sodium and calcium voltage-dependent channels [2]. Various side effects of ASMs include dizziness, blurred vision, dysarthria, ataxia, somnolence, and psychomotor slowing.

While treating epileptic patients, clinicians must continuously monitor the levels of ASMs in blood, referred to as Therapeutic Drug Monitoring (TDM). This practice is critical in order to enhance drug dosage, minimize toxicity, eliminate undesirable dug interactions, and ensure proper compliance. Current TDM is conducted via frequent phlebotomy visits, and has several limitations such as: a) drug levels are affected by numerous conditions of which some are unpredictable; b) CBZ levels in blood greatly vary with time of measurement (the levels before taking the CBZ are different than after taking the CBZ); c) going to clinics and waiting for extended periods of time

for blood collection is time-consuming, tedious, and may hinder patients from following a strict blood sampling schedule.

Common reported techniques utilized for the detection and quantification of CBZ can be categorized into electrochemical based methods such as CV [3], differential pulse voltammetry (DPV) [4]-[6], and amperometry [7],[8], and non-electrochemical based methods such as high performance liquid chromatography (HPLC) [9]-[11], and spectrophotometry [12]. The latter offer the highest sensitivity and selectivity, however, require bulky equipment, trained clinicians, and sample pre-treatment. Furthermore, such methods are cumbersome and cannot be rendered miniature or portable. On the other hand, electrochemical based methods possess great attributes such as sensitivity, speed, low-cost, simplicity, and portability making them good candidates to be utilized in environmental and medical applications. However, contemporary electrochemical based sensors rely on commercially available electrodes that lack selectivity to the target molecules. To the best of our knowledge, no reported miniaturized detection biosensor can selectively measure the CBZ concentration within a complex medium.

Fortunately, MIPs overcome such limitation. They are alternatives to natural antibodies that are robust, easy to fabricate and could be prepared by various methods. MIPs have been widely coupled with electrochemical techniques improving sensor's selectivity and sensitivity. [13] reports the successful detection of streptomycin residues in food using magnetic MIP based on nanogold-encapsulated poly(o-phenylenediamine) shell on magnetic iron oxide cores. Furthermore, MIPs have been reported for bisphenol A (BPA) detection [14], insecticide fenamiphos (FEN) detection [15] ceftizoxime detection [16], epinephrine detection [17], and amyloid-β protein [18]. As presented in Figure 5.1, a template of interest is chosen to be imprinted within the polymer during the polymerization process. Post-polymerization, the template is extracted from the polymer leaving a gap similar to its structure. Due to the presence of such gaps, the MIP has a high affinity towards the imprinted template. MIPs demonstrated their ability to be vigorous, efficient, and most importantly, inexpensive. Amongst the various methods of MIP synthesis, to date, addition polymerization has been used for CBZ detection. This preparation technique involves a monomer, a cross-linker, a porogen, an initiator along with the template/analyte of interest. Despite their effectiveness, both controlling the thickness of chemically synthesized MIPs and their deposition on the electrodes' surfaces is challenging.

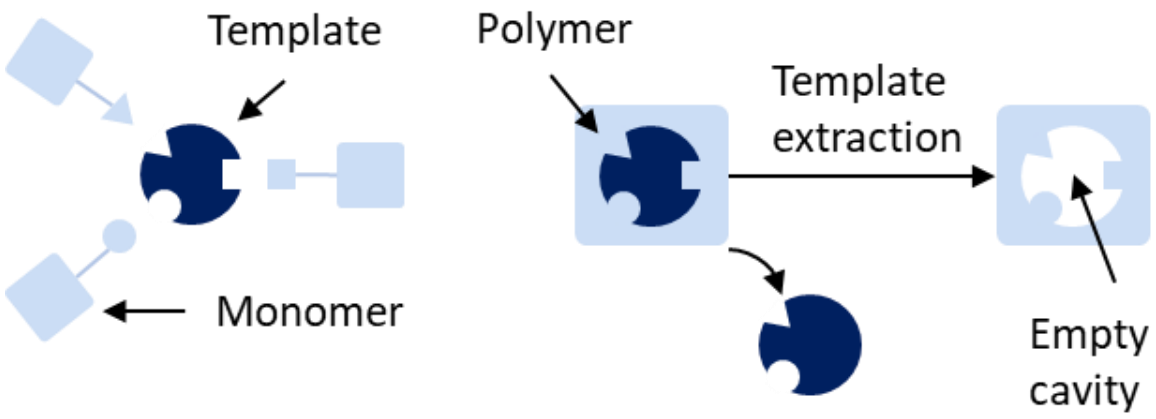

Figure 5.1 Molecular imprinting principle

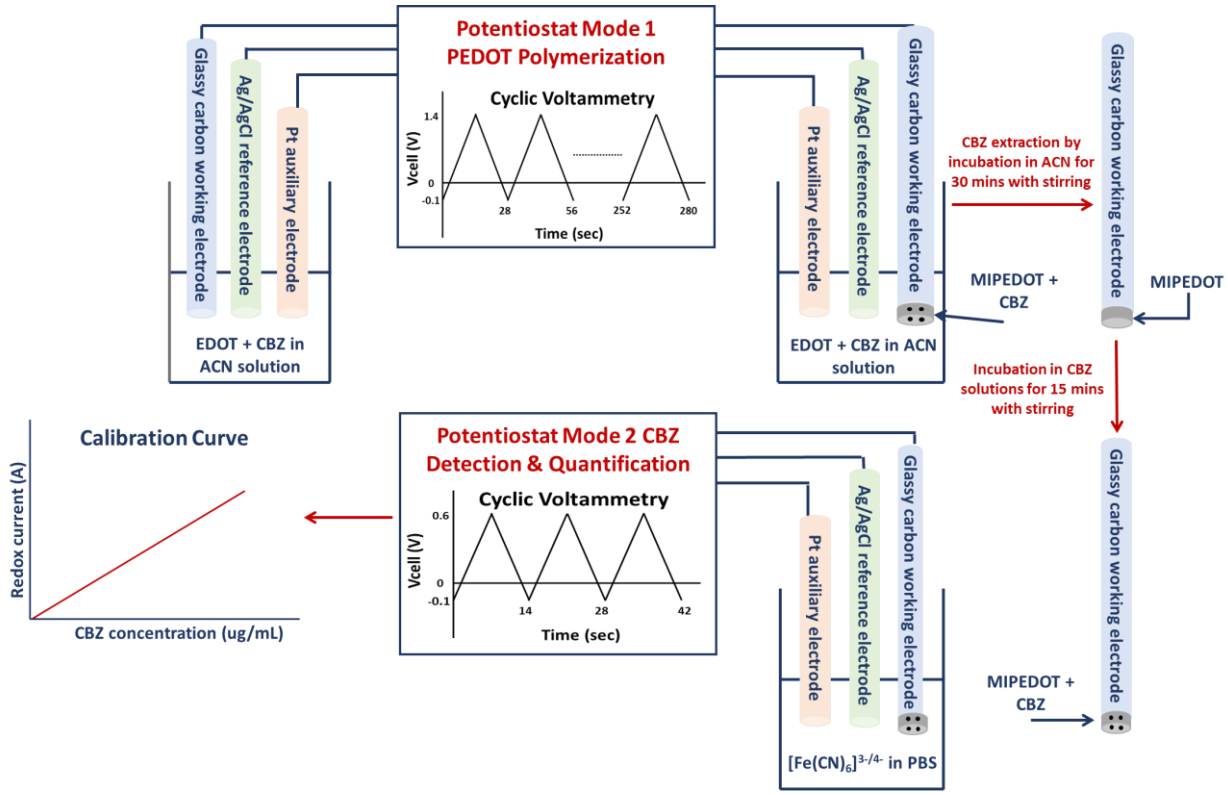

Figure 5.2 Proposed sensor's overall design. Mode 1 is for molecular imprinted polymer polymerization, and mode 2 is for CBZ detection and quantification

Electropolymerization is an alternative method to synthesize MIPs. It permits the direct formation of controlled thickness MIP layers on the electrode's surface through adjusting the various electrochemical conditions such as monomer concentration, applied voltage, number of cycles, etc. Poly-3,4-Ethylenedioxythiophene (PEDOT) is a popular biocompatible polymer synthesized by electropolymerization. It has proven to enhance electrodes' sensitivity and fidelity [19]. Additionally, PEDOT has been successfully deployed in nucleic acid detection systems in order to enhance the flexibility of two-dimensional transition-metal carbonitrides $Ti_3C_2T_x$ MXene whilst preserving its conductive properties [20]. Other PEDOT applications are reported in [21] synthesizing a pressure based sensor PEDOT:PSS modified sponge for highly sensitive detection of carcinoembryonic antigen (CEA). PEDOT synthesis requires less time, less skill, and is low-cost compared to additional polymerization.

A biosensor capable of selectively detecting CBZ must consist of an interface circuit connected to specifically modified CBZ sensing electrodes. As part of our previous work, we have reported the development of MIP modified electrodes capable of selectively capturing CBZ molecules overcoming the limitation of miniature electrochemical sensors for CBZ detection [22]. The MIP was based on the electropolymerization of PEDOT on GCEs by CV.

In this paper we present a solution to selectively target CBZ molecules by developing a miniaturized potentiostat-based biosensor capable of the electropolymerization of a PEDOT-based MIP on the biosensing electrodes followed by successive detection of CBZ molecules by CV as shown in Figure 5.2. In the remainder of this paper, in section II, we present the electrode-electrolyte model, followed by a system overview analysis and design considerations in Section III. Afterwards, Section IV encompasses post-layout simulations along with results of the fabricated chip and *in vitro* experiments. Finally, in Section V we present a conclusion of our work.

5.2.3 An Electrochemical Cell

Understanding the electrode-electrolyte interface is crucial to enable design of an effective potentiostat and to simulate accurately its behavior. Figure 5.3 presents the adopted electrical model circuit of the electrode-electrolyte interface for the 3-electrode cell. R_s is the solution resistance that exists between combinations of working electrode (WE), counter electrode (CE) and reference electrode (RE).

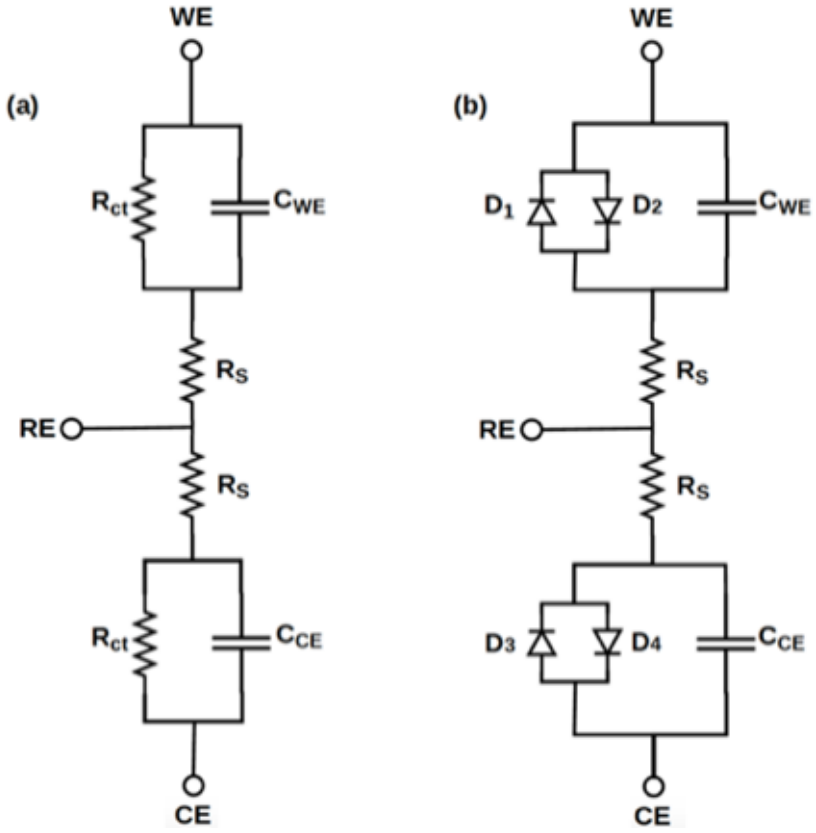

Figure 5.3 Electrode-electrolyte interface electrical model: (a) Three-electrode electrochemical cell; (b) Charge transfer resistance replaced by diodes

R_S can be determined by Eq. (1), Values of R_S have been reported in the range of 10 to 220 Ω [23].

$$Rs = \frac{\rho}{4r} \tag{1}$$

where r denotes the radius of the electrodes and ρ is the resistivity of the solution.

The current path across the electrode-electrolyte interface is represented by a capacitance in parallel with a non-linear resistance. C_{WE} and C_{CE} are the capacitances at the WE-electrolyte and the CE-electrolyte interfaces respectively. The Gouy-Chapman-Stern model offers a derivation of the

interface capacitance as a series combination of the double layer capacitance, known as the Helmholtz capacitance C_H, and the diffusion layer capacitance, known as the Gouy-Chapman capacitance C_G. This theoretical derivation is determined by Eq. (2). Depending on different electrolyte compositions and modifications to the WE surface, [23], [24] report the values of C_{WE} in the order of 1 to 100 μF cm^{-2}.

$$\frac{1}{C} = \frac{1}{C_H} + \frac{1}{C_G} = \frac{d_{OHP}}{\varepsilon_0 \varepsilon_r} + \sqrt{\frac{\varepsilon_0 \varepsilon_r U_t}{2 n^0 z^2 q}} \cdot \frac{1}{\varepsilon_0 \varepsilon_r \cosh\left(\frac{z\phi_0}{2U_t}\right)} \tag{2}$$

where d_{OHP} and ε_r are the double layer's thickness and relative permittivity respectively. ε_0 is the permittivity of free space, z is the solution's ion charge, ϕ_0 is the applied potential, U_t is the thermal voltage, q is the elementary charge, and n^0 is the concentration of ions in the bulk solution.

The non-linear resistance depends on several mechanisms such as the charge transfer at the electrode's surface, the chemical reactions and the diffusion of reactants to and from the electrode's surface along with the crystallization process. However, both the crystallization process and chemical reactions may be ignored. Therefore, this resistance is mainly due to the charge transfer resistance represented by R_{ct} and can be determined by Eq. (3).

The resistance R_{ct} has been reported to range between 1 and 10 MΩ [25]. This resistance decays exponentially to a couple of kΩ at large overpotentials, and could be replaced by two diode-connected MOSFETs in reverse parallel as shown in Figure 5.3(b).

$$R_{ct} = \left(\frac{V_t}{J_0 z}\right) \frac{1}{\cosh\left(\frac{z\eta}{2V_t}\right)} \tag{3}$$

In Eq. (4), J_0 is the absolute value of the oxidation and reduction current at equilibrium, η is the overpotential, Vt = kT/q which denotes the thermal voltage, $\Delta\psi_0$ denotes the equilibrium potential,

β denotes the symmetry factor, k_c denotes the reduction reaction rate constant, and c_A denotes the electron-acceptor ions' concentration.

$$J_0 = Fk_c c_A e^{\frac{\beta \Delta \psi_0}{V_t}} \quad (4)$$

5.2.4 System Overview

Figure 5.4 presents the architecture of a basic 3-electrode potentiostat cell. It consists of a control amplifier followed by a current to voltage converter circuit. The core function of the potentiostat stems from the regulation of the WE node potential to match the RE node potential, while measuring the current flowing through WE, and ensuring that no current flows into RE.

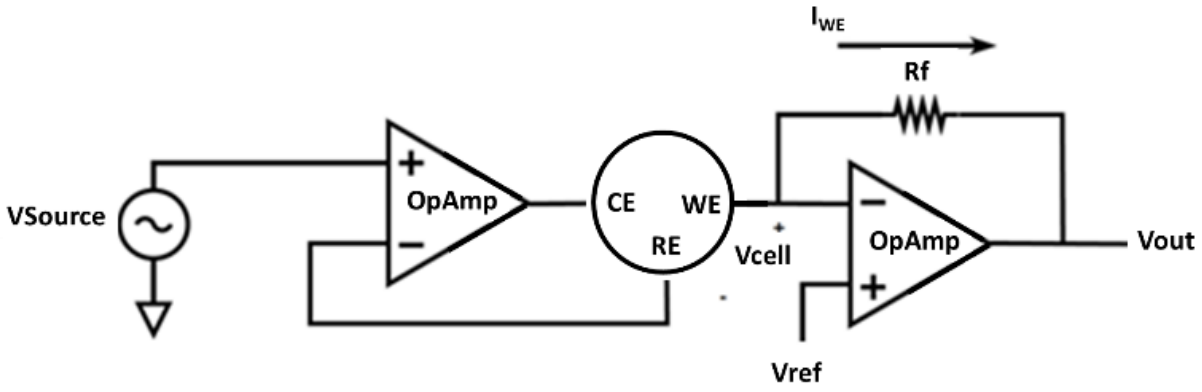

Figure 5.4 Basic potentiostat design of a 3-electrode electrochemical cell

The applied potential VSource is the same as the potential on RE, since the voltage at both +ve and –ve terminals of the Op-Amp are nominally equal, if the amplifier has a negligible offset. Similarly, since the +ve terminal of the second Op-Amp is connected to Vref, the potential at WE is set to Vref. These two settings enable the regulation of the WE potential to match that on RE.

Given that the Op-Amp's input impedance is high, no current flows through it. Therefore, all the current flows from CE through WE with no current passing through RE. Additionally, the second Op-Amp is utilized to measure the current passing through WE. This current is converted into a

potential drop across the feedback resistor Rf. These fundamental functions of the potentiostat necessitate the design of high gain and high input impedance Op-Amps.

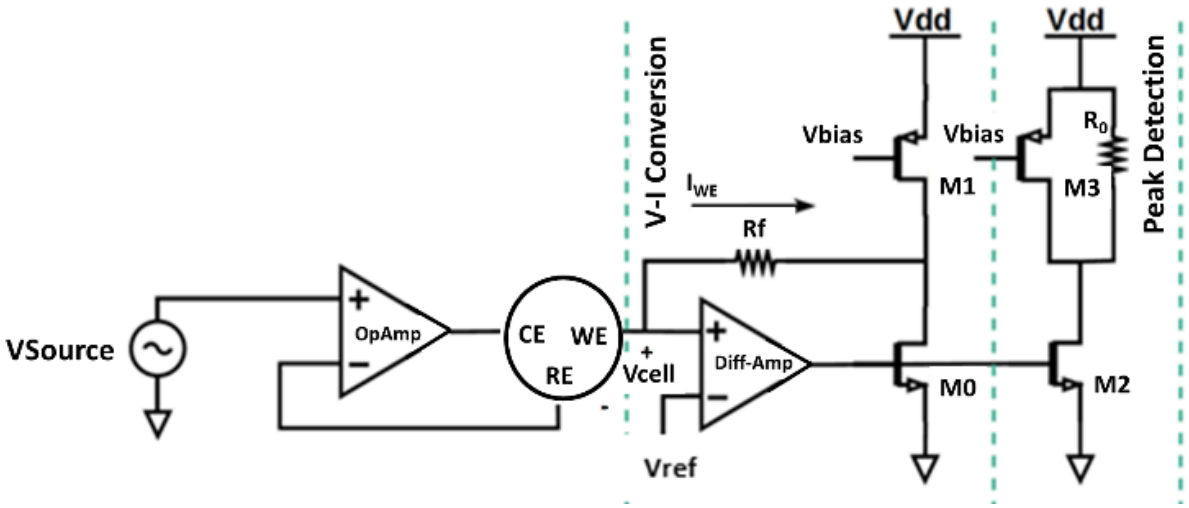

Figure 5.5 Proposed potentiostat design with I-V conversion and peak detection circuitry

The proposed design in Figure 5.5 occupies 0.55x0.55 mm2 chip area and was fabricated in a standard 180nm CMOS process. It consists of a sensing channel and a control amplifier used to regulate the cell voltage across WE with respect to RE. Additionally, the sensing channel compromises a current to voltage conversion and a peak detection stage. The biosensor detects CBZ molecules through a two-step process. First, by applying a cyclic voltage signal to form the MIP on the electrode's surface, followed by another cyclic voltage signal for CBZ detection. The resulting anodic and cathodic currents result in a proportional voltage that could be measured across the feedback resistance at the transimpedance amplifier stage. On the other hand, the peak detection circuitry detects the peak redox currents for different CBZ concentrations.

5.2.4.1 Control Amplifier Design

In a 3-electrode CV experiment, a cyclic voltage signal is set across WE and RE, and the resulting current through WE and CE is recorded. As previously mentioned, the first operation of the

biosensor is the PEDOT polymerization on the electrode's surface obtained by applying a cyclic potential of -0.1 V to +1.4 V across Vcell. Secondly, another CV potential of -0.1 V to +0.6 V across Vcell is applied to analyze CBZ levels' effect on the resulting current. Hence, the control amplifier was designed to have an input voltage range of -0.0 V to +1.5 V. Another important design factor was the output stage current which limits the flow of current through WE. This current was set to 3mA to ensure proper operation. Finally, the compliance voltage, which is the maximum voltage required between WE and RE throughout the electrochemical system, was measured *in vitro* to be 2 V, therefore it was necessary to minimize the saturation voltages of the output PMOS transistor to obtain 2 V bias between WE and CE.

The control amplifier was designed to be a high gain 2-stage Op-Amp with a power supply of 3.3V and a bias current of 100 μA. The measured gain was 53.07 dB and with a phase margin of 85.76° as shown in Figure 5.6. A 1 pF Miller capacitor was added to ensure stability of the Op-Amp over a wide range of capacitive load.

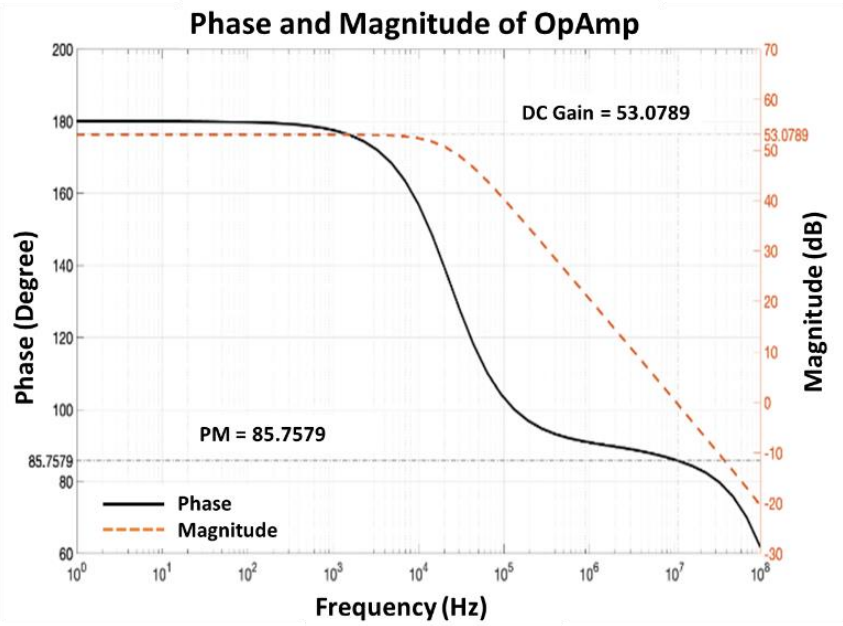

Figure 5.6 AC phase margin and gain of the designed Op-Amp

5.2.4.2 I-V Conversion Circuit

The sensing channel consists of a 2-stage Op-Amp with a feedback resistor in a transimpedance configuration as presented in Figure 5.7. The choice of the resistor value is critical to the sensitivity of the sensing amplifier. According to our previous reports, the redox currents could be as high as 800 μA, therefore Rf value was chosen to be 1 kΩ to ensure good sensitivity.

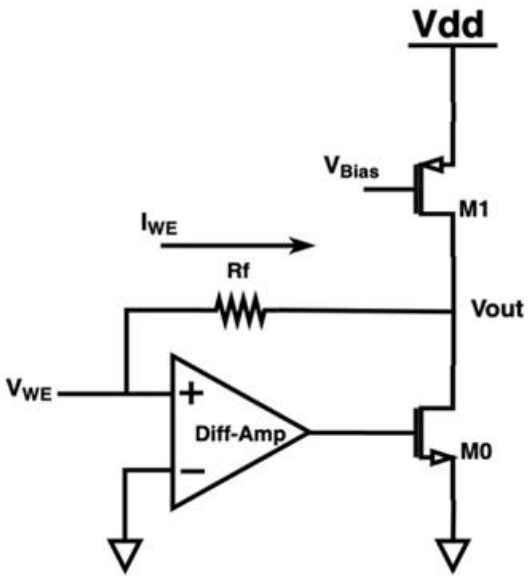

Figure 5.7 Transimpedance current to voltage conversion circuit

The -ve terminal of the amplifier was set to ground and the +ve terminal was connected to WE. By applying KCL we obtain.

$$V_{out} - V_{WE} = \frac{I_{WE}}{R_f} \tag{5}$$

$$I_{WE} = \frac{V_{out} - V_{WE}}{R_f} \tag{6}$$

$$I_{WE} = \frac{V_{out} - Vref}{R_f} \tag{7}$$

Since both input terminals of the amplifier have similar voltages due to the high-input impedance, the voltage on WE will become Vref.

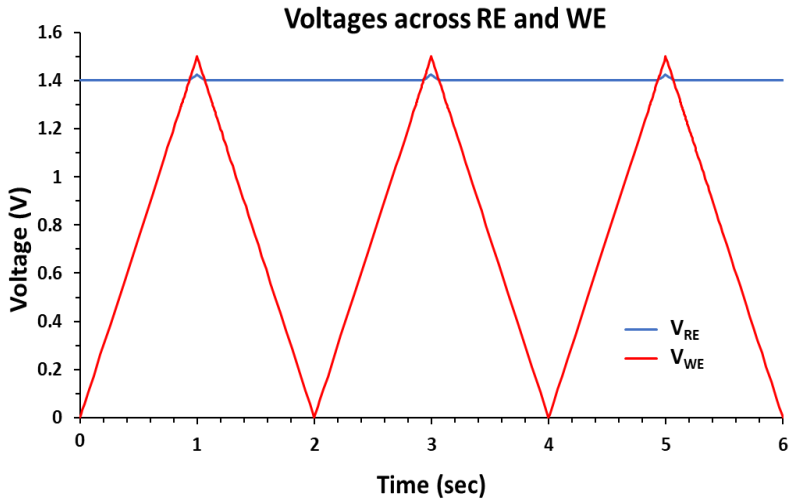

Figure 5.8 Recorded potential at WE and RE after applying a cyclic input voltage of -0.0 V to +1.5 V with a step size of 100 mV/s

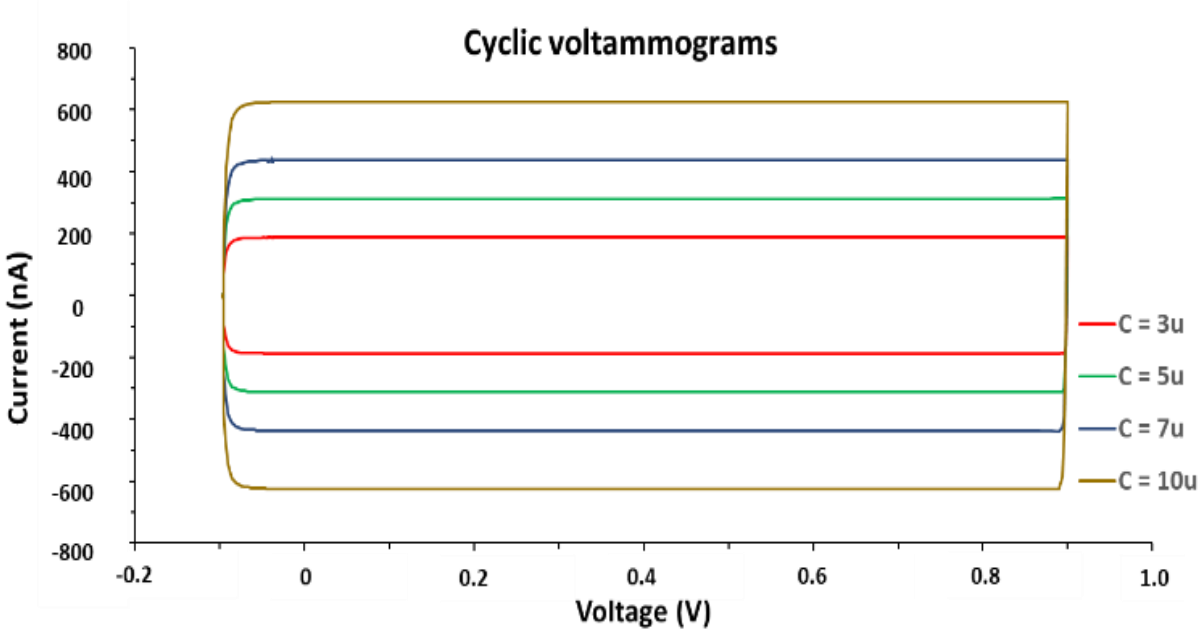

Figure 5.9 Electric double layer capacitance plots. Recorded voltammograms of current vs cell voltage with C_{WE} and C_{CE} of 3uF, 5uF, 7uF and 10uF

A cyclic voltage signal from 0 to 1.5 V with a step size of 100 mV/s was applied at the source of the control amplifier and the voltage Vref was set at 1.4 V which to match Vcell of -0.1 to +1.4 V, which is the maximum voltage required for the polymerization of the imprinted matrix. Afterwards the voltage at WE was measured along with the voltage across RE. Figure 5.8 shows that indeed throughout the applied signal, the voltage V_{WE} remained at 1.4 V and V_{RE} was a replica of the source validating successful manipulation of the cell voltage Vcell.

To further test the stability of the potentiostat, the current I_{WE} through the WE was recorded whilst varying C_{CE} and C_{WE} from 1 to 10 μF. The effect of different electric double layer capacitance is provided in Figure 5.9.

5.2.4.3 Peak Detection Circuit

Peak detection enables us to promptly draw a correlation between CBZ concentration and the anodic peak currents produced. The configuration of the proposed peak detection circuit is provided in Fig. 5. I_{WE} was mirrored through transistors M2 to M3 to the peak detection stage. This current then passes through the resistor R_O. The voltage drop signal across R_O, V_R, is identical in form to that of the redox current I_{WE}. The output resistance value R_O was chosen to be 2 kΩ. The differential amplifier utilized in the current to voltage conversion is similar to the differential amplifier stage in the control Op-Amp with a bias current of 100 μA. Figure 5.10 presents the graph of V_R throughout different solution resistance R_S values. As R_S increases the current I_{WE} decreases yielding a decrease in V_R. On the other hand, as R_S decreases, the current I_{WE} increases, yielding an increase in V_R. The same observation could be drawn with respect to changes in the charge transfer resistance R_{ct}.

5.2.5 Experimental Results

This section validates the chip fabrication, the *in vitro* setup used to test it, and obtained experimental results. Initially, the fabricated chip was utilized to electropolymerize the molecular imprinted PEDOT on the electrode's surface. Followed by SEM to validate the polymer's formation along with its uniform deposition. Furthermore, CV tests were conducted in order to

measure the sensor's response to different therapeutic CBZ levels using $[Fe(CN)_6]^{3-/4-}$ as a redox mediator in PBS. Throughout the experiments, CBZ removal from the imprinted sites was validated through UV-vis spectroscopy.

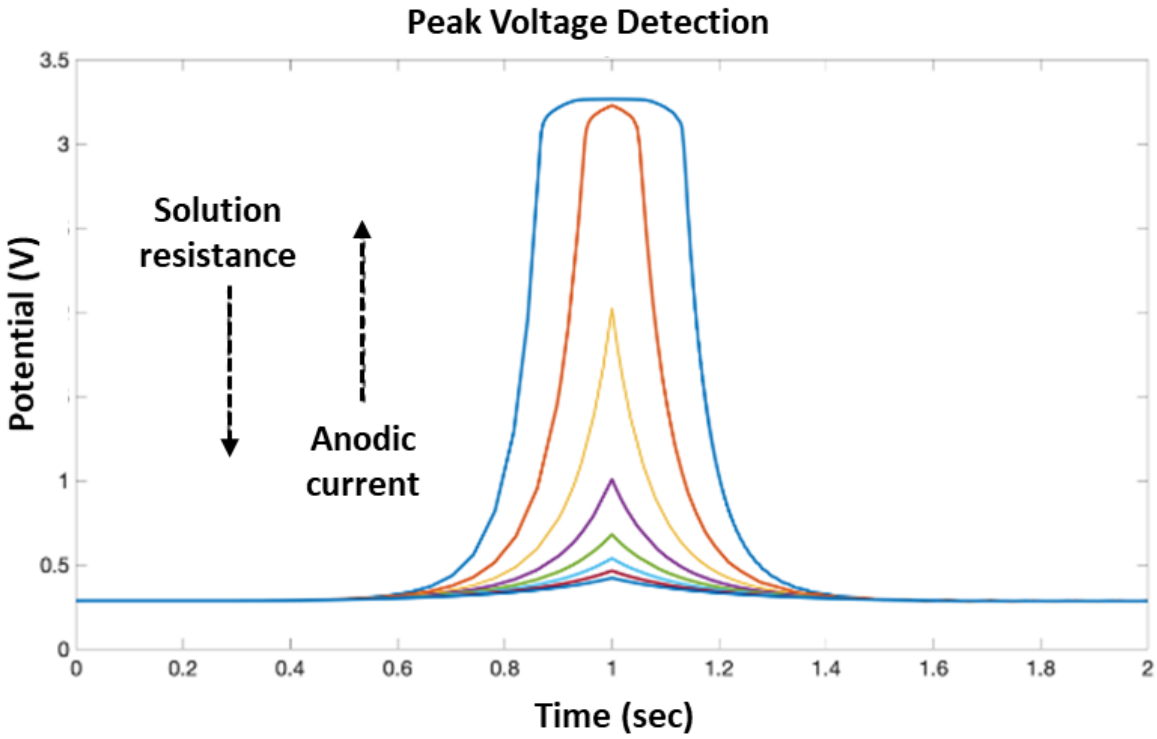

Figure 5.10 Peak voltage V_R versus solution resistance

5.2.5.1 Chip Fabrication

The proposed CMOS biosensor was assembled by Taiwan Semiconductor Manufacturing Company (TSMC), that has a minimum feature size of 0.18 μm and operates at a nominal power supply voltage of 3.3 V. The 1×1 mm^2 chip was packaged and mounted on a socket adapter and then placed on a breadboard for testing. Figure 5.11 presents a microscopic image of the fabricated chip along with layout and floorplan consisting of two blocks: the control amplifier and the sense amplifier. The packaged chip mounted on the adapter socket and the 3-electrode system is shown in Figure 5.12.

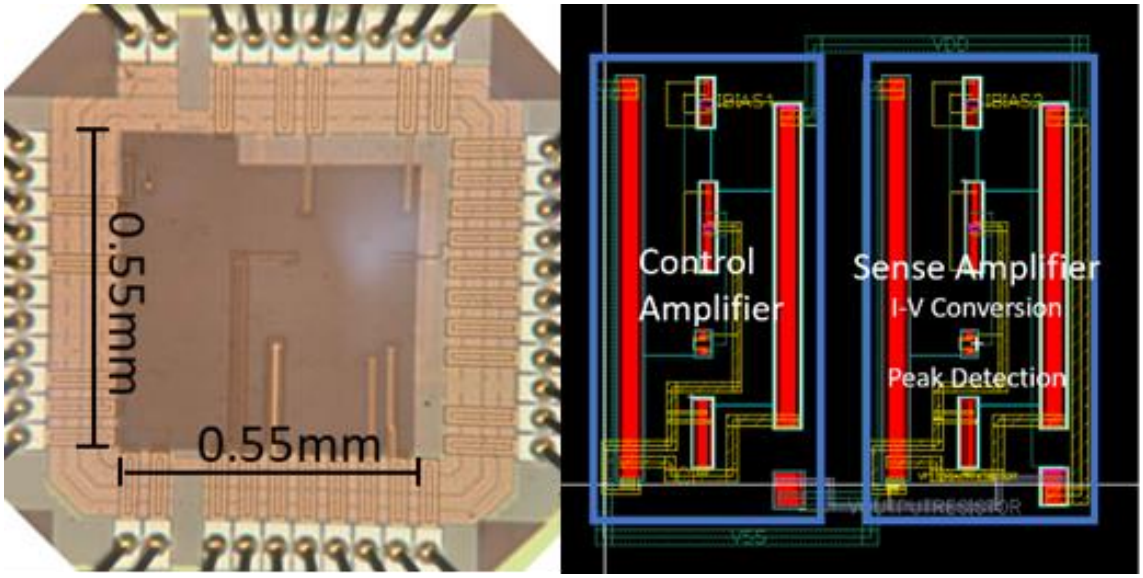

Figure 5.11 Photomicrographic image of the fabricated chip along with its layout floorplan

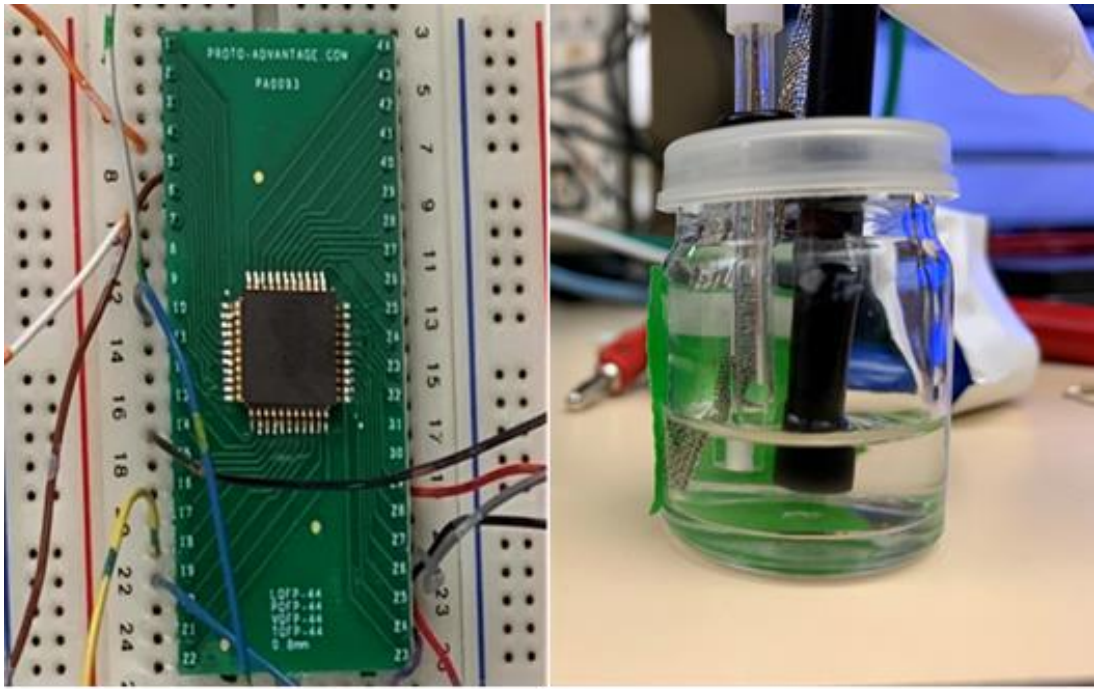

Figure 5.12 Test setup (a) packaged chip on adapter socket and breadboard (b) 3-electrode solution testing

5.2.5.2 Reagents

CBZ powder along with valproic acid (VPA) and phenytoin (PHT) were supplied by Sigma-Aldrich. All other analytical grade reagents were purchased commercially. The 3,4-Ethylenedioxythiophene (EDOT) monomer was also supplied by Sigma-Aldrich. It was purified by distillation, purged by nitrogen, and stored in darkness at a temperature of 4 °C. PBS was used as the electrolyte. CBZ, VPA and PHT stock solutions were prepared in a mixture of methanol/water (20:80) and stored at a temperature of 4 °C.

5.2.5.3 Test Setup Apparatus

All measurements were conducted in a 3-electrode setup: a molecular imprinted PEDOT modified GCE (MIPEDOT-GCE) (diameter = 2 mm) as the WE; a Pt wire electrode as the CE; and a potassium chloride (KCl)-saturated Ag/AgCl electrode as the RE. A 33210A Keysight Waveform/Function Generator was utilized to apply a CV signal across the cell along with a MDO4104-6 Tektronix mixed domain oscilloscope to probe output signals. SEM images were conducted at an electron acceleration voltage of 10 kV.

5.2.5.4 Preparation of CBZ Imprinted PEDOT Films

Prior to use, the bare GCEs were polished using 0.3 μm and 0.05 μm alumina slurry. Afterwards, the electrodes were sonicated in distilled water and ethanol for 5 minutes each. Furthermore, the GCEs were immersed in an ACN solution containing 0.2 M Bu_4NBF_4, 0.2 M EDOT, and 0.015 M CBZ. PEDOT was electropolymerized to form the imprinted sites on the electrode's surface, a cyclic signal across Vcell with a potential range of -0.1 V to +1.4 V and a period of 28 s was applied for a duration of 280 s. The electrodes were then immersed in ACN and stirred constantly for a duration of 30 min. This resulted in the extraction of the CBZ molecules trapped inside polymer matrix. Similarly, non-imprinted PEDOT modified GCEs (NIPEDOT-GCEs) were constructed in absence of CBZ to serve as control electrodes. Figure 5.13 provides a SEM image of the MIP post CBZ extraction depicting successful formation of a porous and uniformly deposited structure.

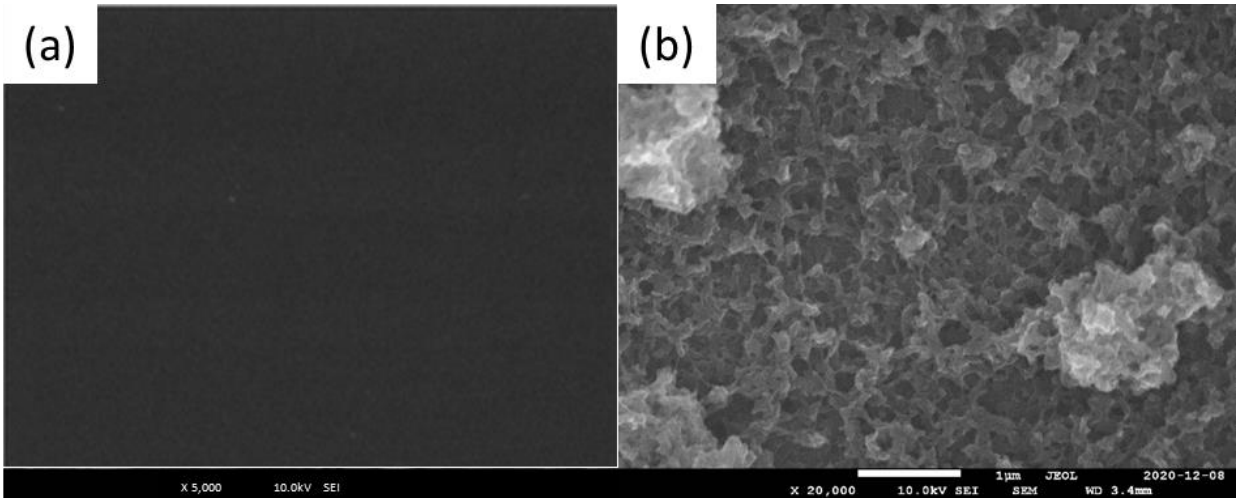

Figure 5.13 Surface morphology of (a) Bare GCE [24] and (b) electropolymerized PEDOT using SEM at 10kV and 20000 times magnification

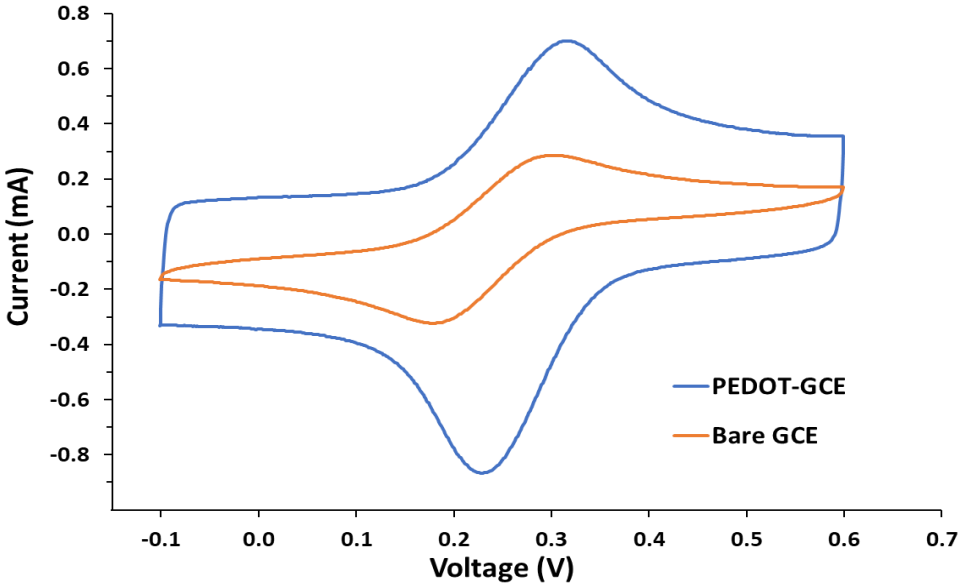

Figure 5.14 Cyclic Voltammograms of PBS solution of 0.01 M $[Fe(CN)_6]^{3-/4-}$ and 0.1 M KCl onto: Bare GCE and PEDOT-GCE

Furthermore, CV measurements portrayed the difference in conductivity of bare GCE's compared to MIPEDOT-GCEs. Hence, a cyclic signal across Vcell with a potential range of -0.1 to +0.6 V

and a period of 14 s was applied for a duration of 42 s. Figure 5.14 provides the recorded cyclic voltammograms.

5.2.5.5 CBZ Extraction Method

The extraction of the CBZ molecules from the imprinted polymer is a main challenge in electropolymerized polymers. Once exposed to harsh conditions, the polymer on the electrode's surface may be delaminated and lose functionality. Therefore, it is necessary to extract the CBZ molecules in gentler methods. As such, ACN was chosen as the extraction medium since it seamlessly dissolves CBZ. The extraction post-entrapment was conducted through incubating the electrode in ACN and constantly stirring for a period of 30 minutes. Proper removal of CBZ molecules from the imprinted sites was then validated through performing UV-vis spectroscopy. The UV spectra of the ACN solution utilized for extraction was generated. Figure 5.15 illustrates a peak at a wavelength of 230 nm distinct to the presence of CBZ molecules validating the removal of the CBZ molecules from polymer sites.

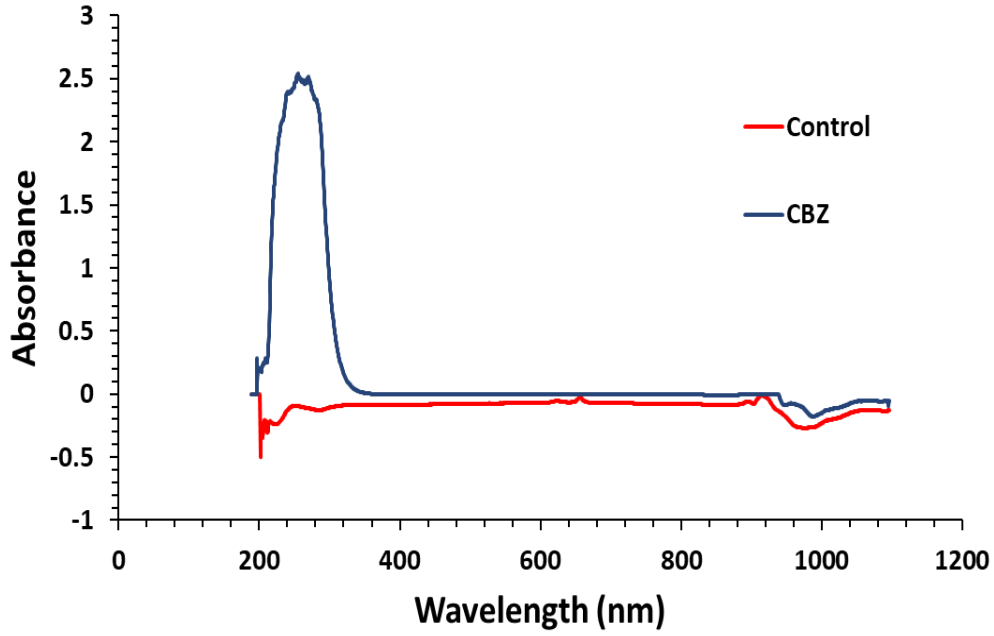

Figure 5.15 UV spectra of CBZ in ACN displaying a peak at 230 nm due to the presence of CBZ in solution vs control without the presence of CBZ

5.2.5.6 MIPEDOT-GCE Calibration Curve

Therapeutic CBZ concentrations in blood have been reported to be within 4-12 mg/L. Therefore, stock concentrations of 1-50 mg/L of CBZ were prepared by dissolving CBZ in a mixture of methanol/water (20:80). Afterwards the MIPEDOT-GCEs were incubated in the prepared solutions for 15 minutes with stirring. They were then removed from the solution and left to dry to dry at room temperature. Finally, the electrodes were transferred into a solution of PBS (PH=7.4) containing 0.01 M $[Fe(CN)_6]^{3-/4-}$ and 0.1 M KCl for CV testing. All measurements were conducted 3 times to confirm results validity.

Following a cyclic signal across Vcell with a potential range of -0.1 to +0.6 V and a period of 14 s applied for a duration of 42 s, the current peaks were recorded by dividing the voltage drop V_R across the resistor's value. It was observed that the sensor's peak current, equivalent to the maximum current through the solution, had a linear response to CBZ concentration. On the other hand, NIPEDOT-GCEs did not provide a response to CBZ concentration variation. Figure 5.16 provides the constructed calibration curve of current variation recorded by the electrode with respect to CBZ concentration. Higher CBZ concentrations inhibited electron transfer at the electrode's surface resulting in a current decrease, hence, a larger current variation with respect to MIPEDOT-GCE response with absence of CBZ.

Both Limit of detection (LOD) and limit of Quantification (LOQ) are terms utilized to describe the smallest concentration of the analyte that can be measured. LOD is defined as the lowest concentration that can be detected with a stated probability, although not quantified as an exact value. On the other hand, LOQ is defined as the lowest concentration that can be quantified with a specified acceptable precision and accuracy [26]. The LOD and LOQ were calculated with respect to the linear regression method [27] and found to be 2.04 and 6.2 μg/mL respectively. The biosensor's sensitivity is highly reliant on the CBZ extraction protocol from within the imprinted polymer. Therefore, through the optimization of the extraction protocol, a larger number of CBZ molecules would free up more gaps within the polymer and enhance detection. Additionally, sensitivity may be enhanced through increasing the conductivity and surface area of the polymer. The latter can be accomplished by adding conductive graphene to the mixture.

5.2.5.7 Selectivity Tests

To test the selectivity of the fabricated sensor, we studied the sensor's response to two competing ASMs. Both PHT and VPA are routine ASMs which may be prescribed along with CBZ. Their therapeutic levels have been established to be 10-20 µg/mL [28] and 50-125 µg/mL respectively [27]. As such stock solutions of PHT and VPA were prepared by dissolving each drug in a methanol/water mixture (20:80). Concentrations were chosen to be with 1-150 µg/mL to cover a range wider than what has been therapeutically reported. Furthermore, the MIPEDOT-GCEs were incubated in each stock solution followed by constant stirring for 15 min. The electrodes were then left to dry before transferring them into a solution of PBS (PH=7.4) containing 0.01 M $[Fe(CN)_6]^{3-/4-}$ and 0.1 M KCl for CV testing. After applying a cyclic signal across Vcell with a potential range of -0.1 to +0.6 V and a period of 14 s applied for a duration of 42 s, no peak current change was measured. This confirms that the fabricated sensor is not influenced by drugs other than CBZ rendering it selective solely to CBZ.

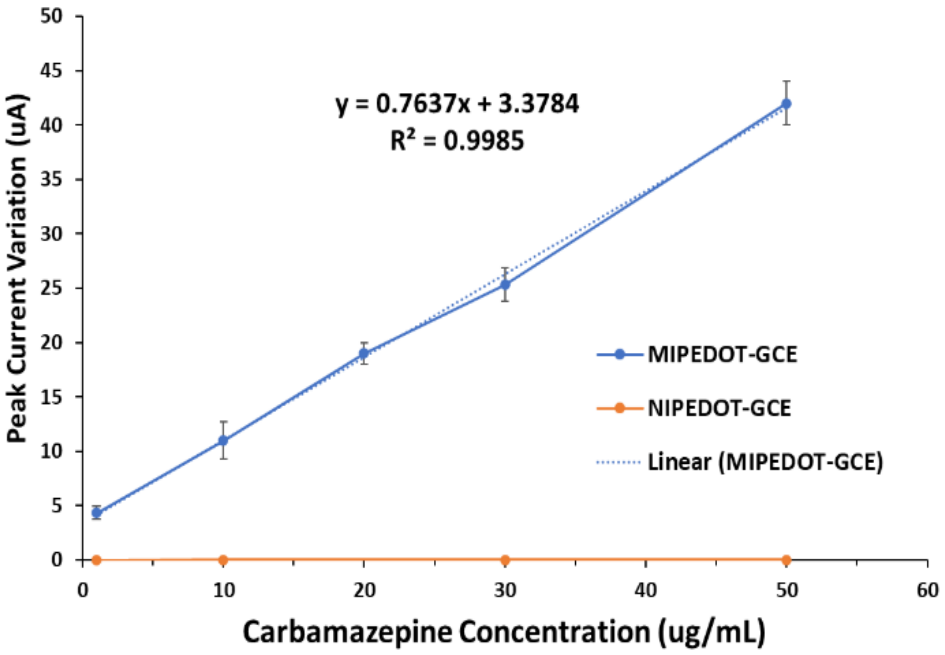

Figure 5.16 Calibration curve of peak current variation through modified MIPEDOT and NIPEDOT-GCE versus CBZ concentrations of 0 to 50 ug/mL

5.2.5.8 Stability Tests

Stability of the fabricated MIP electrodes was studied by recording their redox peak currents in a PBS solution containing 0.01 M $[Fe(CN)_6]^{3-/4-}$ and 0.1 M KCl while applying a cyclic cell voltage of -0.1 to +0.6 V with a period of 14 s for 42 s. Throughout a duration of 2 months, the electrodes showed no noticeable decline in performance and their respective peak currents remained constant.

5.2.5.9 Proposed Sensor's Advantages

Table 5.1 summarizes the most recent CBZ detection sensors based on electrochemical methods. Sensors are classified based on their selectivity and sensitivity and must possess both attributes in order to successfully target a molecule within a complex medium. Compared to the existing sensors, the proposed sensor is the only sensor capable of selective detection of CBZ, rendering it the most effective in complex media. Despite their superior sensitivity, existing sensors lack selectivity and therefore suffer from interfering drugs or substances. Additionally, another advantage of the proposed sensor is its ability to be tailored towards the detection of various drugs. This can be achieved by using another drug as a template while imprinting the PEDOT polymer. Hence, the proposed sensor is not limited to the detection of CBZ but potentially a wider variety of ASMs.

Table 5.1 Comparison with recent CBZ electrochemical-based detection sensors

Material	**Method**	**LOD**	**Selectivity**	**Reference**
GO-g-C3N4	Amp.	10.5 nM	No	[7]
NiSe2	Amp.	18.2 nM	No	[29]
Au@AgPdNPs-β-CD-IL/GCE	CV	0.089 μM	No	[30]
Ce-ZnO/rGO/GCE	DPV	1.2 nM	No	[31]
MIPEDOT-GCE	CV	8.6 μM	**Yes**	This work

5.2.5.10 Future Work and Limitations

In the present study, a simplified architecture potentiostat was implemented for electrochemical measurements. However, signal to noise ratio and sensitivity could be greatly improved by using a differential potentiostat topology as suggested in [32] along with proper offset cancelation [33]. Additionally, the use of a multichannel potentiostat [34] would enable concurrent measurements and greatly reduce measurement time whilst enhancing sensitivity and sensor's performance.

Furthermore, the use of integrated electrodes may greatly improve signal to noise ratio by eliminating the effect of connectors thus enhancing sensors sensitivity. Along with that, it is of great importance to optimize the CBZ extraction protocol liberating more imprinted sites for better template removal.

5.2.6 Conclusion

The presented biosensor is intended for therapeutic drug monitoring of patients with epilepsy through the electropolymerization of molecular imprinted PEDOT on GCEs, and the successful detection and quantification of CBZ molecules. It is composed of a TSMC180nm CMOS chip coupled with a 3-electrode electrochemical cell. The circuit operates at a nominal supply voltage of 3.3 V and is capable of performing CV required for both PEDOT polymerization and CBZ detection. A cyclic input signal with a potential range of 0 to +1.4 V and a period of 28 s was applied for 280 s to successfully polymerize molecular imprinted PEDOT on the GCE's surface. This was validated by SEM images presenting the uniform deposition and porous morphology of the polymer.

Furthermore, a cyclic input signal with a potential range of -0.1 to +0.6 V and a period of 14 s was applied for 42 s to trigger the redox currents of the mediator pair $[Fe(CN)_6]^{3-/4-}$ enabling the successful quantification of CBZ molecules entrapped within the polymer matrix. The LOD and LOQ of the biosensor were found to be 2.04 and 6.2 μg/mL respectively. These values are significantly better than previously reported values of 231.5 and 791.0 μg/mL respectively [22]. Additionally, the sensors were selectivity validated by incubation in PHT and VPA. No response due to such incubation was measured. Further sensor optimization could be done by integrating the

electrodes withing the chip, enabling multi-channel detection, and enhancing the potentiostat's performance by increasing its signal-to-noise ratio.

5.2.7 Acknowledgments

The authors would like to thank NSERC Canada for funding the research, along with Dr. Steen B. Schougaard for offering access to his facilities.

5.2.8 References

[1] R. D. Thijs, R. Surges, T. J. O'Brien, and J. W. Sander, "Epilepsy in adults," The Lancet, vol. 393, no. 10172, pp. 689–701, 2019.

[2] S. L. Moshé, E. Perucca, P. Ryvlin, and T. Tomson, "Epilepsy: new advances," The Lancet, vol. 385, no. 9971, pp. 884–898, 2015.

[3] N. Lavanya, C. Sekar, S. Ficarra, E. Tellone, A. Bonavita, SG. Leonardi, and G Neri, "A novel disposable electrochemical sensor for determination of carbamazepine based on Fe doped SnO2 nanoparticles modified screen-printed carbon electrode," Materials Science and Engineering: C, vol. 62, pp. 53–60, 2016.

[4] WY. Lin, ML. Pan, HY. Wang, YO. Su, and PW. Huang, "Analysis of carbamazepine serum by differential pulse voltammetry (DPV) and comparison with fluorescence polarization immunoassay (FPIA): an animal study," Medicinal Chemistry Research, vol. 21, no. 12, pp. 4389–4394, 2012.

[5] HY. Wang, ML. Pan, YL. O. Su, SC. Tsai, CH. Kao, SS. Sun, and WY. Lin, "Comparison of Differential Pulse Voltammetry (DPV)—a new method of carbamazepine analysis—with Fluorescence Polarization Immunoassay (FPIA)," Journal of Analytical Chemistry, vol. 66, no. 4, pp. 415–420, 2011.

[6] ML. Pan, WY. Lin, HY. Wang, SC. Tsai, PF. Hsieh, YLO Su, and PW. Huang, "Determination of carbamazepine: a comparison of the differential pulse voltammetry

(DPV) method and the immunoassay method in a clinical trial," Journal of analytical chemistry, vol. 69, no. 1, pp. 57–61, 2014.

[7] P. Balasubramanian, TST. Balamurugan, SM. Chen, TW, Chen, M. A. Ali, F. MA. Al-Hemaid, and MS. Elshikh. "An amperometric sensor for low level detection of antidepressant drug carbamazepine based on graphene oxide-g-C3N4 composite film modified electrode," Journal of The Electrochemical Society, vol. 165, no. 3, pp. B160–B166, 2018.

[8] B. Unnikrishnan, V. Mani, and SM. Chen, "Highly sensitive amperometric sensor for carbamazepine determination based on electrochemically reduced graphene oxide--single-walled carbon nanotube composite film," Sensors and Actuators B: Chemical, vol. 173, pp. 274–280, 2012.

[9] C. A. A. de Almeida, C. GB. Brenner, L. Minetto, C. A. Mallmann, and A. F. Martins, "Determination of anti-anxiety and anti-epileptic drugs in hospital effluent and a preliminary risk assessment," Chemosphere, vol. 93, no. 10, pp. 2349–2355, 2013.

[10] R. H. C. Queiroz, C. Bertucci, W. R. Malfará, S. A. C. Dreossi, A. R. Chaves, D. A. R. Valério, and M. E. C. Queiroz, "Quantification of carbamazepine, carbamazepine-10, 11-epoxide, phenytoin and phenobarbital in plasma samples by stir bar-sorptive extraction and liquid chromatography," Journal of pharmaceutical and biomedical analysis, vol. 48, no. 2, pp. 428–434, 2008.

[11] N. M. Shah, AF. Hawwa, JS. Millership, PS. Collier, and JC. McElnay, "A simple bioanalytical method for the quantification of antiepileptic drugs in dried blood spots," Journal of Chromatography B, vol. 923, pp. 65–73, 2013.

[12] HN Deepakumari, and HD Revanasiddappa, "Development and Validation of a UV-Spectrophotometric Method for the Quantitative Determination of Oxcarbazepine and Study of its Degradation Profile," Chemical Sciences Journal, vol. 5, 2014.

[13] B. Liu, D. Tang, B. Zhang, X. Que, H. Yang, and G. Chen, "Au (III)-promoted magnetic molecularly imprinted polymer nanospheres for electrochemical determination of streptomycin residues in food," Biosensors and Bioelectronics, vol. 41, pp. 551-556, 2013.

[14] G. Cai, Z. Yu, and D. Tang, “Actuating photoelectrochemical sensing sensitivity coupling core-core-shell Fe3O4@ C@ TiO2 with molecularly imprinted polypyrrole,” Talanta, vol. 219, p. 121341, 2020.

[15] H. Karimi-Maleh et al., “A novel detection method for organophosphorus insecticide fenamiphos: Molecularly imprinted electrochemical sensor based on core-shell Co3O4@ MOF-74 nanocomposite,” Journal of colloid and interface science, vol. 592, pp. 174-185, 2021.

[16] M. Beytur et al., “A highly selective and sensitive voltammetric sensor with molecularly imprinted polymer based silver@ gold nanoparticles/ionic liquid modified glassy carbon electrode for determination of ceftizoxime,” Journal of Molecular Liquids, vol. 251, pp. 212-217, 2018.

[17] M. L. Yola and N. Atar, “Development of molecular imprinted sensor including graphitic carbon nitride/N-doped carbon dots composite for novel recognition of epinephrine,” Composites Part B: Engineering, vol. 175, p. 107113, 2019.

[18] N. Özcan, H. Medetalibeyoglu, O. Akyıldırım, N. Atar, and M. L. Yola, “Electrochemical detection of amyloid-β protein by delaminated titanium carbide MXene/multi-walled carbon nanotubes composite with molecularly imprinted polymer,” Materials Today Communications, vol. 23, p. 101097, 2020.

[19] C. Bodart et al., “Electropolymerized poly (3, 4-ethylenedioxythiophene)(PEDOT) coatings for implantable deep-brain-stimulating microelectrodes,” ACS applied materials & interfaces, vol. 11, no. 19, pp. 17226-17233, 2019.

[20] R. Zeng et al., “CRISPR-Cas12a-driven MXene-PEDOT: PSS piezoresistive wireless biosensor,” Nano Energy, vol. 82, p. 105711, 2021.

[21] L. Huang, Z. Yu, J. Chen, and D. Tang, “Pressure-Based Bioassay Perceived by a Flexible Pressure Sensor with Synergistic Enhancement of the Photothermal Effect,” ACS Applied Bio Materials, vol. 3, no. 12, pp. 9156-9163, 2020.

[22] A. Hammoud, D. Chhin, D. Nguyen, and M. Sawan, “A new molecular imprinted PEDOT glassy carbon electrode for carbamazepine detection,” Biosensors and Bioelectronics, vol. 180, p. 113089, 2021.

[23] C. Lei, Y. Pu-Xuan, F. You-Jun, Z. Hua-Hong, and L. Hong, “Mathematical Expression and Quantitative Analysis of Impedance Spectrum on the Interface of Glassy Carbon Electrode,” Journal of Electrochemistry, p. 201, 2020.

[24] B. Chen et al., “Penetrating glassy carbon neural electrode arrays for brain-machine interfaces,” Biomedical Microdevices, vol. 22, pp. 1-10, 2020.

[25] M. M. Ahmadi and G. A. Jullien, “Current-mirror-based potentiostats for three-electrode amperometric electrochemical sensors,” IEEE Transactions on Circuits and Systems I: Regular Papers, vol. 56, no. 7, pp. 1339-1348, 2008.

[26] E.-P. Replaces, “Protocols for determination of limits of detection and limits of quantitation; approved guideline.”

[27] A. Shrivastava and V. B. Gupta, “Methods for the determination of limit of detection and limit of quantitation of the analytical methods,” Chronicles of young scientists, vol. 2, no. 1, pp. 21-25, 2011.

[28] A. Jain, I. Haque, V. Tayal, and V. Roy, “Valproic acid-induced acute pancreatitis,” Indian journal of psychiatry, vol. 61, no. 4, p. 421, 2019.

[29] S. Veeralingam and S. Badhulika, “Two-Dimensional Metallic NiSe2 Nanoclusters–Based Low-Cost, Flexible, Amperometric Sensor for Detection of Neurological Drug Carbamazepine in Human Sweat Samples,” Frontiers in Chemistry, vol. 8, p. 337, 2020.

[30] L. Daneshvar and G. H. Rounaghi, “An electrochemical sensing platform for carbamazepine determination based on trimetallic Au-Ag-Pd dendritic nanopatricles, supramolecular β-cyclodextrin and [bmim] NTF2 ionic liquids,” Journal of The Electrochemical Society, vol. 164, no. 6, p. B177, 2017.

[31] N. Dhanalakshmi, T. Priya, and N. Thinakaran, “Highly electroactive Ce-ZnO/rGO nanocomposite: ultra-sensitive electrochemical sensing platform for carbamazepine determination,” Journal of Electroanalytical Chemistry, vol. 826, pp. 150-156, 2018.

[32] S. Subhan, S. Khapli, Y.-A. Song, and S. Ha, “A Fully Differential Potentiostat Circuit with Integrated Time-based ADCs,” in 2019 IEEE Biomedical Circuits and Systems Conference (BioCAS), 2019: IEEE, pp. 1-4.

[33] M. Duwe and T. Chen, “Low power integrated potentiostat design for μ electrodes with improved accuracy,” in 2011 IEEE 54th International Midwest Symposium on Circuits and Systems (MWSCAS), 2011: IEEE, pp. 1-4.

[34] G. Massicotte, S. Carrara, G. Di Micheli, and M. Sawan, “A CMOS amperometric system for multi-neurotransmitter detection,” IEEE transactions on biomedical circuits and systems, vol. 10, no. 3, pp. 731-741, 2016.

CHAPTER 6 GENERAL DISCUSSION

The aim of this thesis was to successfully detect and monitor ASMs within blood, in order to provide clinicians with valuable information aiding them in personalized therapeutic treatments. Specifically, the objective of the research was to design and fabricate a miniature biosensor possessing the capabilities of both selective and precise detection. Blood is a very complex medium in which multiple molecules co-exist; this poses a challenge to selective detection. It is often impossible to quantify a molecule without the need of sophisticated methods. Furthermore, existing selective ASM quantification techniques rely on bulky equipment and tedious sample preparation. Therefore, designing such biosensor requires providing solutions to two major challenges.

The first challenge is implementing a detection technique capable of being integrated within a lab-on-chip. Hence, the utilization of CMOS technology to design an electrochemical based sensor as provided in chapter 3. Electrochemical techniques consume little power, require low sampling times and low sample quantities with least destruction. Furthermore, EIS is an electrochemical technique which provided a linear response with different CBZ concentrations based on the variation of electrical impedance on the electrode's surface. Despite the high precision offered by that technique, it lacked the ability of selective detection.

The second challenge in designing the biosensor was enabling it to selectively detect ASM molecules whilst relying on electrochemical techniques. The electrode is susceptive to various interactions at its surface and multiple molecules might have a similar effect on the electrode's impedance or conductive characteristics. Therefore, the isolation of the targeted molecule's response is necessary. In chapter 4 of this thesis, we presented a MIP technique capable of selective binding to ASMs. Once the targeted molecule binds to the MIP at the electrode's surface, electrochemical detection is employed for characterization. The performed study utilizing a large scale commercial potentiostat showed that CBZ molecules were successfully entrapped within the polymer matrix and had an isolated effect on the electrode's electrochemical response. Thus, the second challenge was overcome.

With the above two solutions, we were finally able to design and fabricate a miniature biosensor capable of selective detection and quantification of ASM based on electrochemical detection. Chapter 4 presents a 0.5 x 0.5 mm^2 CMOS biosensor chip fabricated in TSMC180nm technology. The biosensor, through CV, polymerizes a uniform layer of MIPEDOT on the electrode's surface

and enables the quantification of the imprinted molecules. The LOD of the proposed biosensor was 2.04 μg/mL which suits our application. Additionally, the biosensor showed no response to tested competing molecules within the medium, such as phenytoin and valproic acid. Hence, selective detection is obtained.

The proposed biosensor presents a promising solution to therapeutic drug monitoring capable of fast, label-free and cost-effective ASM detection. Moreover, the proposed approach can be utilized in diverse applications and for the detection of various molecules.

CHAPTER 7 CONCLUSION AND RECOMMENDATIONS

7.1 Conclusion

Epilepsy is the most-common neurological disease after stroke and the first line-of treatment is through the prescription of ASMs. Unfortunately, to date, no direct relationship has been established between treatment and the prescribed drugs. There also exists no biosensor capable of constantly monitoring ASM concentrations within blood. The ability to monitor ASM concentrations would enormously aid in personalized medicine permitting clinicians to have more data when treated epileptic patients. In this thesis we presented the first biosensor combining electrochemical CV detection with MIP technology. This biosensor provides excellent selectivity, which is often hard to obtain with miniature detection systems. Despite its high sensitivity, the biosensor offers great selectivity towards the targeted drug, thanks to molecular imprinting.

The biosensor comprised of two main blocks, a potentiostat as the transducing element, and a MIP electrode as part of its biosensing element. This tandem allows implementing the biosensing element capable of targeting and binding to the ASM of interest, and in turns, the transducing element measures the signal vs concentration present at the electrode's surface. CV is the adopted electrochemical technique that was successfully exploited in the implemented micro-chip solution.

The formation of a biocompatible and conductive polymer, PEDOT, was conducted through CV and validated through SEM images. This was shown to increase the conductivity at the electrode's surface. Furthermore, template imprinting within the polymer along with the template's extraction were validated by studying the redox peaks of cyclic voltammograms and by conducting UV-vis spectroscopy. Finally, the successful binding and detection of ASM CBZ was studied by CV in order to generate a calibration curve of CBZ concentrations vs redox currents.

The proposed sensor was highly sensitive with a LOD of 2.04 μg/mL. This selectivity was confirmed by showing that there were no recorded signals generated by interfering drugs. It is simple to construct, easy to operate and was tested within PBS, which possesses characteristics similar to human blood. We believe that the proposed sensor is a great step towards personalized medicine and may be effective in epileptic treatment by informing clinicians about ASM concentrations in order to explore the relationship between drug concentrations and effective treatment.

7.2 Research contributions

The main contribution of this research is the fabrication of a biosensor based on MIP technology capable of fully detecting and quantifying the concentrations of ASMs. Aided by a MIP for selective detection, the sensor may be utilized to detect any ASM of interest. Following detection, CV is deployed in order to measure the concentration of the drug. The biosensor was constructed in CMOS technology and tested in PBS. Detailed contributions are listed below:

1. **Design and simulation of a CMOS electrical impedance spectroscopy-based system capable of detecting the electrical impedance at an electrode's surface along with conducting EIS *in vitro* measurements on CBZ molecules.**

   This was an initial approach to quantify ASMs based on their effect on the electrical impedance of the electrode's surface. *In vitro* measurements illustrated that indeed CBZ concentration in a solution has a linear relationship with the electrical impedance of gold electrode's surface. However, due to multiple factors that might affect impedance in a complex medium, EIS alone cannot be adopted for selective detection.

2. **Design and synthesis of CBZ selective electrodes which in tandem with CV as an electrochemical technique could both bind to CBZ within a complex medium and enable quantification.**

   As a solution to the selectivity drawback in existing miniature biosensors, an electrode based on the molecular imprinting of CBZ molecules was synthesized. Cyclic voltammetry graphs illustrated the electrode's effectiveness in targeting CBZ molecules. Furthermore, the redox currents of the redox pair $[Fe(CN)_6]^{3-/4-}$ illustrated a direct correlation with CBZ concentrations.

3. **Design and fabrication of a miniature CMOS biosensor capable of performing the necessary electrochemical techniques to synthesize the imprinted polymer and enable selective detection of CBZ.**

   We combined the sensitivity of a miniature electrochemical sensor to the selectivity of the proposed electrodes. CV was conducted to successfully imprint and form the polymer on the electrode's surface. Again, CV was utilized in order to record the redox current variations due to the change on CBZ concentrations within the solution. The biosensor

achieved great sensitivity and selectivity and may be useful for the detection of a vast selection of drugs.

7.3 Recommendations for future work

Despite its effectiveness and high precision, there are numerous potential improvements which may be applied to the proposed biosensor. Amongst these improvements are enhancing the potentiostat design, designing a multi-channel system, integrating the electrode setup within the CMOS chip, studying the sensor's stability in biological conditions, studying the impact of different fabrication parameters on the electrode's quality, improving the polymer's thickness, improving the extraction protocol and enabling multi-ASM imprinting.

1. The potentiostat is the main electrical component of the biosensor and plays a vital role in sensor's sensitivity. Single input systems similar to the one proposed suffer from background currents that are not related to the concentration of the targeted molecule. That current may be generated by various sources, such as interfering electro-active molecules and capacitive current in the electrical double layer. This problem can be eliminated with a differential input topology. Indeed, the addition of a second WE electrode and adopting a differential configuration minimizes the propagation of unwanted background signals and hence, improves sensor's sensitivity and signal-to-noise ratio.
2. A multi-channel electrode array system may greatly increase throughput. The addition of an electrode array presents more statistical data to the user enabling various data processing applications such as signal averaging and outlier elimination. Developing such approach could lead to implementing high electrode density arrays of 8x8, 64x64, and 124x124.
3. Furthermore, for high-throughput applications, it would be helpful to integrate the electrodes within a CMOS chip. This has several advantages, such as the optimization of the distance between the WE, RE and the CE, and reducing noise due to unwanted wiring and connections. In order to generate accurate measurements, it is important to have a fixed distance between the electrodes, this condition could always be satisfied with the use of integrated electrode arrays. Also, integrated arrays with close proximity to the transducing unit eliminates the need for long wiring that tend to add unnecessary noise to the system.

4. Various factors play an important role in the sensors ability to target a wider concentration of ASM and its reproducibility. Amongst these factors are the polymer's thickness and the template extraction protocol. Therefore, studying the effect of the polymer's thickness versus the number of imprinted sites would greatly help optimize the sensors' performance. Furthermore, adopting an extraction technique that is capable of fully freeing up the imprinted gaps post quantification would increase the linear range of the sensor's operation.
5. Finally, the sensor has a great potential of imprinting various ASM. As a proof of concept, CBZ was chosen to be imprinted within the polymer matrix. However, it is possible to imprint a wide variety of ASMs. This is especially important in the context of epileptic treatment, since often, multiple drugs are prescribed concurrently. Hence, the detection and quantification of a wider variety of ASMs is necessary.

REFERENCES

[1] R. D. Thijs, R. Surges, T. J. O'Brien, and J. W. Sander, "Epilepsy in adults," *The Lancet,* vol. 393, no. 10172, pp. 689-701, 2019.

[2] S. Liu, W. Yu, and Y. Lü, "The causes of new-onset epilepsy and seizures in the elderly," *Neuropsychiatric disease and treatment,* vol. 12, p. 1425, 2016.

[3] M. M. Goldenberg, "Overview of drugs used for epilepsy and seizures: etiology, diagnosis, and treatment," *Pharmacy and Therapeutics,* vol. 35, no. 7, p. 392, 2010.

[4] M. Bialer, "Extended-release formulations for the treatment of epilepsy," *CNS drugs,* vol. 21, no. 9, pp. 765-774, 2007.

[5] V. K. Sehgal and R. Kumar, "Phenytoin beyond Epilepsy," *International Journal of Medical and Dental Sciences,* vol. 4, no. 2, pp. 743-744, 2018.

[6] K. Mani, G. Rangan, H. Srinivas, V. Sridharan, and D. Subbakrishna, "Epilepsy control with phenobarbital or phenytoin in rural south India: the Yelandur study," *The Lancet,* vol. 357, no. 9265, pp. 1316-1320, 2001.

[7] J. Patocka, Q. Wu, E. Nepovimova, and K. Kuca, "Phenytoin–An anti-seizure drug: Overview of its chemistry, pharmacology and toxicology," *Food and Chemical Toxicology,* vol. 142, p. 111393, 2020.

[8] L. Dean, "Phenytoin therapy and HLA-B* 15: 02 and CYP2C9 genotypes," 2017.

[9] A. Beydoun, S. DuPont, D. Zhou, M. Matta, V. Nagire, and L. Lagae, "Current role of carbamazepine and oxcarbazepine in the management of epilepsy," *Seizure,* vol. 83, pp. 251-263, 2020.

[10] A. P. Santhosh *et al.,* "Carbamazepine versus levetiracetam in epilepsy due to neurocysticercosis," *Acta Neurologica Scandinavica,* vol. 143, no. 3, pp. 242-247, 2021.

[11] A. Zybina *et al.,* "Nanoparticle-based delivery of carbamazepine: A promising approach for the treatment of refractory epilepsy," *International journal of pharmaceutics,* vol. 547, no. 1-2, pp. 10-23, 2018.

[12] Y. Al Khalili, S. Sekhon, and S. Jain, "Carbamazepine toxicity," *StatPearls [Internet],* 2020.

[13] S. Chateauvieux, F. Morceau, M. Dicato, and M. Diederich, "Molecular and therapeutic potential and toxicity of valproic acid," *Journal of Biomedicine and Biotechnology,* vol. 2010, 2010.

[14] M. Romoli *et al.*, "Valproic acid and epilepsy: from molecular mechanisms to clinical evidences," *Current neuropharmacology,* vol. 17, no. 10, pp. 926-946, 2019.

[15] M. Rahman and H. Nguyen, "Valproic Acid," *StatPearls [Internet],* 2021.

[16] A. Jain, I. Haque, V. Tayal, and V. Roy, "Valproic acid-induced acute pancreatitis," *Indian journal of psychiatry,* vol. 61, no. 4, p. 421, 2019.

[17] K. S. McKeating, A. Aubé, and J.-F. Masson, "Biosensors and nanobiosensors for therapeutic drug and response monitoring," *Analyst,* vol. 141, no. 2, pp. 429-449, 2016.

[18] I. J. Arfman, E. A. Wammes-van der Heijden, P. G. Ter Horst, D. A. Lambrechts, I. Wegner, and D. J. Touw, "Therapeutic drug monitoring of antiepileptic drugs in women with epilepsy before, during, and after pregnancy," *Clinical pharmacokinetics,* vol. 59, no. 4, pp. 427-445, 2020.

[19] F. Polo and G. Toffoli, "Point-of-care for therapeutic drug monitoring of antineoplastic drugs," *Med. Chem.(Los. Angeles),* vol. 6, no. 6, 2016.

[20] R. Griss *et al.*, "Bioluminescent sensor proteins for point-of-care therapeutic drug monitoring," *Nature chemical biology,* vol. 10, no. 7, pp. 598-603, 2014.

[21] L.-S. Huang, Y. Pheanpanitporn, Y.-K. Yen, K.-F. Chang, L.-Y. Lin, and D.-M. Lai, "Detection of the antiepileptic drug phenytoin using a single free-standing piezoresistive microcantilever for therapeutic drug monitoring," *Biosensors and Bioelectronics,* vol. 59, pp. 233-238, 2014.

[22] S. Carrara, A. Cavallini, V. Erokhin, and G. De Micheli, "Multi-panel drugs detection in human serum for personalized therapy," *Biosensors and Bioelectronics,* vol. 26, no. 9, pp. 3914-3919, 2011.

[23] A. Lacam and C. Chateau, "High-pressure measurements at moderate temperatures in a diamond anvil cell with a new optical sensor: SrB4O7: Sm2+," *Journal of Applied Physics,* vol. 66, no. 1, pp. 366-372, 1989.

[24] B. H. Weigl *et al.*, "Optical triple sensor for measuring pH, oxygen and carbon dioxide," *Journal of biotechnology,* vol. 32, no. 2, pp. 127-138, 1994.

[25] S. Unser, I. Bruzas, J. He, and L. Sagle, "Localized surface plasmon resonance biosensing: current challenges and approaches," *Sensors,* vol. 15, no. 7, pp. 15684-15716, 2015.

[26] V. Myroshnychenko *et al.*, "Modelling the optical response of gold nanoparticles," *Chemical Society Reviews,* vol. 37, no. 9, pp. 1792-1805, 2008.

[27] K. C. Bantz *et al.*, "Recent progress in SERS biosensing," *Physical chemistry chemical physics,* vol. 13, no. 24, pp. 11551-11567, 2011.

[28] R. L. McCreery, *Raman spectroscopy for chemical analysis*. John Wiley & Sons, 2005.

[29] R. Aroca, *Surface-enhanced vibrational spectroscopy*. John Wiley & Sons, 2006.

[30] C. I. Cheng, Y.-P. Chang, and Y.-H. Chu, "Biomolecular interactions and tools for their recognition: focus on the quartz crystal microbalance and its diverse surface chemistries and applications," *Chemical Society Reviews,* vol. 41, no. 5, pp. 1947-1971, 2012.

[31] C. Sousa *et al.*, "Direct and fast detection of Alexandrium minutum algae by using high frequency microbalance," *Journal of microbiological methods,* vol. 104, pp. 49-54, 2014.

[32] P. Samorì, *STM and AFM Studies on (bio) molecular Systems: Unravelling the Nanoworld*. Springer Science & Business Media, 2009.

[33] F. Huber, H. Lang, N. Backmann, D. Rimoldi, and C. Gerber, "Direct detection of a BRAF mutation in total RNA from melanoma cells using cantilever arrays," *Nature nanotechnology,* vol. 8, no. 2, pp. 125-129, 2013.

[34] K. M. Hansen *et al.*, "Cantilever-based optical deflection assay for discrimination of DNA single-nucleotide mismatches," *Analytical Chemistry,* vol. 73, no. 7, pp. 1567-1571, 2001.

[35] G. Wu, R. H. Datar, K. M. Hansen, T. Thundat, R. J. Cote, and A. Majumdar, "Bioassay of prostate-specific antigen (PSA) using microcantilevers," *Nature biotechnology,* vol. 19, no. 9, pp. 856-860, 2001.

[36] D. Skoog, D. West, F. Holler, and S. Crouch, "Fundamentals of analytical chemistry: Nelson Education," *Fundamentals of Analytical Chemistry:,* 2013.

[37] F. A. Settle, *Handbook of instrumental techniques for analytical chemistry*. Prentice Hall PTR, 1997.

[38] S. Jansod, M. G. Afshar, G. A. Crespo, and E. Bakker, "Phenytoin speciation with potentiometric and chronopotentiometric ion-selective membrane electrodes," *Biosensors and Bioelectronics,* vol. 79, pp. 114-120, 2016.

[39] Y. K. Al-Bayati and R. R. Karabat, "Potentiometric Study of Phenytoin–PVC Membrane Electrodes for Determination of Phenytoin in pharmaceutical preparations."

[40] H. Wang *et al.*, "Comparison of Differential Pulse Voltammetry (DPV)—a new method of carbamazepine analysis—with Fluorescence Polarization Immunoassay (FPIA)," *Journal of Analytical Chemistry*, vol. 66, no. 4, pp. 415-420, 2011.

[41] E. T. ACAR and A. N. Onar, "Square wave voltammetric determination of valproic acid in pharmaceutical Preparations," *Turkish Journal of Chemistry*, vol. 40, no. 1, pp. 106-116, 2016.

[42] H. Haruta, *The impedance measurement handbook: a guide to measurement technology and techniques*. Agilent Technologies, 2000.

[43] J. S. Daniels and N. Pourmand, "Label-free impedance biosensors: Opportunities and challenges," *Electroanalysis*, vol. 19, no. 12, pp. 1239-1257, 2007.

[44] A. Johnson, Q. Song, P. Ko Ferrigno, P. R. Bueno, and J. J. Davis, "Sensitive affimer and antibody based impedimetric label-free assays for C-reactive protein," *Analytical chemistry*, vol. 84, no. 15, pp. 6553-6560, 2012.

[45] F. Lisdat and D. Schäfer, "The use of electrochemical impedance spectroscopy for biosensing," *Analytical and bioanalytical chemistry*, vol. 391, no. 5, pp. 1555-1567, 2008.

[46] A. Hammoud, D. Nguyen, and M. Sawan, "Detection methods and tools of administered anti-epileptic drugs-a review," *Biosens Bioelectron Open Acc: BBOA-146. DOI*, vol. 10, pp. 2577-2260, 2018.

[47] M. Cremer, *Über die Ursache der elektromotorischen Eigenschaften der Gewebe, zugleich ein Beitrag zur Lehre von den polyphasischen Elektrolytketten*. R. Oldenbourg, 1906.

[48] W. R. Heineman and W. B. Jensen, "Leland c. clark jr.(1918–2005)," *Biosensors and Bioelectronics*, vol. 8, no. 21, pp. 1403-1404, 2006.

[49] B. Nikhil, J. Pawan, F. Nello, and E. Pedro, "Introduction to biosensors," *Essays Biochem*, vol. 60, no. 1, pp. 1-8, 2016.

[50] P. Mehrotra, "Biosensors and their applications–A review," *Journal of oral biology and craniofacial research*, vol. 6, no. 2, pp. 153-159, 2016.

[51] A. Turner, I. Karube, and G. S. Wilson, *Biosensors: fundamentals and applications*. Oxford university press, 1987.

[52] D. G. Myszka and R. L. Rich, "Implementing surface plasmon resonance biosensors in drug discovery," *Pharmaceutical science & technology today,* vol. 3, no. 9, pp. 310-317, 2000.

[53] N. Formisano *et al.,* "Optimisation of an electrochemical impedance spectroscopy aptasensor by exploiting quartz crystal microbalance with dissipation signals," *Sensors and Actuators B: Chemical,* vol. 220, pp. 369-375, 2015.

[54] P. Jolly, N. Formisano, and P. Estrela, "DNA aptamer-based detection of prostate cancer," *Chemical Papers,* vol. 69, no. 1, pp. 77-89, 2015.

[55] P. Jolly, N. Formisano, J. Tkáč, P. Kasák, C. G. Frost, and P. Estrela, "Label-free impedimetric aptasensor with antifouling surface chemistry: A prostate specific antigen case study," *Sensors and Actuators B: Chemical,* vol. 209, pp. 306-312, 2015.

[56] G. Rea *et al.*, "Structure-based design of novel Chlamydomonas reinhardtii D1-D2 photosynthetic proteins for herbicide monitoring," *Protein Science,* vol. 18, no. 10, pp. 2139-2151, 2009.

[57] V. Scognamiglio *et al.,* "Biosensors for effective environmental and agrifood protection and commercialization: from research to market," *Microchimica Acta,* vol. 170, no. 3, pp. 215-225, 2010.

[58] D. D. Reddy, *Biosensors and bioelectronics*. New Delhi: I K International Publishing House (in English), 2013.

[59] C. Lowe, "An introduction to the concepts and technology of biosensors," *Biosensors,* vol. 1, no. 1, pp. 3-16, 1985.

[60] E. P. Replaces, "Protocols for determination of limits of detection and limits of quantitation," *Approved Guideline,* 2004.

[61] K. L. Adams, M. Puchades, and A. G. Ewing, "In vitro electrochemistry of biological systems," *Annu. Rev. Anal. Chem.,* vol. 1, pp. 329-355, 2008.

[62] P. N. Patsalos *et al.,* "Antiepileptic drugs—best practice guidelines for therapeutic drug monitoring: a position paper by the subcommission on therapeutic drug monitoring, ILAE Commission on Therapeutic Strategies," *Epilepsia,* vol. 49, no. 7, pp. 1239-1276, 2008.

[63] S. L. Moshé, E. Perucca, P. Ryvlin, and T. Tomson, "Epilepsy: new advances," *The Lancet,* vol. 385, no. 9971, pp. 884-898, 2015.

[64] G. Bahrami, S. Mirzaeei, and A. Kiani, "Sensitive analytical method for Topiramate in human serum by HPLC with pre-column fluorescent derivatization and its application in human pharmacokinetic studies," *Journal of Chromatography B,* vol. 813, no. 1-2, pp. 175-180, 2004.

[65] T. Ishida, K. Kudo, M. Hayashida, and N. Ikeda, "Rapid and quantitative screening method for 43 benzodiazepines and their metabolites, zolpidem and zopiclone in human plasma by liquid chromatography/mass spectrometry with a small particle column," *Journal of Chromatography B,* vol. 877, no. 25, pp. 2652-2657, 2009.

[66] J. Kuhn, C. Götting, and K. Kleesiek, "Sample cleanup-free determination of mycophenolic acid and its glucuronide in serum and plasma using the novel technology of ultra-performance liquid chromatography–electrospray ionization tandem mass spectrometry," *Talanta,* vol. 80, no. 5, pp. 1894-1898, 2010.

[67] R. H. C. Queiroz *et al.*, "Quantification of carbamazepine, carbamazepine-10, 11-epoxide, phenytoin and phenobarbital in plasma samples by stir bar-sorptive extraction and liquid chromatography," *Journal of pharmaceutical and biomedical analysis,* vol. 48, no. 2, pp. 428-434, 2008.

[68] N. A. Santagati, R. Gotti, and G. Ronsisvalle, "Simultaneous determination of phenytoin and dextromethorphan in urine by solid-phase extraction and HPLC–DAD," *Journal of separation science,* vol. 28, no. 11, pp. 1157-1162, 2005.

[69] T. Vermeij and P. Edelbroek, "High-performance liquid chromatographic and megabore gas—liquid chromatographic determination of levetiracetam (ucb L059) in human serum after solid-phase extraction," *Journal of Chromatography B: Biomedical Sciences and Applications,* vol. 662, no. 1, pp. 134-139, 1994.

[70] A. Khedr, M. Moustafa, A. B. Abdel-Naim, A. Alahdal, and H. Mosli, "High-performance liquid chromatographic method for determination of phenytoin in rabbits receiving sildenafil," *Analytical chemistry insights,* vol. 3, p. ACI. S658, 2008.

[71] W. J. Lough and I. W. Wainer, *High performance liquid chromatography: fundamental principles and practice*. CRC press, 1995.

[72] V. R. Meyer, *Practical high-performance liquid chromatography*. John Wiley & Sons, 2013.

[73] D. L. Pavia, *Introduction to Organic Laboratory Techniques: Chemistry 36, Stanford University*. Thomson/Wadsworth, 2006.

[74] M. I. Churchwell, N. C. Twaddle, L. R. Meeker, and D. R. Doerge, "Improving LC–MS sensitivity through increases in chromatographic performance: Comparisons of UPLC–ES/MS/MS to HPLC–ES/MS/MS," *Journal of Chromatography B,* vol. 825, no. 2, pp. 134-143, 2005.

[75] B. Matuszewski, M. Constanzer, and C. Chavez-Eng, "Strategies for the assessment of matrix effect in quantitative bioanalytical methods based on HPLC− MS/MS," *Analytical chemistry,* vol. 75, no. 13, pp. 3019-3030, 2003.

[76] N. M. Shah, A. Hawwa, J. Millership, P. Collier, and J. McElnay, "A simple bioanalytical method for the quantification of antiepileptic drugs in dried blood spots," *Journal of Chromatography B,* vol. 923, pp. 65-73, 2013.

[77] X. Su *et al.*, "Dried blood spots: An evaluation of utility in the field," *Journal of infection and public health,* vol. 11, no. 3, pp. 373-376, 2018.

[78] R. S. George and S. J. Moat, "Effect of dried blood spot quality on newborn screening analyte concentrations and recommendations for minimum acceptance criteria for sample analysis," *Clinical chemistry,* vol. 62, no. 3, pp. 466-475, 2016.

[79] C. A. A. de Almeida, C. G. Brenner, L. Minetto, C. A. Mallmann, and A. F. Martins, "Determination of anti-anxiety and anti-epileptic drugs in hospital effluent and a preliminary risk assessment," *Chemosphere,* vol. 93, no. 10, pp. 2349-2355, 2013.

[80] H. Hashem, A. A. Gouda, and H. Saleh, "Development and validation of rapid stability indicating HPLC-determinations of antiepileptic drugs phenobarbital in suppositories and phenytoin in capsules as well as in urine sample," *Journal of Liquid Chromatography & Related Technologies,* vol. 36, no. 16, pp. 2292-2306, 2013.

[81] R. Shah and R. Shah, "Development and validation of RP-HPLC method for phenytoin sodium and phenobarbitone in bulk and pharmaceutical dosage form," *International Journal of Pharmacy and Pharmaceutical Sciences,* vol. 9, no. 10, pp. 224-229, 2017.

[82] N. Khansili, G. Rattu, and P. M. Krishna, "Label-free optical biosensors for food and biological sensor applications," *Sensors and actuators B: chemical,* vol. 265, pp. 35-49, 2018.

[83] W. W. Lee, C. P. McCoy, R. F. Donnelly, and S. E. Bell, "Swellable polymer films containing Au nanoparticles for point-of-care therapeutic drug monitoring using surface-enhanced Raman spectroscopy," *Analytica chimica acta,* vol. 912, pp. 111-116, 2016.

[84] P. Damborský, J. Švitel, and J. Katrlík, "Optical biosensors," *Essays in biochemistry,* vol. 60, no. 1, pp. 91-100, 2016.

[85] K. Basavaiah, N. Rajendraprasad, M. Cijo, K. Vinay, and P. Ramesh, "Development and validation of stability indicating spectrophotometric methods for determination of oxcarbazepine in pharmaceuticals," 2011.

[86] M. Gandhimathi and T. Ravi, "Use of Folin-Ciocalteu phenol reagent and 3-methyl-2-benzothiazolinone hydrazine hydrochloride in the determination of oxcarbazepine in pharmaceuticals," *Acta Pharmaceutica,* vol. 58, no. 1, p. 111, 2008.

[87] C. M. Krishna, S. V. Rao, N. M. Rao, and C. Rambabu, "Spectrophotometric determination of Oxcarbazepine by condensation reactions using 2-chlorophenylhydrazine and anthranilic acid," *Journal of Pharmacy Research,* vol. 10, no. 4, pp. 3317-3319, 2011.

[88] N. Rajendraprasad, K. Basavaiah, and K. Vinay, "Application of 3-methylbenzothiazolin-2-one hydrazone for the quantitative spectrophotometric determination of oxcarbazepine in pharmaceuticals with cerium (IV) and periodate," *Journal of Applied Spectroscopy,* vol. 79, no. 4, pp. 616-625, 2012.

[89] N. Rajendraprasad, K. Basavaiah, and K. B. Vinay, "Titrimetric and spectrophotometric assay of oxcarbazepine in pharmaceuticals using N-bromosuccinimide and bromopyrogallol red," *International journal of analytical chemistry,* vol. 2011, 2011.

[90] C. Ramaa, P. Chothe, A. Naik, and V. Kadam, "Spectrophotometric method for the estimation of oxcarbazepine in tablets," *Indian journal of pharmaceutical sciences,* vol. 68, no. 2, 2006.

[91] H. Revanasiddappa, H. Deepakumari, and S. Mallegowda, "Development and validation of indirect spectrophotometric methods for lamotrigine in pure and the tablet dosage forms," *Analele Universitatii din Bucuresti-Chimie,* vol. 20, no. 1, pp. 49-55, 2011.

[92] H. Deepakumari and H. Revanasiddappa, "Development and validation of a uvspectrophotometric method for the quantitative determination of oxcarbazepine and study of its degradation profile," *Chemical Science Journal,* vol. 5, p. 1, 2014.

[93] Z. Rezaei, B. Hemmateenejad, S. Khabnadideh, and M. Gorgin, "Simultaneous spectrophotometric determination of carbamazepine and phenytoin in serum by PLS regression and comparison with HPLC," *Talanta,* vol. 65, no. 1, pp. 21-28, 2005.

[94] J. A. Arancibia, A. C. Olivieri, and G. M. Escandar, "First-and second-order multivariate calibration applied to biological samples: determination of anti-inflammatories in serum and urine," *Analytical and bioanalytical chemistry,* vol. 374, no. 3, pp. 451-459, 2002.

[95] A. M. de la Peña, M. Moreno, I. Durán-Merás, and F. Salinas, "Synchronous fluorimetric determination of salicylic acid and diflunisal in human serum using partial least-squares calibration," *Talanta,* vol. 43, no. 8, pp. 1349-1356, 1996.

[96] E. Dinç, C. Serin, F. Tuğcu-Demiröz, and T. Doğanay, "Dissolution and assaying of multicomponent tablets by chemometric methods using computer-aided spectrophotometer," *International journal of pharmaceutics,* vol. 250, no. 2, pp. 339-350, 2003.

[97] M. A. Lomillo, O. D. Renedo, and M. A. Martınez, "Resolution of ternary mixtures of rifampicin, isoniazid and pyrazinamide by differential pulse polarography and partial least squares method," *Analytica chimica acta,* vol. 449, no. 1-2, pp. 167-177, 2001.

[98] A. J. Nepote, L. Vera-Candiotti, M. a. R. Williner, P. C. Damiani, and A. C. Olivieri, "Development and validation of chemometrics-assisted spectrophotometry and micellar electrokinetic chromatography for the determination of four-component pharmaceuticals," *Analytica chimica acta,* vol. 489, no. 1, pp. 77-84, 2003.

[99] S. Šašić and Y. Ozaki, "Short-wave near-infrared spectroscopy of biological fluids. 1. Quantitative analysis of fat, protein, and lactose in raw milk by partial least-squares regression and band assignment," *Analytical chemistry,* vol. 73, no. 1, pp. 64-71, 2001.

[100] Ö. Üstündağ and E. Dinç, "Simultaneous resolution of a binary mixture of captopril and hydrochlorothiazide in tablets by bivariate and multivariate spectral calibrations," *Die Pharmazie-An International Journal of Pharmaceutical Sciences,* vol. 58, no. 9, pp. 623-628, 2003.

[101] E. Fu *et al.*, "SPR imaging-based salivary diagnostics system for the detection of small molecule analytes," *Annals of the New York Academy of Sciences,* vol. 1098, no. 1, pp. 335-344, 2007.

[102] R. Dwivedi *et al.*, "Correlation of saliva and serum free valproic acid concentrations in persons with epilepsy," *Seizure,* vol. 25, pp. 187-190, 2015.

[103] J. P. Brody, T. D. Osborn, F. K. Forster, and P. Yager, "A planar microfabricated fluid filter," *Sensors and Actuators A: Physical,* vol. 54, no. 1-3, pp. 704-708, 1996.

[104] J. P. Brody and P. Yager, "Diffusion-based extraction in a microfabricated device," *Sensors and Actuators A: Physical,* vol. 58, no. 1, pp. 13-18, 1997.

[105] P. Yager *et al.*, "Microfluidic diagnostic technologies for global public health," *Nature,* vol. 442, no. 7101, pp. 412-418, 2006.

[106] V. V. Coşofreţ and R. P. Buck, "A poly (vinylchloride) membrane electrode for determination of phenytoin in pharmaceutical formulations," *Journal of pharmaceutical and biomedical analysis,* vol. 4, no. 1, pp. 45-51, 1986.

[107] S. Pruneanu *et al.*, "Novel graphene-gold nanoparticle modified electrodes for the high sensitivity electrochemical spectroscopy detection and analysis of carbamazepine," *The Journal of Physical Chemistry C,* vol. 115, no. 47, pp. 23387-23394, 2011.

[108] J. B. Raoof, M. Baghayeri, and R. Ojani, "A high sensitive voltammetric sensor for qualitative and quantitative determination of phenobarbital as an antiepileptic drug in presence of acetaminophen," *Colloids and Surfaces B: Biointerfaces,* vol. 95, pp. 121-128, 2012.

[109] N. S. Lawrence, R. P. Deo, and J. Wang, "Biocatalytic carbon paste sensors based on a mediator pasting liquid," *Analytical chemistry,* vol. 76, no. 13, pp. 3735-3739, 2004.

[110] J. Liu *et al.*, "Electrochemical microfluidic chip based on molecular imprinting technique applied for therapeutic drug monitoring," *Biosensors and Bioelectronics,* vol. 91, pp. 714-720, 2017.

[111] M. Queiroz, S. Silva, D. Carvalho, and F. Lancas, "Determination of lamotrigine simultaneously with carbamazepine, carbamazepine epoxide, phenytoin, phenobarbital, and primidone in human plasma by SPME-GC-TSD," *Journal of chromatographic science,* vol. 40, no. 4, pp. 219-223, 2002.

[112] N. Lavanya *et al.*, "A novel disposable electrochemical sensor for determination of carbamazepine based on Fe doped SnO2 nanoparticles modified screen-printed carbon electrode," *Materials Science and Engineering: C,* vol. 62, pp. 53-60, 2016.

[113] W. Lin, M. Pan, H. Wang, Y. Su, and P. Huang, "Analysis of carbamazepine serum by differential pulse voltammetry (DPV) and comparison with fluorescence polarization immunoassay (FPIA): an animal study," *Medicinal Chemistry Research,* vol. 21, no. 12, pp. 4389-4394, 2012.

[114] P. Balasubramanian *et al.*, "An amperometric sensor for low level detection of antidepressant drug carbamazepine based on graphene oxide-g-C3N4 composite film modified electrode," *Journal of The Electrochemical Society,* vol. 165, no. 3, p. B160, 2018.

[115] M. Amiri, H. Salehniya, and A. Habibi-Yangjeh, "Graphitic carbon nitride/chitosan composite for adsorption and electrochemical determination of mercury in real samples," *Industrial & Engineering Chemistry Research,* vol. 55, no. 29, pp. 8114-8122, 2016.

[116] M. Sadhukhan and S. Barman, "Bottom-up fabrication of two-dimensional carbon nitride and highly sensitive electrochemical sensors for mercuric ions," *Journal of Materials Chemistry A,* vol. 1, no. 8, pp. 2752-2756, 2013.

[117] L. Magos and T. W. Clarkson, "Overview of the clinical toxicity of mercury," *Annals of clinical biochemistry,* vol. 43, no. 4, pp. 257-268, 2006.

[118] M. Pan *et al.*, "Determination of carbamazepine: a comparison of the differential pulse voltammetry (DPV) method and the immunoassay method in a clinical trial," *Journal of Analytical Chemistry,* vol. 69, no. 1, pp. 57-61, 2014.

[119] A. Bahlmann, J. Falkenhagen, M. G. Weller, U. Panne, and R. J. Schneider, "Cetirizine as pH-dependent cross-reactant in a carbamazepine-specific immunoassay," *Analyst,* vol. 136, no. 7, pp. 1357-1364, 2011.

[120] P. Datta, D. Scurlock, and A. Dasgupta, "Analytic performance evaluation of a new turbidimetric immunoassay for phenytoin on the ADVIA 1650® analyzer: effect of phenytoin metabolite and analogue," *Therapeutic drug monitoring,* vol. 27, no. 3, pp. 305-308, 2005.

[121] A. Hatch *et al.*, "A rapid diffusion immunoassay in a T-sensor," *Nature biotechnology,* vol. 19, no. 5, pp. 461-465, 2001.

[122] F. Parant, M. Moulsma, M. C. Gagnieu, and G. Lardet, "Hydroxyzine and metabolites as a source of interference in carbamazepine particle-enhanced turbidimetric inhibition immunoassay (PETINIA)," *Therapeutic drug monitoring,* vol. 27, no. 4, pp. 457-462, 2005.

[123] E. Z. Reineks, S. E. Lawson, K. E. Lembright, and S. Wang, "Performance characteristics of a new levetiracetam immunoassay and method comparison with a high-performance liquid chromatography method," *Therapeutic drug monitoring,* vol. 33, no. 1, pp. 124-127, 2011.

[124] J. F. Wilson, L. M. Tsanaclis, J. E. Perrett, J. Williams, J. Wicks, and A. Richens, "Performance of techniques for measurement of therapeutic drugs in serum. A comparison based on external quality assessment data," *Therapeutic drug monitoring,* vol. 14, no. 2, pp. 98-106, 1992.

[125] X. Yang, J. Janatova, J. M. Juenke, G. A. McMillin, and J. D. Andrade, "An ImmunoChip prototype for simultaneous detection of antiepileptic drugs using an enhanced one-step homogeneous immunoassay," *Analytical biochemistry,* vol. 365, no. 2, pp. 222-229, 2007.

[126] F. Chapuis, V. Pichon, F. Lanza, S. Sellergren, and M. C. Hennion, "Optimization of the class-selective extraction of triazines from aqueous samples using a molecularly imprinted polymer by a comprehensive approach of the retention mechanism," (in English), *Journal of chromatography. A,* vol. 999, no. 1-2, pp. 1-2, 2003.

[127] C.-M. Dai, J. Zhang, Y.-L. Zhang, X.-F. Zhou, Y.-P. Duan, and S.-G. Liu, "Selective removal of acidic pharmaceuticals from contaminated lake water using multi-templates molecularly imprinted polymer," *Chemical engineering journal,* vol. 211, pp. 302-309, 2012.

[128] A. Hillberg, K. Brain, and C. Allender, "Molecular imprinted polymer sensors: implications for therapeutics," *Advanced drug delivery reviews,* vol. 57, no. 12, pp. 1875-1889, 2005.

[129] F. Khalilian and S. Ahmadian, "Molecularly imprinted polymer on a SiO2-coated graphene oxide surface for the fast and selective dispersive solid-phase extraction of Carbamazepine from biological samples," *Journal of separation science,* vol. 39, no. 8, pp. 1500-1508, 2016.

[130] F. Lanza *et al.*, "Development of a semiautomated procedure for the synthesis and evaluation of molecularly imprinted polymers applied to the search for functional monomers for phenytoin and nifedipine," *Analytica chimica acta,* vol. 435, no. 1, pp. 91-106, 2001.

[131] Y. Liu, Q.-J. Song, and L. Wang, "Development and characterization of an amperometric sensor for triclosan detection based on electropolymerized molecularly imprinted polymer," *Microchemical Journal,* vol. 91, no. 2, pp. 222-226, 2009.

[132] S. A. Mohajeri and S. A. Ebrahimi, "Preparation and characterization of a lamotrigine imprinted polymer and its application for drug assay in human serum," *Journal of separation science,* vol. 31, no. 20, pp. 3595-3602, 2008.

[133] Y.-L. Zhang, J. Zhang, C.-M. Dai, X.-F. Zhou, and S.-G. Liu, "Sorption of carbamazepine from water by magnetic molecularly imprinted polymers based on chitosan-Fe3O4," *Carbohydrate polymers,* vol. 97, no. 2, pp. 809-816, 2013.

[134] L.-S. Huang, C. Gunawan, Y.-K. Yen, and K.-F. Chang, "Direct determination of a small-molecule drug, valproic acid, by an electrically-detected microcantilever biosensor for personalized diagnostics," *Biosensors,* vol. 5, no. 1, pp. 37-50, 2015.

[135] M. B. Gholivand, G. Malekzadeh, and M. Torkashvand, "Determination of lamotrigine by using molecularly imprinted polymer–carbon paste electrode," *Journal of Electroanalytical Chemistry,* vol. 692, pp. 9-16, 2013.

[136] K. Hoshina, S. Horiyama, H. Matsunaga, and J. Haginaka, "Molecularly imprinted polymers for simultaneous determination of antiepileptics in river water samples by liquid chromatography–tandem mass spectrometry," *Journal of Chromatography A,* vol. 1216, no. 25, pp. 4957-4962, 2009.

[137] J. Liu *et al.*, "Electrochemical sensor based on molecularly imprinted polymer for sensitive and selective determination of metronidazole via two different approaches," *Analytical and bioanalytical chemistry,* vol. 408, no. 16, pp. 4287-4295, 2016.

[138] J. Kuhn and C. Knabbe, "Fully validated method for rapid and simultaneous measurement of six antiepileptic drugs in serum and plasma using ultra-performance liquid chromatography–electrospray ionization tandem mass spectrometry," *Talanta,* vol. 110, pp. 71-80, 2013.

[139] H. Heidari and B. Yari, "Multivariate Optimization of an Ultrasound-Assisted Deep Eutectic Solvent-Based Liquid-Phase Microextraction Method for HPLC–UV Analysis of Carbamazepine in Plasma," *Chromatographia,* vol. 83, no. 12, pp. 1467-1475, 2020.

[140] S. Veeralingam and S. Badhulika, "Two-Dimensional Metallic NiSe2 Nanoclusters–Based Low-Cost, Flexible, Amperometric Sensor for Detection of Neurological Drug Carbamazepine in Human Sweat Samples," *Frontiers in Chemistry*, vol. 8, p. 337, 2020.

[141] S. Zhou, L. Xu, L. Liu, H. Kuang, and C. Xu, "Development of a monoclonal antibody-based immunochromatographic assay for the detection of carbamazepine and carbamazepine-10, 11-epoxide," *Journal of Chromatography B*, vol. 1141, p. 122036, 2020.